How Energy Accumulation and Disposal Affect the Rates of Reactions

SIMON H. BAUER

Department of Chemistry, Cornell University, Ithaca, New York 14853

Received March 31, 1977 (Revised Manuscript Received October 27, 1977)

Contents

I. Introduction 147
A. Definitions 147
B. Orders of Magnitude for Energy Transfer Probabilities 148
1. Gas Phase 148
2. Condensed Phases 150
3. Intramolecular Energy Transfer 150
C. Assumptions—Sometimes Stated and Often Implied 151
D. The Characteristic Intervals of Chemical Kinetics 152
E. Occurrence of a Reaction and Its Degree of Advancement 153
II. When a Single Energy Pool is Adequate 155
A. Implications of the Arrhenius Expression 155
B. Success of RRKM Theory for Unimolecular Reactions 155
C. The Kinetic Isotope Effect 155
D. Estimation of Rate Parameters for Elementary Steps 156
E. Model Calculations 156
III. When Several Energy Pools Are Indicated 156
A. Molecular Rate Parameters vs. Ensemble Rate Constants 156
B. Ion–Molecule Reactions 157
C. Sensitivity of Rate Parameters to Translation, Rotation, and Orientation 159
1. Total Kinetic Energy (Center of Mass Coordinates) 159
2. Available Rotational Energy 161
3. Reactions between Oriented Molecules 161
D. Vibrational Energy Pools 163
1. Abstraction and Displacement Reactions by H, X, or M Atoms 163
2. Elimination Reactions 165
3. Other Insertion and Elimination Reactions 167
4. Photodissociation and Recombination Reactions 168
E. IR Laser-Induced Reactions 168
1. On Distinguishing Vibration-Specific from Thermal Effects 168
2. Excited Diatoms 169
3. Excited Small Polyatomics 171
4. Laser Augmented Rates for Large Molecules 172
F. Do Conventional Kinetic Experiments Indicate Multiple Energy Pools? 174
1. Nonlinear Arrhenius Graphs 174
2. Diatom Dissociations 175
IV. Comments on Theory 175
A. Trajectory Calculations 176
B. The "Surprisal" Formulation for Nonrandom Systems 178
V. Conclusions 180
VI. Appendix 180
VII. Key to Symbols 180
VIII. References and Notes 181

0009-2665/78/0778-0147$05.00/0

I. Introduction

A. Definitions

This review is a discourse on the role of rotational and vibrational excitation in controlling the rates of chemical reactions. It was written for nonprofessional kineticists and focuses on some of the concepts which underlie every day discussions among chemists. To minimize ambiguity it is essential that common terms be defined in the present context, even though the distinctions which are thus introduced may appear (unavoidably) arbitrary. We propose to disect several types of *elementary steps* and to inspect the parts of which they are constituted. The presumption is that for each complex reaction a mechanism has been developed, and that acceptable arguments have been marshalled for the postulated intermediate species, based (possibly) on recorded transient spectra, on isolated adducts of scavenged intermediates, or inferred from careful analyses of product distributions, the retention or loss of chirality, etc. Because the models implied by the language we use are not always identical with the quantitative formulations utilized in data reduction, it is essential that there be an agreement as to the meaning of the following terms.

(i) A molecule or a fragment is a *reaction intermediate* if it has an identifiable structure; i.e., it has a unique connectivity and conformation, AND, a mean lifetime greater than the mean time between collisions (τ_c) with the ambient molecules. Thus, the boat and chair forms of cyclohexane are considered to be distinct species, but excited states which are structurally equivalent, OR have a mean lifetime shorter than τ_c, are not classified as distinct. (Since τ_c is dependent on sample density, this definition obviously does not apply to experiments performed under "single collision" conditions; one must then fall back on another operational detectability criterion.) On this basis, electronically excited species are considered reaction intermediates.

(ii) In conventional kinetics an elementary step describes structurally identifiable changes which connect any two species, either of which may be an initial reagent, reaction intermediate, or reaction product. Thus, gauche $\rightleftarrows$ trans conformational changes are elementary steps but (*i,j*) transitions or (*s–s*) conversions (defined below) are not.

(iii) Designate transfers between energized *states* (which may have the same or different total energies), *without changes in structure* as (*i,j*) transitions; in the present context these are not elementary steps. Clearly, there is a fuzzy region in phase space which connects highly excited species, which we recognize as reactants, to other similarly excited species, which we recognize as products.

(iv) Designate the very rapid sequence of structures (the lifetimes of which are in the 0.01–0.1-ps range) through which a reactant passes to become the product, in a single elementary step, as a *structure–sequence* graph; call the transformation an (*s–s*) *conversion.* This process is distinguished from a "mechanism" as used by kineticists for a collection of elementary steps in a complex reaction.

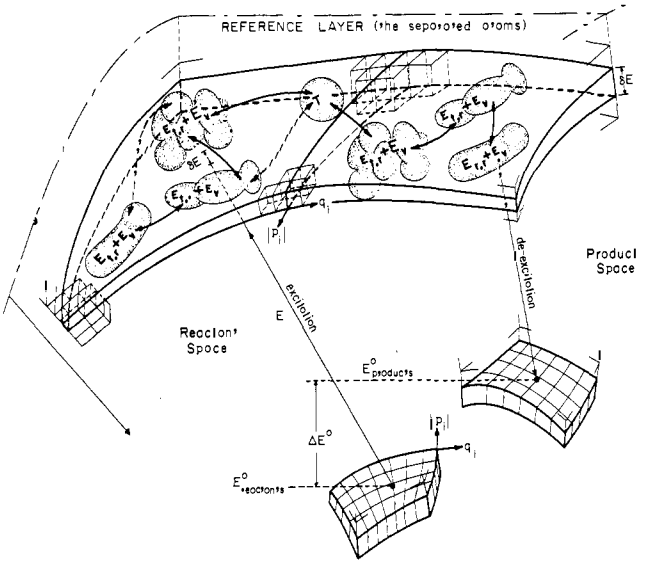

Figure 1. A phase space diagram which shows the migration of a representative point during a reaction. Note the possible partition of energy in the reactant and product spaces and the possibility that there may be several T regions (in a many atom system) which correspond to distinct product channels. The number of cells in an E layer rises rapidly with increasing $(E - E^0_R)$ or $(E - E^0_P)$.

A pictorial representation (Figure 1) will aid in clarifying these distinctions. Imagine a stacked set of layers to represent the E scale (total internal energy, which includes the kinetic energy of relative motion of a colliding pair, their internal vibrational energies, and internal rotational energies). Each of these layers is multidimensional, such that the location of a representative point within a given layer (that is, within a cell) specifies all the coordinates (q_i) and the momenta ($|\vec{p}_i|$) of the atoms in the reacting unit. This phase-space representation shows that for low E there is no continuity of cells which link the reactant space to the product space; there are no combinations of p's and q's which look like a transition structure and still have the indicated total energy. However, for a layer of thickness δE such that E is greater than E^*, there is a group of cells (T), which *do bridge* the reactant and product spaces. The stacked multidimensional layer model underscores the concept that upon specifying the total internal energy of a reacting unit one locates the representative point in a particular E layer, but he leaves ambiguous its location within that layer. The partition of the energy with respect to relative translation, internal rotation, and vibration may prove significant. Thus, (i,j) transitions refer to a random-walk motion of the representative point between adjacent E layers or between cells within a layer, but the point remains either in the reactant space or the product space; an $(s–s)$ conversion refers to motion of the representative point within or through T space, between the reactant and product spaces.

Figure 1 provides no clues regarding the forces which induce migration of the representative point; however, the principle of microscopic reversibility provides a relation between the probability for any step and its reverse. Transitions between cells in adjacent E layers, either of the (i,j) or (s–s) type, require collisions with the ambient molecules. Transitions which are restricted to a single layer can be induced either by gentle collisions (that is, the encounters merely reshuffle the distribution of energies and alter the phases of the vibrations) or they may occur spontaneously, provided the reacting unit is sufficiently energized and is polyatomic. Thus, during intervals between perturbing collisions with the ambient molecules a highly energized polyatomic species or a colliding pair (as a unit) may undergo (i,j) transitions (intramolecular energy transfer) or $(s–s)$ conversions.

For the random walk of representative points through phase space, one may reasonably postulate that small steps are more probable than large jumps (the adiabatic principle[1]); ergo, translational and rotational energy exchanges (with very few exceptions) occur essentially at every collision. For small molecules in modest vibrational excitation, the gaps in the vibrational energy spectrum range from $\approx 10^2$ to 10^3 cm^{-1} (0.3–3.0 kcal/mol), and one may anticipate substantial survival factors for vibrational excitation, such that the probability for conversion per collision of vibrational to translation-rotational energy is considerably less than unity. Let $Z_{i\to j}(T)$ be the mean number of collisions with the ambient gas at temperature T, required to deexcite the molecule from state i to state j. Then for the reverse process:

$$Z_{j\to i} = Z_{i\to j} \exp[-(E_i - E_j)/kT]$$

The following is a capsule summary of the large body of data now available on the magnitudes of such survival factors.

B. Orders of Magnitude for Energy Transfer Probabilities[2]

1. Gas Phase

One should pause to contemplate the enormous number of pairwise combinational $(i\to j)$ which exist even for the simplest target molecule, keeping in mind that the energy transfer efficiency depends not only on the interaction potential between the collision partners but also on both initial states. To illustrate the wide range of observed magnitudes, note that for tightly bound homatomic diatomics, in collision with inert species at room temperature [N_2 on $N_2(v = 1)$, for example], $Z_{1\to 0} \approx 10^7$; for unsymmetrical polyatomics values $10 \leq Z_{1\to 0} \leq 10^3$ have been reported. Empirical correlations for these two classes of compounds have been proposed by Millikan and White,[3] and Lambert and Salter,[4] respectively. The magnitudes of log $Z_{1\to 0}$ generally decrease with increase in T as does $T^{-1/3}$. For a relatively small number of cases it has been experimentally determined that $Z_{1\to 0}(T)$ passes through a broad maximum at intermediate temperatures; for HF and DF these appear at 900 and 700 K, respectively.[5] Also, $1 \leq Z_{v\to(v-1)} = v^n Z_{1\to 0}$, with $n = 1$ for harmonic oscillators and $1.5 \leq n \leq 2.5$ for anharmonic cases.[6] [However, for HF(v) + H → HF($v - 1$) + H, $Z_{3\to 2} \approx 4Z_{2\to 1} \approx 100Z_{1\to 0}$.[7]] An almost universal correlation, derived in theoretical analyses of v–T transfer probabilities, is that $Z_{1\to 0}$ decreases with the depth of penetration of the collider into the repulsive shell of the excited species, and with the steepness of the repulsive potential at the collision turnaround point. It follows that the deeper the attractive term of the potential function for the colliding pair, the steeper and closer is the net repulsive curve and the greater the probability for deactivation. Examples: impact type collisions show the lowest $Z_{1\to 0}$'s;[8] deactivation by atoms (not in $^1S_0$ states) is generally very efficient[9] (Table I); so are H-bonded pairs, $CO_2 + H_2O$[10] and DF + $(DF)_n$.[11] Nonadiabatic electronic curve crossing provides strong coupling,[12] as does intermediate complex formation.[13] With few exceptions, all polyatomics show a single relaxation time for conversion of vibrational excitation to translation and rotation. These $Z_{1\to 0}$'s correlate with the lowest characteristic frequency in the molecule, irrespective of the vibrational mode which is excited.[4b] For a given lowest frequency, molecules which incorporate hydrogen atoms have lower $Z_{1\to 0}$'s than those devoid of hydrogen. Sound dispersion data indicate dual relaxation times for SO_2, CH_2Cl_2, CH_2Br_2, and C_2H_6; theoretically C_2N_2 should be in this group.

The observation that v–R–T energy transfers are characterized by a single relaxation time indicates that collisionally induced intra species vibration–vibration transfers are considerably faster than v–R–T energy exchanges. Two types of intra species v–v transfers are possible: collisions which leave almost all of the vibrational energy in the originally excited molecule but re-

TABLE I. Relative Deexcitation Efficiencies

Vibrationally excited molecule	Colliding atom	Temp range, K	Ratio of relaxation times
HF	H	~300	$\frac{HF-HF}{HF-H} \sim 0.01$ (?)
HF	F	1400–4100	$\frac{HF-HF}{HF-F} \sim 18$
HF	F	1890–3340	$\frac{HF-HF}{HF-F} \sim 26$
HF	Cl	1400–4100	$\frac{HF-HF}{HF-Cl} \geq 5$
HCl	Cl	~300	$\frac{HCl-Cl_2}{HCl-Cl} \sim 2000$
DCl	Cl	294	$\frac{DCl-DCl}{DCl-Cl} \sim 820$
HBr	Br	294	$\frac{HBr-HBr}{HBr-Br} \sim 147$
N_2	O	3000–4500	$\frac{N_2-O_2}{N_2-O} \sim 10$
CO	H	1400–2800	$\frac{CO-CO}{CO-H} \sim 10^4$
CO	O	1800–4000	$\frac{CO-CO}{CO-O} \sim 10^2$ to 10^3
O_2	O	1600–3300	$\frac{O_2-O_2}{O_2-O} \sim 300$
NO	O	~2700	$\frac{NO-NO}{NO-O} \sim 42$
NO	Cl	~1700	$\frac{NO-NO}{NO-Cl} \sim 33$
CO_2	O	~300	$\frac{CO_2-CO_2}{CO_2-O} \sim 10$

distribute it among the normal modes, and collisions which transfer most of the energy to the impinging (unexcited) molecule, and into an internal distribution unlike that of the original molecule. To date, no gas-phase experiments have been reported which demonstrate this distinction, but it has been established that the *combined* transition probability per average collision decreases with the amount of energy converted to translation + rotation.[14] Several types of interspecies energy transfers are possible, depending on the combination of concurrent changes which occur in the various quantum numbers and in the relative kinetic energy (g); symbolically, $[v_1,J_1;v_2,J_2;g] \rightarrow [v_1',J_1';v_2',J_2';g']$. While some correlations have been established, no adequate general theory has been proposed.[15] Of special current interest are studies of the vibrational deexcitation of small molecules with potentially reactive atoms. Here the distinction between relaxation without and with atom exchange is often difficult to demonstrate experimentally.[9b,16]

For single quantum *inter*species v–v transfers,

$$AB(v = 1) + CD(v = 0) = AB(v = 0) + CD(v = 1) + \Delta\epsilon$$

the magnitudes of probabilities range from 10^{-7} ($CO \leftarrow O_2$ at room temperature; $\Delta\epsilon = 587$ cm^{-1}) to 4×10^{-2} ($CS \leftarrow N_2O$; $\Delta\epsilon = -13$ cm^{-1}); most values are in the 10^{-3}–10^{-4} range.[17] The energy-transfer efficiencies decline with increasing $\Delta\epsilon$, but

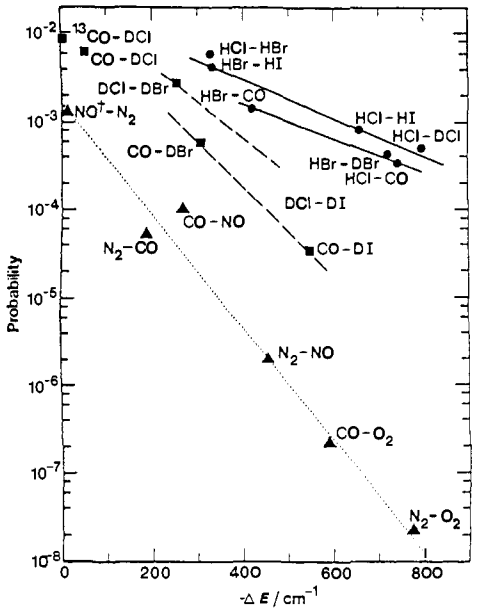

Figure 2. Probability for interspecies v–v transfer, as a function of the energy defect (ΔE) (reproduced from ref 18).

the absolute values depend on structural and dynamic factors[18] as illustrated in Figure 2. An example wherein the reduced mass and the magnitude of Δv modifies the $\Delta\epsilon$ dependence is provided by the relative efficiencies for deexcitation of H_2 and D_2 by CO:[19]

	obsd k(300 K) (cm^3 mol^{-1} s^{-1})
$H_2(v = 1) + CO(v = 0) = H_2(v = 0)$ + CO {if to $v = 2$, $\Delta\epsilon = 100$ cm^{-1}; if to $v = 1$, $\Delta\epsilon = 2016$ cm^{-1}}	8.7×10^7
$D_2(v = 1) + CO(v = 0) = D_2(v = 0)$ + $CO(v = 1)$ $\Delta\epsilon = 847$ cm^{-1}	2.6×10^9

The effect of the energy mismatch, while significant, is only one of several factors which determine whether the transfer probability varies directly or inversely with temperature. It is presumed that for dipole–dipole interactions only small energy defects ($\leq$20 cm^{-1}) lead to an inverse relation, whereas for longer range forces (dipole–quadrupole, etc.) the energy mismatch could be larger, $\Delta E < 250$ cm^{-1}.[20] Molecules which are large enough to be interesting to chemists have high densities of vibrational and rotational states even at intermediate excitation levels. Consequently, only small energy discrepancies are involved in v–v transfers, and one presumes that the corresponding probabilities are in the 0.01–0.30 range. The application of lasers for pumping specific vibrational states led to the discovery of "mode specific" v–v energy transfers. Flynn and co-workers[21] found that in $CH_3F/SO_2/Ar$ mixtures, where the ν_3 mode of methyl fluoride (1049 cm^{-1}) was pumped and fluorescence from the sulfur dioxide recorded, the rise time for the ν_2 mode (517.7 cm^{-1}) was found to be almost two orders of magnitude *slower* than that for ν_3 (1361.8 cm^{-1}) indicating a more rapid v–v crossover to the stretching modes. Fluorescence from directly pumped OCS also indicates selective mode to mode transfers.

Reports on electronic to vibrational energy transfer measurements ($\epsilon \rightarrow v$) are appearing with increasing frequency as sharp state-to-state selective diagnostics become available.[304] These cover a wide range of species, states of excitation, and transfer efficiencies. Because such investigations are peripheral to our topic few examples are cited. The vibrational distribution in product CO(v) from:

$$Na(3^2P_{1/2,3/2}) + CO(X^1\Sigma^+, v = 0) \rightarrow Na(3^2S_{1/2}) + CO(X^1\Sigma^+, v > 0)$$

was measured by Lin and Hsu[22] via infrared resonance absorption of CO laser radiation. While vibrational states close to the available limit ($v = 7$; $\Delta E = 48.5$ kcal mol^{-1}) were populated, the maximum in population appeared at $v = 2$; the $\epsilon \rightarrow v$ transfer efficiency is ≈35%. Differential cross sections for $\epsilon \rightarrow v$ transfer from Na* to eight simple gases were also determined by Hertel et al.[23] The deactivation of metastable $Hg(6^3P_2)$ by ten species, with product states determined from the spectra of light emitted from the region of intersection of crossed molecular beams, was investigated by Liu and Parson.[24] Vibrational deactivation rates of the $\nu_4 = 1$ level of the ($\tilde{A}$, $^1A_2$) excited electronic state of formaldehyde were measured for ten buffer gases. Cross sections range from 100 Å^2 (self) to 20 Å^2 (Ar, O_2) for $\nu_4 = 1 \rightarrow 0$.[305]

2. Condensed Phases

Thus far we have distinguished three types of energy transfers: $v \rightarrow R, T$, $v \rightarrow v$ (inter and intra species) which involve substantial redistributions of internal energies, and $v \rightarrow v_i$ (intramolecule, via gentle collisions), which leave the internal energies of the target molecules substantially unaltered. There is a fourth class, the *collisionless* redistribution of energy in highly excited polyatomics ($v \rightarrow v_r$). A cogent question is whether such distinctions are meaningful for energy-transfer processes in condensed phases. An affirmative answer is indicated by a variety of experiments. The time scales are determined by the magnitudes of the terms which internally couple the intramolecular oscillators relative to those which couple them to the characteristic vibrations of the bulk specimen. At one extreme, the vibrational relaxation time in liquid N_2–CO mixtures (77 K) is radiatively dominated at 56 ± 10 s, but the CO ↔ N_2 vibration equilibration time is of the order of 1 μs.[25] Infrared emissions from CO trapped in noble gas matrices were recorded by Dubost and Charneau.[26] For highly purified samples the fluorescence decay times were found to be 20.6 ms in Ne and 14.5 ms in Ar. They concluded that radiationless relaxation was unimportant because the CO oscillators are weakly coupled to the lattice vibrations, but long-range dipole–dipole interaction results in fast v–v transfer. A very large number of diatomics and simple polyatomics were investigated in Ar matrices by Legay and co-workers;[27] they found a wide range of coupling parameters with the lattice. Energy transfer within isolated $(O_2)_2$ dimers, in solid neon host (4.2 K), were studied via high-resolution spectra; vibrational energy transfer times are ~14 ps from one O_2 ($^1\Delta_g$) to another.[313]

In polyatomic liquids at room temperature vibrational relaxation occurs at the (1–10) picosecond time scale.[28,29] The shortest times are associated with rapid dephasing of the oscillating molecules without loss of vibrational energy ($v \rightarrow v_i$). A theoretical analysis of vibrational relaxation in liquids was presented by Oxtoby and Rice.[30] Chandler and Pratt[31] developed a classical statistical mechanics formalism which describes how intermolecular forces alter the average intramolecular structures of nonrigid molecules, and how these forces affect the equilibrium constants of chemically reacting species.

Exploration of state distributions generated by visible or ultraviolet laser pulses of picosecond duration, via frequency and time shifted probing picosecond pulses, opened a time domain which is three orders of magnitude shorter than is electronically accessible. The large organic molecules which have been studied show very rapid (1–10 ps) vibrational relaxation times within excited electronic or ground states, as well as rapid internal conversion between singlet states, and intersystem singlet–triplet crossings.[32] However, electronic states at surfaces of solids pumped by localized chemiexcitation (radical recombination or CO oxidation) are not always effectively coupled to the frequency spectrum of the bulk materials, such that their radiative lifetimes are shorter than internal relaxation times; characteristic emission spectra were observed.[33]

There is now a large body of data on v–R–T energy transfers from molecules in highly energized states, at or above the critical levels for unimolecular reaction. An exhaustive summary and analysis has been prepared by Tardy and Rabinovitch.[34] Efficiencies for deexcitation are primarily derived from the measured shift in the falloff curves, i.e., the dependence of (k_{uni}/k^∞) values on the pressures of the added, nonreactive gases. Sickman and Rice[35] first called attention to the disparity between the low efficiencies for vibrational relaxation derived from sound dispersion (and similar types of measurements which operate at low levels of vibrational excitation) and the near unit efficiencies for deexcitation of critically energized molecules. Since absolute values for $Z(v_{critical} \rightarrow v_{subcritical})$ are difficult to obtain, most of the experimental results for the added foreign gases are expressed relative to the reacting substrates; these factors range from ≈0.2 for monotomic species, 0.2–0.6 for diatomic and small linear molecules, to 0.5–1.1 for polyatomics. The magnitudes depend somewhat on the substrate but correlate best with the boiling points of the chaperone species. Estimates of the mean energy transferred per collision are sensitive to the model used to deconvolute the experimental results. Here also the magnitudes correlate with the structure of the chaperone species. $\langle \Delta E \rangle$'s range from 0.5–1.0 kcal/mol for monotomic chaperones, 1.5–2.0 for small linear molecules to 3–15 kcal/mol for polyatomics. Values of $\langle \Delta E \rangle$ increase somewhat with increasing total energy in the excited state but (possibly) vary *inversely* with temperature.

3. Intramolecular Energy Transfer

Discussions of intramolecular energy redistribution ($v \rightarrow v_r$) constitute a significant portion of unimolecular reaction theory.[36] Two characteristic times must be considered under collisionless conditions: τ_r, the mean time required for dispersal of localized excitations, and τ_ℓ, the mean time which passes, in highly energized molecules ($E > E^*$), before a threshold amount E^* accumulates, via intramolecular random fluctuations, at the reaction site to generate the transition (T) structure. [Since these terms are not sufficiently explicit and are sometimes misinterpreted, refer to the following section.] Note that all the critical experiments were performed with samples which were excited well above the threshold for conversion, with $E^* \geq 30RT$. Then $\tau_\ell \leqq 1$ ps. In the semiclassical limit of RRKM theory,

$$(\tau_r^*)^{-1} = \nu^* = \prod_{i=1}^{s} \nu_i^\dagger \left(\prod_{j=1}^{s-1} \nu_j^\# \right)^{-1} \quad (1)$$

ν^* is a geometric-mean frequency which spans the R and T spaces; s is the number of coupled harmonic oscillators required to represent the vibrations of the reacting species; $\nu_i^\dagger$ are the oscillator frequencies of the energized molecule; while $\nu^\#$ are the characteristic frequencies of the transition state. It is generally asserted that

$$\tau_\ell^{-1}(E) = \nu^* \frac{\rho^*(E - E^*)}{\rho(E)} \quad (2)$$

where $\rho(E)$ is the density of states in the E layer for R at R†, and $\rho^*(E - E^*)$ is the corresponding expression for the T configuration. For a system which is close to a Boltzmann distribution, treated classically,[37]

$$\langle \tau_\ell^{-1} \rangle \approx \nu^* \left(1 + \frac{E^*}{skT} \right)^{1-\langle s \rangle}$$
$$\langle s \rangle \approx \frac{\text{vibrational heat capacity}}{R} \quad (3)$$

During the past four decades kineticists extracted useful

generalizations from carefully designed experiments with highly energized reactants produced within relatively narrow energy bands by "chemical activation". More recently developed techniques permit the exploration of entirely new portions of phase space. For example, highly energized molecules can be prepared by multiphoton absorption in the infrared; nonthermalized distributions occur in shock initiated reactions, and reaction cross-sections for state selected reagents can be estimated from studies of reactive scattering with molecular beams, from a variety of ion–molecule reactions, and in highly exoergic systems which chemiluminesce and provide media for lasing. In the following sections we shall also consider examples which do not conform to the above generalizations for intra $v \rightarrow v_r$ energy transfers. Intramolecular energy transfer in electronically excited molecules, gas phase, was reviewed by Lee.[305]

C. Assumptions—Sometimes Stated and Often Implied

Given the above definitions and time scales, it is interesting to examine the models generally implied during discussions of *s–s* graphs. Of primary concern to most chemists are structural features of the reactants which affect rates in a *relative way*. The arguments imply energetic considerations; *entropic* factors are introduced to account for departures from expected rates. Chemists draw graphs to show a sequence of "minimal energy structures"; they rarely incorporate analyses based on molecular dynamics. [Lest there be any doubt as to the essential difference between (*s–s*) conversions and the dynamics of a chemical transformation, the reader is directed to the brief report by Wang and Karplus[38] which shows typical trajectories for the insertion of singlet methylene into molecular hydrogen. These trajectories were obtained by integration of the equations of motion on a CNDO potential energy surface for five atoms.] Furthermore, *most chemists talk as though:*

(a) Theyconsider a single molecular event; i.e., they follow the fate of a single activated molecule, or of a fragment, or of a pair of colliding species in strong interaction.

(b) For each type of molecular event a unique potential energy surface exists; however, one quickly replaces this multidimensional surface by a one-dimensional (lowest potential) path, which connects the sequence of smoothly varying geometries from reactant to product. The complex atomic motions are collapsed unto a single *reaction coordinate* (*s*) (refer to Figure 3).

(c) There is a unique configuration (T) characterized by a unique total internal energy [E_T^0]; E^* is associated with the highest point along this minimal potential energy path, measured from E_R^0.

(d) Reactions occur only when the reactant accumulates a threshold internal energy, E^* (exclusive of the translational energy of the center mass of the entire unit, and its overall rotational energy).

(e) The "driving force" for reaction is the condition that E_P^0 be more negative than E_R^0, but the *rate* is determined by the magnitude of ($E_R - E^*$).

The ingenuity demonstrated by those concerned with the *exploration of reaction paths* is admirable. They ascertained the qualitative features of $V(s)$ functions by plotting rational (*s–s*) graphs, and they were successful in evolving predictive rules by considering an array of closely related curves for a sequence of reactions involving different (electronic) substituents, or initial configurations, or locked-in geometries, or the consequences of isotopic substitutions. These chemical procedures are currently being augmented by orbital symmetry correlation schemes, and approximate MO calculation for assumed sequences of structures. Thus, the shapes of the potential functions along the *s* coordinate, in the transition region, have been estimated for selected types of reactions.[39] Occasionally such calculations indicate that the *s* coordinate for a minimum potential energy path does not follow the most direct structural conversion from R to P; that is, there are significant exceptions to the assumption that (*s–s*) conversions follow a path of minimal displacement of atomic coordinates.

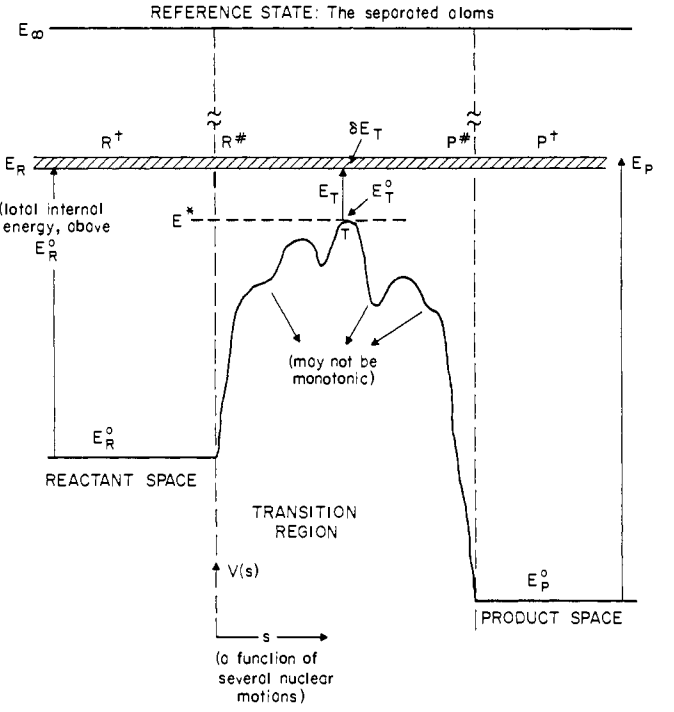

Figure 3. Potential energy representation for an (s–s) graph. $V(s)$, the generalized internuclear potential, is the lowest electronic energy path which connects the reactant and product spaces. Note: Figures 1 and 3 demonstrate quite distinct aspects. In the former, there is no clue as to the cause of, or the magnitudes of, the probabilities for transition from one cell to another; that information must be derived from the solution of the dynamical equations on an appropriate potential energy surface. In the latter, the s path represents the intersection of two hypersurfaces, for which the ordinate is an energy scale, and the abscissa is a special scale. The complete surface is needed to solve the dynamical problem.

Consider now the above list of assumptions. It is evident that assumption (b) does not apply to photoexcitation which propels the reactant to an excited electronic state, or to reactions, such as the unimolecular decomposition of dioxetanes, wherein the products are generated in excited electronic states. The latter reactions involve two, possibly intersecting, potential energy surfaces. More important, there is a serious difficulty with any model which focuses on single molecular events and then applies postulate (e). In the absence of perturbing collisions, any sufficiently energized molecule or reacting pair is constrained to remain at its specified energy level [$E_R = E_T = E_P$], irrespective of the space it happens to be in. In the absence of additional information, the probability for finding a molecule, or an interacting pair, in some designated portion of the E layer [R, T, or P] depends only on the total number of cells in that region (Figure 1), since the *prior expectation for cell occupancy is uniform*. [One could argue that $\Sigma_{E\ layer}\rho(\vec{p},q)\delta\vec{p}\delta q\}_{P\ space}$ is larger than $\Sigma_{E\ layer}\rho(\vec{p},q)\delta\vec{p}\delta q\}_{R\ space}$ merely because ($E_P - E_P^0$) $\geq E^*$ is greater than ($E - E_R^0$) $\geq E^*$; but this is not necessarily the case for all exoergic reactions.]

The obvious response is to reinterpret (a). One imagines—not a single event—but a *representative* event which is characteristic of a narrow group of molecules immersed in a macroscopic assembly of similar molecules, at a specified temperature. Then the "driving force" is produced by the much larger population of sufficiently energized reactant species which drift toward T than of product species, which drift in the opposite

direction, because $(E_T^0 - E_R^0)$ is less than $(E_T^0 - E_P^0)$. In the same spirit one should reinterpret assumption (c): T is symbolic of a *class* of configurations of similar structure with electronic energy in the vicinity of E_T^0. A further refinement is to note that in a *thermalized* system the net rate of conversion R → P is the difference between the (total) unidirectional fluxes:

$$\int_{E'}^{E_\infty} \frac{\rho^*(E_R - E_T^0)}{\rho(E_R)} \rho(E_R) \exp(-E_R/kT)\, dE_R - \int_{E'}^{E_\infty} \frac{\rho^*(E_P - E_T^0)}{\rho(E_P)} \rho(E_P) \exp(-E_P/kT)\, dE_P \quad (4)$$

At this point additional (and crucial) postulates are implied:

(f) All forms of molecular energy are assigned equal effectiveness, be they the relative translational energy of a colliding pair, internal rotation, or molecular vibrations. In Figure 3 there is a single ordinate, and no distinctions were introduced for the partition of energy among the various degrees of freedom. The only dynamics included is the one-dimensional translation of the representative point through the T region, but this detail cancels out in all quantitative treatments.[40]

(g) It is also assumed that (*i,j*) transitions are much more probable, and hence occur very much more frequently, than (*s–s*) conversions; $\tau_\ell \gg \tau_r$; $\tau_{i\to j}$. When this applies, each stack of states, R and P, is maintained close to its Boltzmann distribution, and only small corrections need to be made for the depletion of populations in high *E* layers in the vicinity of *T* due (*s–s*) conversions.[41] Obviously, assumptions (f) and (g) are coupled; thus, if the latter is valid, then the measured rates of R → P are not sensitive to the partition of energy among the reactant states.

The following very simple argument emphasizes the significance of assumption (g). Consider the five-state model (used in discussions of unimolecular reactions):

$$\mathrm{R} \underset{\kappa_1}{\overset{\kappa_{-1}}{\rightleftharpoons}} \mathrm{R}^\dagger \qquad \mathrm{R}^\dagger \underset{\tau_{r,R}^{-1}}{\overset{\tau_{\ell,R}^{-1}}{\rightleftharpoons}} \mathrm{R}^\# \cdot \mathrm{T} \cdot \mathrm{P}^\# \underset{\tau_{\ell,P}^{-1}}{\overset{\tau_{r,P}^{-1}}{\rightleftharpoons}} \mathrm{P}^\dagger \qquad \mathrm{P}^\dagger \underset{\kappa_4}{\overset{\kappa_{-4}}{\rightleftharpoons}} \mathrm{P} \quad (5)$$

[κ_1, κ_{-1}, κ_4, κ_{-4} each include the pressure of the ambient gas.] Under steady-state conditions for all transient species ($R^\dagger$, T, $P^\dagger$),

$$\frac{d[P]}{dt} = \tau_\ell^{-1} \left(\frac{\kappa_1}{\kappa_{-1}}\right) \frac{1}{1 + 1/\kappa_{-1}\tau_\ell} [R] \quad (6)$$

Then, when $1/\kappa_{-1}\tau_\ell \ll 1$, i.e., when (*i,j*) transitions occur much more frequently than (*s–s*) conversions, the rate of production of the P species is given approximately by the product of the "equilibrium" concentration of $R^\dagger$ $(=\kappa_1/\kappa_{-1})[R]$ and τ_ℓ^{-1}. This gross rate carries no information on either the dynamics of excitation or of conversion: $R^\dagger \to T \to P^\dagger$. Below we shall discuss experiments devised to measure specific cross sections for such steps. In the "fall-off" regime, when $1/\kappa_{-1}\tau_\ell > 1$, d[P]/d*t* is limited by the R → $R^\dagger$ step. Then, the gross rate is affected by the depletion of population of highly energized $R^\dagger$ states (close to E*), for which the steady-state levels are below the high-pressure (Boltzmann) values. The assertion that τ_ℓ^{-1} is proportional to the ratio of state densities (under assumption (g)) is plausible but it remains to be validated. Approximate potential surfaces are generally used to compute state desnities, not for solving the difficult dynamical problem for (*s–s*) conversions.

D. The Characteristic Intervals of Chemical Kinetics

At this stage it should be evident that the basic operational parameters in kinetic processes are the instantaneous state populations and the characteristic times which control changes in these populations. The following comments may prove helpful in utilizing the symbols we introduced (refer to section VII). The smallest time units which are significant for structural changes are the periods of molecular vibrations (10^{-13}–10^{-14} s). For bimolecular processes there is a second basic interval, the *mean* time between collisions (τ_c) to which a target molecule is subjected. It is dependent on the ratio $(\mu/T)^{1/2}$ and inversely proportional to the density of the ambient gas; $(3 \times 10^{-10}/P_{atm})$ s is typical. One should not forget that in all experiments one deals with an exponential distribution of collision intervals (and of the corresponding free paths) so that a substantial fraction of molecules suffer collisions during considerably shorter periods. For intermolecular vib–rot–transl energy transfers, $\tau_{v\to R,T} \approx (10$–$10^4)\tau_c$, while for inter vib–vib transfers, $\tau_{v\to v} \approx (3$–$300)\tau_c$. Little is known about the efficiency for intramolecular vib–vib redistributions which are assisted by "gentle" collisions. We estimate $\tau_{v\to v_l} \approx (0.1$–$2)\tau_c$, since τ_c's are calculated on the basis of translational momentum transfer cross sections, whereas cross sections for vibrational dephasing may be an order of magnitude larger. Approximate expressions for τ_r and τ_ℓ were given (eq 1 and 2); numerically they are 10^{-12} and $(10^{-9}$–$10^{-6})$ s for a typical hexatomic molecule, respectively.

In discussions of energy partition in energized molecules (or in strongly interacting pairs), the terms *localized* and *random* properly refer to the *distribution of representative points in phase space for a macroscopic sample*, not to a reaction site in the molecule. This dictum applies to experiments conducted either under single or multiple collision conditions. To emphasize this concept consider a few (idealized) techniques of the many used to "prepare" systems so as to initiate reaction.

Case α. Expose a sample to a heavy dose of monochromatic infrared radiation, such that many molecules are propelled to a highly excited but unique vibrational state (in the E layer), which can be described by a specific combination of normal modes. For each of the molecules in that group the representative point resides in a closely bunched group of cells, and the corresponding distribution is a spike which persists until collisions or other perturbations destroy this localized condition. Note that *all* the atoms in these molecules move with finite amplitudes and fixed phases relative to each other. If similar (adjacent) states were thus populated, the initial distribution would be sharply peaked around the most popular cell. The same type of representation applies when molecules are placed in excited electronic states by absorption of monochromatic UV photons.

Case β. Inject a micromole of CD_2's into an equivalent amount of

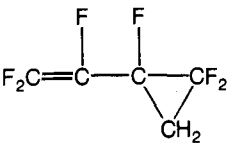

thus generating a highly energized bicycloaddition product, which (we imagine) is initially excited at the deuterated end. Here also there will be a period during which the representative points for the mixture are localized in a small region of the E layer, *symbolically* represented by

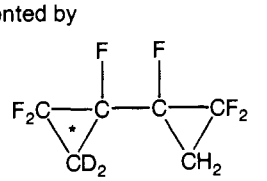

Case γ. Imagine crossing a molecular beam of H_3CNC with an energetic beam of He (or Xe) atoms, such that their relative kinetic energy (rke) in their center of mass system is 40 kcal mol^{-1}. (E^* for isomerization is 37.85 kcal mol^{-1}.) Classical

trajectory calculations show[42] that the mean vibrational excitation of the isocyanide molecules is somewhat less than 1.6 kcal mol^{-1} and that characteristically nonuniform distributions of energy among the vibrational modes are induced.

To describe the evolution of these systems one must first answer several questions: (1) Are the anharmonic oscillations which comprise the reactants sufficiently tightly coupled such that without the imposition of external perturbations, after some short time (τ_r), the spiked distributions drift (1/e) of the way toward a uniform (random; when each cell is assigned equal probability for being occupied) distribution? The τ_r's are somewhat different for the R and P spaces (eq 1); indeed, it is conceivable that for each mode of excitation there may be several characteristic times depending on the location of the initial spikes in the R and P spaces. The magnitudes of the vibrational or electronic coupling constant (λ_c) are critical.[307] Rice[43] briefly summarized the results of analytical and numerical studies for model systems as follows. Let the motion of n nonlinear, coupled oscillators be determined by the Hamiltonian

$$\mathcal{H} = H_0[p^{(n)};q^{(n)}] + \lambda_c V[p^{(n)};q^{(n)}]$$

where H_0 describes the harmonic, weakly coupled case. Then there is a threshold value, $\lambda_c \geq \lambda^*$, for which a random distribution of vibrational excitation is rapidly attained; for $\lambda_c < \lambda^*$ some periodicity in molecular motion remains (i.e., the wandering of the representative points is thereby circumscribed in phase space). A similar but more specific formulation was developed by Brumer and Duff.[44] They calculated the minimum critical energy which a coupled set of anharmonic oscillators must have so as to exhibit rapid intramolecular energy flow. In case α, an intriguing, currently debated question concerns the minimal number of IR photons which must be absorbed by molecules (relative to the number required for fragmentation) to bring them within the anharmonic, tightly coupled regime, for rapid vibrational energy redistribution.[45]

(2) For tightly coupled systems, what is the mean time (τ_ℓ) required for a sample initially in a uniform distribution to attain some specified spike distribution, due to random intramolecular fluctuations? The latter may be representative of a particular conformation, which we recognize as one of several possible T states. Thus, in case β, τ_r refers to the mean time for randomization of the chemiexcitation energy, and τ_ℓ is the mean time for the accumulation of sufficient energy in the

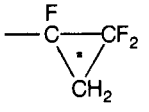

end of the molecule to eject a CF_2 from the CH_2 terminus. This corresponds to a recognizably different but entirely similar spiked distribution to the one originally synthesized.

(3) What characteristic τ_r's are appropriate for the nonrandom distributions generated by many (s–s) conversions, i.e., for molecules immediately after passage through the T region? This question did not appear in conventional kinetics discussions until recently. It is now a dominant problem, first, because it is recognized that in some systems substantial wandering back and forth through the T region (prior to randomization) may occur, and second, in many cases the nascent state populations can be measured and found to be nonrandom so that "energy disposal" has become a challenging topic for both theoretical and experimental investigations.

The experimental evidence for very short $\tau_{r,R}$'s is based on early chemiexcitation studies of Kistiakowsky and Butler,[46] and recently amplified by Rabinovitch's carefully designed experiments, illustrated as case β.[47] Indirect analyses[45a,c] of the dependence of the isotopic fractionation $^{32}S/^{34}S$ during multiphoton absorption by SF_6, on the pressure, laser power, and specific irradiating frequency, is consistent with the assumption of rapid randomization ($\tau_r < 1$ ns) for $SF_6^{(n)}$ [$nh\nu \gg D_0$(S–F)] $\rightarrow SF_5 + F$. Molecular beam studies of the translational energy distributions of fragments resulting from multiphoton dissociation of SF_6 also indicate that an RRKM treatment is satisfactory.[48] In other words, the most probable path followed in phase space by a *highly energized* molecule depends only on the E layer but not on its previous history, whether excitation was a consequence of molecular collisions or the absorption of radiation; however, the distribution of population among and within E layers is a sensitive function of the mode of excitation. Contrast low levels of photon excitation {$H_3BPF_3(3\nu_3) + H_3B \rightarrow B_2H_6 + PF_3$}, when the orthogonality of normal modes appears to be retained.[49]

A partial answer to question 3 is that the probabilities for transition R $\rightarrow$ T($\tau_{\ell,R}^{-1}$), and P $\rightarrow$ T($\tau_{\ell,P}^{-1}$) are *symmetrically* related:

$$\rho_R(E)\frac{\tau_{\ell,R}^{-1}(E)}{\tau_{r,R}^{-1}(E)} = \rho_T^*(E - E^*) = \frac{\tau_{\ell,P}^{-1}(E)}{\tau_{r,P}^{-1}(E)}\rho_P(E) \qquad (2')$$

This merely restates the proposition that, for a random distribution of representative points in either the R or P spaces, the diffusion rate to T is directly proportional to the relative numbers of accessible cells in each of these delineated regions. Because the process is random, the fraction of the originally excited molecules which remain in R (for example) after time t is,

$$N_R(t) = N_R(t_0)\exp\left(-\frac{t - t_0}{\tau_{\ell,R}}\right) \qquad (7)$$

(the random life assumption). Equation 7 applies to bimolecular processes, wherein long-lived intermediates are generated, as well as to strictly unimolecular conversions. However, dynamical factors may restrict the nascent distribution so that partition is not random. In all cases, *emergence from* any E ($>E^*$) layer in either the R or the P spaces occurs through the intervention of collisions. If there are dynamical constraints which selectively limit the rates of filling of cells, either through intramolecular processes or by preferential intermolecular energy transfer, then several $\tau_r(\vec{p};q)_{initial}$ are needed, and the above purely statistical arguments (eq 2′ and 7) must be replaced by detailed dynamical calculations.

E. Occurrence of a Reaction and Its Degree of Advancement

Several of the designations in Figure 1 were inserted because of chemical convenience; they are strictly arbitrary. There are no inherent distinctions in that model between R, T, and P spaces; neither are there differences between (i,j) and (s–s) transitions. Nevertheless, when one focuses on a single representative point for an energized molecule and follows its random walk, he finds that the vast majority of its hops can be unequivocally classified as being either one or the other type. On rare occasions only will the point wander about for a significant period in T space, for there are *relatively* few cells in that ambiguous region. However, in the strict application of this model the question whether an R $\rightarrow$ P transformation had occurred is not meaningful. Imagine that for some reaction *all* the interstate transition probabilities are known ($\kappa_{i\rightarrow j}$) and the initial population distribution (N_i^0, N_j^0, . . .) is specified; then one could solve for the time evolution of the populations of all the states. Indeed, if the transitions were first order in the populations [the reactants are highly diluted, and the (s–s) conversion is intramolecular, or if one of the reactants is present in very large excess], a formal analytical solution is available for the set of coupled differential rate equations:

$$N_i(t) = A_i + \Sigma B_{iz}\exp(-\lambda_z t) \qquad (8)$$

Here the decay parameters λ_z are the roots of a secular deter-

minant, which includes *all* the κ's. This model provides no basis for a discussion of when a reaction "has occurred", it is meaningful only to inquire how close the population of the *i*th state is to its equilibrium value. After a sufficient time post-initiation, all population will approach their equilibrium values with the same longest time constant ($1/\lambda_0$), characteristic of the *system:*

$$[N_i(t) - N_i(\infty)] = A_i + B_{i0}\exp(-\lambda_0 t) \qquad (9)$$

To most chemists the distinction between the smoothed-out time-path of an individual phase space point and the statistical evolution of a reacting system is not sharply delineated because averaging over the ensemble is introduced at different stages in the various formulations of chemical kinetics. According to the prevalent use of absolute reaction rate theory, "over the hill is out". It is assumed that after a negligible initial transient all states are filled to their Boltzmann levels. The net rate is then determined by the averaged flux of representative points that reach the T region, with translational vectors directed toward the product space; this terminates consideration of their fates. One must assume that both the geometric and dynamic structures of the transition state are known so that its partition function can be calculated. In 1939 Hirschfelder and Wigner[50] presented a refined analysis of the transmission process.

A clear-cut but purely formal criterion for reaction is incorporated in Slater's theory for unimolecular reactions;[51] here averaging is introduced midway in the analysis. He proposed that one select a distinctive interatomic distance or bond angle which is substantially altered during the conversion from reactants to products (q_1); then, he expressed its magnitude as a linear combination of normal mode amplitudes. One must also specify a critical value for its extension (q_{10}). Slater showed that for a system in a Boltzmann distribution the minimum total energy (ϵ_0, set equal to the *measured* high-pressure activation energy) which the molecule must have to attain q_{10} is

$$\epsilon_0 = q_{10}^2/\Sigma\alpha_{1\eta}^2$$

where $\alpha_{1\eta}$ are the coefficients in the expansion of the mean amplitude of the q_1 coordinate in terms of mean amplitudes of normal coordinates, $\langle Q_\eta \rangle$. Slater's model was tested for cases where $E^*/RT \geq 40$ and failed because it limits the deposition of vibrational energy into orthogonal states which are superpositions of normal modes. He postulated that while collisional excitation generated essentially uniform distributions of energized states, some $\tau_r(p;q)_R$ were very long, so that R $\rightarrow$ T transitions occurred only from selected regions in R space. The concept that the criterion for reaction, for instance, an amplitude of the fluctuating distance between two atoms, is dependent on the partition of energy among the normal modes, rather than on the total energy content, is intriguing. He solved for the mean time for first extension beyond some specified limit of a critical internal coordinate, with zero time set at the instant the excited molecule was last involved in a collision. This may be a good representation when (E^*/RT) is small,[51d] as in a conformational change, or when vibrational energy is injected via a small number of photons; it clearly is not applicable to chemical activation, whereby much energy is injected in a geometrically localized manner.

The sharpest criterion for reaction appears in trajectory calculations, and in the corresponding quantum mechanical scattering processes. First, numerous individual events are examined and the results of large numbers of trajectories are combined in appropriately weighted proportions, to represent a real system. A Monte Carlo procedure for selecting random combinations of initial states provides optimum sampling of states from the reactant space. The position and momenta parameters at the trajectory termini show whether an event should be classified as nonreacted (elastic or inelastic) or reacted, and show the partition of the total energy between translation, rotation, and vibration.[52] There seems to be no difficulty in deciding whether trajectory termini are in the reactant or product spaces, presumably because for total energy somewhat above E_T^0 there are many more cells which are clearly either in the R or P categories compared with those in T space. Generally smoothed state-to-state cross sections are summed and weighted by a Boltzmann distribution of initial populations in R space. While such calculations are limited to reactions involving a small number of atoms (3–8), they do provide insight as to the significance of initial energy partition in the reactants, and the manner of energy disposal in the products. However, serious questions remain whether classical mechanics provides an adequate vehicle for such calculations.[53]

The proper solution for a kinetic analysis based on trajectories, but one which is seldom used,[54] is to insert the statistically deduced transition probabilities from initial states to final states into a master equation, and to solve for the relaxation parameters of the system, as indicated by eq 8. Since relations between the κ's and λ's are complicated, most writers by-pass this route and argue as follows. Assume that the relative population in the fuzzy T region is negligible, so that the net rate of production of the now well defined product species is,

$$\frac{d[P]}{dt} = \sum_{i,z}\kappa\binom{i,R}{z,P}N_i^R - \sum_{i,z}\kappa\binom{z,P}{i,R}N_z^P \qquad (10)$$

where N_i^R and N_z^P are the time-dependent state populations, and $\kappa\binom{i,R}{z,P}$ is the state-to-state transition probability (i in R space; z in P space) which includes the concentration of chaperone species. If one further assumes that within the R and P spaces the transitions are very rapid ($\tau_{i\rightarrow j}$ and τ_r are small), such that Boltzmann distributions of state populations are approximately maintained even in the vicinity of the T region, then

$$N_i^R \doteq N_0^R\exp\left(-\frac{E_i - E_R^0}{kT}\right);\quad N_z^P \doteq N_0^P\exp\left(-\frac{E_z - E_P^0}{kT}\right);$$

$$N^R = \sum_i N_i^R$$

$$\frac{d[P]}{dt} \doteq \left[\sum_{i,z} k\binom{i,R}{z,P}\exp\left(-\frac{E_i - E_R^0}{kT}\right)\right]_R N_0^R - \left[\sum_{i,z}\kappa\binom{z,P}{i,R}\exp\left(-\frac{E_z - E_P^0}{kT}\right)\right]_P N_0^P = k_f N^R - k_r N^P \qquad (11)$$

Note that the bracketed terms $[\kappa_f]_R$ and $[\kappa_r]_P$, which under this assumption (but not in general) are functions of the temperature only, measure the total unidirectional fluxes. These can be much large than the phenomenological forward and reverse rate constants, k_f and k_r, respectively, although their ratio is equal to K_{eq}.[55]

An instructive example which illustrates the difference between *flux coefficients* and *phenomenological rate constants* is provided by the three-state case:[56]

$$A \underset{\kappa_{-1}}{\overset{\kappa_1}{\rightleftharpoons}} B \underset{\kappa_{-2}}{\overset{\kappa_2}{\rightleftharpoons}} C$$

The steady-state condition on B, $(B)_{ss} = (\kappa_1 A + \kappa_{-2}C)/(\kappa_{-1} + \kappa_2)$ leads to:

$$-\frac{dA}{dt} = \left[\frac{\kappa_1\kappa_2}{\kappa_{-1} + \kappa_2}\right]A - \left[\frac{\kappa_{-1}\kappa_{-2}}{\kappa_{-1} + \kappa_2}\right]C = k_f A - k_r C \qquad (12)$$

To calculate the *flux*, an arbitrary boundary must be inserted either between A and B or between B and C. If the latter is assumed, the flux into C is

$$fl(B \rightarrow C) = \kappa_2(B)_{ss} = \left\{\frac{\kappa_1 + \kappa_{-2}(C/A)}{\kappa_{-1} + \kappa_2}\right\}\kappa_2 A \equiv \mathcal{R}A$$

where the flux coefficients $\mathcal{R}$ is defined by the above equation; it is evidentally time dependent. The flux out of the C state is

$\kappa_{-2}C = \mathcal{R}'C$. These flux coefficients must satisfy two conditions: first, $(\mathcal{R}A - \mathcal{R}'C)$ must be equal to $(k_fA - k_rC)$, which is the overall rate for the reaction; second, at equilibrium $(\mathcal{R}/\mathcal{R}')$ must equal the equilibrium constant. In this simple example, it can be readily shown that the two conditions are satisfied. Were the boundary placed between A and B,

$$\text{fl}(A\rightarrow B) = \kappa_1 A \equiv \mathcal{R}A, \text{ and } \text{fl}(B\rightarrow A) = \kappa_{-1}B$$

Thus the unidirectional flux coefficients are not uniquely defined and may be time dependent. Finally the values of $\mathcal{R}$ and $\mathcal{R}'$ are *always greater* than k_f and k_r, respectively. Since at equilibrium,

$$\lim_{t\rightarrow\infty}(\mathcal{R}/\mathcal{R}') = \kappa_1\kappa_2/\kappa_{-1}\kappa_{-2} = k_f/k_r$$
$$\mathcal{R}/k_f = 1 + \kappa_2/\kappa_{-1} = \mathcal{R}'/k_r \qquad (13)$$

A quantitative example incorporating a large number of states, as in the dissociation of a diatomic molecule, was described by Bauer et al.[57]

Discussion of criteria for completion of a reaction and measures of its degree of advancement generally imply *collapsed categories* of states, when mean lifetimes within any one *category* are longer than the lifetimes within any one *state*. One must question whether this is the case when E^*/RT is small (5–20), particularly for gas-phase reactions.

II. When a Single Energy Pool Is Adequate

In the preceeding section we called attention to the significance of the several time constants which characterize all reacting systems, and emphasized that their magnitudes determine the adequacy of the models used to represent the dynamical behavior of macroscopic samples. Below we briefly listed five broad categories of evidence which indicate that in most, but not all, macroscopic systems at moderate gas pressures, or in liquids, the kinetic relations are well represented by a model in which all the internal energy of the energized molecules may be lumped into a single pool, because either $\tau_\ell \gg \tau_r$, or rapid energy redistribution is maintained by collisions so that $\tau_\ell \gg \tau_{i\rightarrow j}$. Generally, conventional kinetics is characterized by: $\tau_r < \tau_{v\rightarrow v} < \tau_{v\rightarrow R,T} < \tau_\ell$ (or τ_{bimol}).

A. Implications of the Arrhenius Expression

That for most elementary reactions the Arrhenius dependence of rate constant on temperature is experimentally verified at first sight seems remarkable. This relation not only states that there is a single temperature (i.e., within the precision of our measurements all energy pools have relaxed to the *same* Boltzmann distribution before any significant reaction occurs, and that during the course of the reaction this distribution is perturbed to an insignificant extent), it also specifies the dependence of reaction rate on internal energy, $\kappa(E;E^*)$. Slater[51] argued via use of a Laplace transform, that if:

$$\kappa[T;E^*] = \int_0^\infty \kappa(E;E^*)\mathbf{P}(E;T)\,dE \rightarrow \nu^* \exp(-E^*/RT) \qquad (14)$$

where $\mathbf{P}(E;T)$ is the internal energy distribution function in statistical equilibrium with a translational temperature, and E^* is the theshold energy for reaction; and if, $\mathbf{P}(E;T)$ is the Boltzmann distribution, then

$$\kappa(E;E^*) \equiv \tau_\ell^{-1}(E) = \nu^* \frac{\rho^*(E-E^*)}{\rho(E)} \quad \text{for } E \gtrsim E^*$$
$$= 0 \quad \text{for } E < E^* \qquad (2'')$$

A general experimental test of eq 2'' in the context of eq 14, for polyatomic molecules for which $E^*/RT \gtrsim 30$, was made on the following basis. Since $\mathbf{P}(E;T)$ incorporates $\rho(E)$ in its numerator while $\kappa(E;E^*)$ has the same function in the denominator, $\kappa[T;E^*]$ should be independent of all molecular features which change $\rho(E)$ without altering E^*, for instance, by increasing the number of oscillators but not changing the nature of the reaction. This is indeed the case for a sequence of cis–trans isomerizations, dehydrohalogenations, etc.[58]

B. Success of RRKM Theory for Unimolecular Reactions[36]

All formulations of unimolecular reaction theory at high pressures incorporate the assumption that all states remain populated according to a Boltzmann distribution appropriate to the measured translational temperature. The fact that they account adequately for a large body of data validates the assumption that a single energy pool need be considered. In quantitatively reproducing the decline of the first-order rate constant with sample pressure, on the basis of the number of effective oscillators, the RRKM formulation additionally supports this proposition for the case where

$$\tau_{i\rightarrow j}\,(\text{intermolecular transfers}) > \tau_\ell \gg \tau_r\,(\text{intramolecule transfers})$$

However, under these multicollision conditions, it is not always clear whether a test confirms the statistical nature of intramolecular energy redistribution or merely the statistical nature of the activation process.

Extension of RRKM theory to the unassisted decomposition of energized ions (designated quasi-equilibrium theory,[59] QET) has been generally successful in explaining the observed *partition* of *product ions* among the possible reaction channels. The lifetimes of the parent ions which currently can be explored cover the range from ≈ 1 μs, when conventional electron impact is used to generate the ions, to (50 ns–5 μs) when ionization is induced by charge exchange with inert gas ions (Ar^+, Kr^+, Xe^+) within a strong homogeneous draw-out field[60] and down to (1 ps–10 μs) for ionization by very strong electric fields [10^9–10^{10} V/cm].[61] In most of the experiments, particularly those using electron impact sources, the ions are generated in imprecisely specified distributions of internal energy. In contrast, charge exchange produces ions which are approximately monoenergetic; photoionization leads to excitation of specific states. The observed product distributions for a very large number of ion fragmentation studies are adequately explained by QET; i.e., the assumption that by rapid radiationless transitions ($\tau_r \leq 1$ ps) the combined electronic and vibrational excess energy in the initially excited states is randomized among the vibrational levels of the ground electronic state. Then the rate constant for any selected channel is given by the ratio of the density of states computed for the corresponding transition structure, to the density of states for the energized parent species. Some very interesting results were obtained with a field ionization technique[61] which permitted the recording of the different time histories of several products (say, $C_3H_7^+$ and $C_3H_6^+$) generated upon the decomposition of the parent ($C_4H_{10}^+$), which was produced with a broad distribution of internal energies.

C. The Kinetic Isotope Effect

Predictions of changes in rate constant due to isotopic substitution rest on calculations of ratios of partition functions for the normal and substituted species, both for the reactants and the postulated transition states. The generally satisfactory agreements between theory and experiment[62] therefore point to the presence of a common temperature for all molecular states which are counted in these partition functions. The most telling arguments are based on correct predictions of *secondary* isotope effects which are entirely a consequence of the population distribution among the rotational and vibrational states.

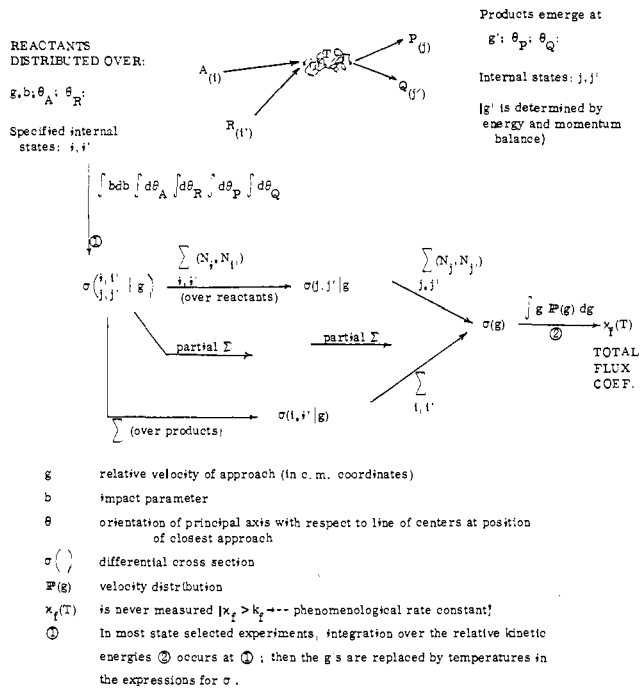

Figure 4. Schematic sequence for partially averaged reactive cross sections.

D. Estimation of Rate Parameters for Elementary Steps

A very general argument for the adequacy of a single energy pool in the analysis of most reactions is the transferability of rate constants for similar transition states, and the concurrent estimation of rate constants by empirical extension from analogous structures.[63] Clearly such a procedure would not apply to distinctly different classes of phase space distributions; for example, the transfer of preexponential factors from conversions in which the most effective activation is derived from the relative translational energy of a colliding pair, to reactions which require substantial vibrational excitations.

E. Model Calculations

The dynamics of dissociation of N_2O, O_3,[64] and HC_2Cl,[65] and the isomerization of H_3CNC,[66] have been extensively modeled via trajectory calculations on reasonable potential surfaces; both harmonic and anharmonic functions were tested. For the triatomics several of the conclusions presented by Bunker are the following.

(a) The normal mode description becomes inadequate when the vibrational amplitudes are large enough for dissociation to occur; also, to account for the low-pressure rates strict harmonicity must *not* to be assumed.

(b) Overall, RRKM theory is checked to within a factor of 2 or better.

(c) The random-life assumption (eq 7) is verified, except when (E^*/RT) is low. Vibrations of sufficiently energized molecules of any size undergo complete intramolecular energy exchange in $\approx$10 ps (except when the excitation is initially injected in X–H stretching vibrations).

(d) Upon dissociation of highly energized triatomic molecules less than half of the energy in excess of that required for bond breaking appears (on the average) as vibrational energy in the product.

There is an *apparent* disagreement between the results of trajectory calculations for chloroacetylene,[65] which show that vibrational energy redistribution is nearly complete within 0.45 ps for sufficiently energized molecules (150–200 kcal mol^{-1}), and photodissociation experiments[67] which indicate that a nonrandom state distribution persists for a much longer time. Theoretical studies[43] show that there may be a critical energy below which τ_r is greater than τ_ℓ. Finally, Monte Carlo calculations for energized H_3CNC suggest an intrinsic non-RRKM behavior for excitation energies as high as 70 kcal mol^{-1}.[68]

III. When Several Energy Pools Are Indicated

A. Molecular Rate Parameters vs. Ensemble Rate Constants

The phenomenological rate equations conventionally used to describe reacting systems, and to express the time dependence of species concentrations, incorporate complex averages of state-to-state cross sections (section II.E), which in turn are characteristic of individual molecules or of pairs of molecules in close contact. For the symbolic reaction A + R $\rightarrow$ P + Q, k_f and k_r should be obtained *either* by solving for the relaxation parameters, à la eq 8, or by empirically fitting the left member to the calculated right member:

$$k_f\left\{[A][R] - \frac{1}{K_{eq}}[P][Q]\right\} = (\text{total flux})_f - (\text{total flux})_r \quad (15)$$

That there are temperature-dependent, concentration-independent, but medium-sensitive phenomenological "rate constants" which do reproduce a large body of kinetic data appears remarkable. Inevitably one is led to inquire whether it is possible to relate more closely than is indicated in Figure 4 these experimental quantities to cross sections derived from single-collision experiments, where partial or complete state selection is achieved. Since most chemists are more concerned with *comparative rates* for a group of similar reactants undergoing a specified type of conversion, rather than with accurate values for the rate constants, one may argue that the approximation $\kappa_f \leftrightarrow k_f$ is equivalent to the assumption that for a specified reaction type these two kinetic parameters are proportional to each other; this is plausible. Intuitively one may also argue that for sufficiently large (E^*/RT) ratios, when the populations of states in the vicinity of the T region is miniscule, the net reaction R $\rightarrow$ P is approximated under steady-state conditions by the forward flux in the low-lying states. Clearly in any experiment, wherein the system is extensively perturbed, either externally or due to rapid reaction (τ_ℓ very short), such that the state populations deviate substantially from a Boltzmann function, eq 14 does not apply. However, in a formal manner it may be extended to systems wherein the various groups of states are individually characterized by distinct temperatures; then[69] the generalized form of eq 14 is:

$$\kappa[T; E_1^* \cdots E_q^*] = \sum_q \omega_q \int_{E_q^*}^{\infty} \kappa_q(E_q;E_q^*)\, \mathbf{P}_q(E_q)\, \mathbf{P}(g,T)\, dE_q\, dg \quad (16)$$

This states that the energy deposited in the qth pools for conversion R $\rightarrow$ P differ in utilization efficiency, each characterized by a specific threshold E_q^*; $\mathbf{P}(g,T)$ is the relative translational energy distribution at T, and ω_q is a weighting factor, since there are various momentum and symmetry restrictions on the ease of transfer of energy between pools. Whether eq 14 or eq 16 applies, the interesting question is what geometric and dynamic molecular features determine the shapes of the $\kappa(E_q; E_q^*)$ functions and the magnitudes of the E_q^*'s?

To a practical chemist the principle of parsimony in developing models may justify a "leap of faith" which correlates molecular structures directly to phenomenological rate constants. However, there are many who find it intellectually attractive to study in detail kinetic phenomena in terms of state-to-state transitions. Indeed, for some applications, such as the development and utilization of chemical lasers, this approach is practically rewarding. Fortunately current developments in

laboratory techniques, use of large and fast computers, and the preoccupation of theoreticians with the very difficult molecular scattering problems, provide the means for indepth investigations of kinetic events on a molecular level. The key words are; studies under single-collision conditions; however, analysis of the effects of perturbations which generate controlled departures from Boltzmann distributions also provide a means for probing different portions of phase space, even in polycollision experiments. In section IV we shall discuss theoretical developments which support the concept that several energy pools may be needed to account for energy requirements and/or disposal in reactions, particularly when the products are viewed under nascent conditions. Section III is a summary of selected experiments which demonstrate the need for multipool models.

It so happens that among the available experimental techniques, diagnostics for state selected product distributions in exoergic reactions are the easiest to implement, and are currently well developed. Next in difficulty are experiments with state selected reactants, in the exoergic direction. State selectivity for endoergic reactions are most difficult to perform with useful levels of specificity, because the overall exponential temperature dependence of rate constants tends to overshadow the fine structure due to structural or dynamic features. Even in trajectory calculations for systems with substantial endoergicity most of the trajectories prove uninteresting (hence the overall computation is expensive) because only a small fraction of the initial combinations of parameters leads to reaction. Consequently, conclusions regarding reactions in the endoergic direction are optimally derived by applying *detailed balance* to the reverse reactions. This must be performed with care for processes which involve partial state selection either in the R or P spaces.[70]

In the usual derivation[71] one starts with the principle of microscopic reversibility, and averages over states in statistical equilibrium. From this it follows that the ratio of the forward to reverse rate constant for a reaction, as written, is the corresponding equilibrium constant, at the translational temperature, T. For a state selected reaction

$$A + BC(v,J) \rightarrow AB(v',J') + C$$

$$\frac{\kappa(v,J\rightarrow v',J';T)}{\kappa(v',J'\rightarrow v,J;T)} = \left(\frac{2J'+1}{2J+1}\right)\left(\frac{\mu'}{\mu}\right)^{3/2} \times \exp\left[-\frac{\Delta E_0 - G_{v,J} + G_{v'J'}}{kT}\right] \quad (17)$$

ΔE_0 is the difference in zero-point energies between the products and the reactants: $\mu = M_A M_{BC}/(M_A + M_{BC})$, and $G_{v,J}$ is the vibrational-rotational energy of that state for the reactants above their zeropoint level. Expressions have been derived[70,72] for various combinations of collapsed initial or final states.

The following are representative samples of reaction types for which there is experimental evidence that all pools do not contribute equally, nor is there a unique threshold energy. For highly exoergic reactions with low E^*'s, this inequality appears in a form of a nonuniform distribution of populations among states in the nascent products.

B. Ion–Molecule Reactions

Extensive reviews have been prepared by Koyano[73] and Lias and Ausloos.[74] Consider first the *unimolecular* decomposition of highly energized ions. In the technique developed by Baer and co-workers[75] the ions are generated (photolytically) in specified internal energy states, and the kinetic energies of the products are determined by "photoelectron coincidence spectroscopy". Thus, absolute fragmentation rates *and* kinetic energy releases can be measured for well-characterized excited species. energy partitioning in the products of ionic decompositions was also investigated by Franklin[76] who utilized a simpler but less precise apparatus. A more refined method was recently described by Ossinger and Weiner.[77] Kinetic energy distributions from unimolecular decay (assuming QET) based on a Langevin collision model for the reverse reaction were derived by Klots.[78] There are sufficient results to date to indicate that the assumption of a single energy pool is an oversimplification. A minimum addendum is to postulate either that: (a) when $(E - E_P^\circ)$ is large, the transition state configuration dissociates directly during a time less than $\tau_{r,P}$; hence the fragments fly apart with internal energy distributions which correspond to T space, rather than P space, *or*, (b) in the preparation of the excited R state, in some instances, two noncommunicating electronic states are involved.[79] The latter applies to the dissociation of the singly charged ions of benzene, 1,2-dichloroethane, monochloroethane, and propargyl chloride. In the loss of X (=Cl, Br, I) from $C_3H_3X^+$ two paths are indicated, leading to different isomeric forms of $C_3H_3^+$ with significantly different kinetic energy releases. On the other hand, the rates of loss of X from $C_6H_5X^+$ are in good agreement with QET.[80] The fragmentation rate of $C_4H_6^+$ ($\rightarrow C_3H_3^+ + CH_3$) is over two orders of magnitude faster than predicted were randomization rapid,[81] as is the loss of HCN from $C_6H_5CN^+$, but the role of angular momentum in determining the kinetic energy release in the fragmentation of $C_4H_6^+$ is qualitatively accounted for by the Klots theory.[82] In their study of the fragmentation of vibrationally excited $C_4H_6F_2^+$, generated by photoionization of vinyl fluoride ($C_2H_3F^+ + C_2H_3F$), Williamson and Beauchamp[83] found that reaction cross sections for all three channels ($\rightarrow C_3H_5^+$; $\rightarrow C_3H_4F^+$; $\rightarrow C_3H_3F_2^+$) decrease with reactant internal energy. For the production of $C_3H_3F_2^+$, 0.18 eV of vibrational excitation is sufficient to reduce the reaction probability by 75%.

Franklin[76] found many cases wherein the measured kinetic energy release departs significantly from values derived on the basis of a statistical model. A typical example is the fragmentation of: $C_3F_8^- \rightarrow F^- + C_3F_7$, for which the average translational energy of the fluoride, when plotted against the excess energy in the parent, is consistently a factor of 2 higher than that predicted from

$$\langle\bar{\epsilon}_{tr}\rangle = \frac{\int_0^E \epsilon_{tr}\rho^\#(E_{v,tr} - \epsilon_{tr})\,d\epsilon_{tr}}{\int_0^E \rho^\#(E_{v,tr} - \epsilon_{tr})\,d\epsilon_{tr}} \xrightarrow[\text{(classical)}]{\text{QET}} \frac{E_{v,tr}}{s} \quad (18)$$

where $\rho^\#$ is the density of vibrational states in the transition structure; $E_{v,tr}$ is the excess vibrational and translational energy possessed by T over that of the fragments in their ground states; and $(s - 1)$ is the number of vibrational modes in T. However, classical trajectory calculations[84] for the fragmentation of variously energized CO_2^- ($\rightarrow CO + O^-$) give average translational energies in good agreement with those observed for low excess energies ($\leq$25 kcal/mol), but they also fall below the observed values for higher excess energies. The measured kinetic energy release distributions during the decomposition of monoenergetic CH_3I^+ [$\rightarrow CH_3^+ + I\,(^2P_{3/2})$] and CD_3I^+ [85] were correctly predicted by QET, formulated in terms of the Langevin model for the reverse association reaction,[78] when the precursor ion energies were less than 0.65 eV. The experimental values fell sharply below the theoretically predicted averages (contrast CO_2^- case) at higher excitations, possibly due to the accessibility of another product channel [$CH_3I^+ \rightarrow CH_3 + I^+\,(^3P_2)$]. All the dissociation rates were too fast to be measured except for CD_3I^+ at its threshold; there $\tau_\ell^{-1} \approx 10^7\ s^{-1}$. This is consistent with the assumption that rapid radiationless transitions occur between the excited electronic state and the vibrational ladder of the ground electronic state. However, note that in the photodissociation of neutral CH_3X (X = Cl, Br, I), energy is partioned in a highly nonstatistical matter.[86] The translational energy distribution of the products ($C_2H_2^+ + HF$) from metastable $C_2H_3F^{+(v)}$ is char-

acterized by an average value of 0.5 eV (half-width ≈0.2 eV), which is 0.69 ± 10% of the total available energy.[87]

The apparent dichotomy wherein, on one hand, QET accounts well for the observed product distributions[88] computed for rational transition structures (with appropriate $E_i^{\dagger}$ values), while, on the other hand, the partition of energy among the product species does not follow from the ratio of state densities, also occurs for uncharged, highly energized radicals generated by chemiactivation (see below). Indeed, there are indications that energy release in the exoergic direction is rarely distributed uniformly among all accessible states. Perhaps the two probes for product states (composition and structure vs. energy partition) are sensitive to different averages over the distribution of reactant species in the E layer. One formal approach is to introduce an "effectiveness function", $\omega(\vec{p};q;E)$, as a measure of the relative probability that a representative point at a given $(\vec{p};q)$ in layer E will reach T during $\tau_{\ell,R}$ (i.e., the $\tau_{r,R}$'s are $\vec{p}$ and q dependent). The utility of such a function could be tested by assigning discrete values to ω for selected localities $(\hat{p}_\gamma;\hat{q}_\gamma)$. Then the relative amounts of products (P_1,P_2) which emerge from any two reactive channels (via transition states T_1 and T_2) is

$$\frac{N(P_1)}{N(P_2)} = \frac{\sum_\gamma \int_{E_1^{\dagger}}^{\infty} \omega_1(\hat{p}_\gamma;\hat{q}_\gamma;E)\rho_1'(|E - E_1'|;\hat{p}_\gamma,\hat{q}_\gamma)\,dE}{\sum_\gamma \int_{E_2^{\dagger}}^{\infty} \omega_2(\hat{p}_\gamma\hat{q}_\gamma;E)\rho_2'(|E - E_2'|;\hat{p}_\gamma,\hat{q}_\gamma)\,dE} \quad (19)$$

When T_1 and T_2 are structurally and energetically similar, as is generally the case, the corresponding "effectiveness functions" will be even more so. The above ratio then reduces, approximately, to $\int_{E_1}^{\infty} \rho_1'(E - E_1')\,dE / \int_{E_2}^{\infty} \rho_2'(E - E_2')\,dE$, which we interpret, possibly incorrectly, as a consequence of a uniform ω function. However, for estimating the mean value of any dynamical quantity, such as the disposal of kinetic energy via channel 1, it is necessary to evaluate:

$$\langle \bar{\epsilon}_{tr(1)} \rangle = \frac{\sum_\gamma \int_0^E \epsilon_{tr}\omega_1(\hat{p}_\gamma,\hat{q}_\gamma;E)\rho_1'(E - \epsilon_{tr})\,d\epsilon_{tr}}{\sum_\gamma \int_0^E \omega_1(\hat{p}_\gamma,\hat{q}_\gamma;E)\rho_1'(E - \epsilon_{tr})\,d\epsilon_{tr}} \quad (20)$$

which is sensitive to the form of the "effectiveness function". Equation 20 allows a residuum of reaction dynamics to be retained in the phase-space formulation.

Ion–molecule reactions as *bimolecular* events are well suited for study of the comparative control of reaction rates by translation vs. vibrational excitation, since the rke of the reacting pair is determined by the controlled draw-out field in the ion source. Furthermore, the ions can be prepared in known states by monochromatic photoionization. A useful compilation of data has been published by Honma, et al.[89] For exoergic *proton* transfers from vibrationally excited ions there is little effect of vibrational energy content on cross section. Thus, for $H_2^+(v) + H_2 \rightarrow H + H_3^+$ there is a slight increase with v for high rke, but at low rke the trend is reversed; then there is a slight *decrease* with increasing $v[\sigma(H_2^+;v = 4)/\sigma(H_2^+;v = 0) \cong 0.8]$.[90] Similarly[89a] there is no marked v dependence for:

$$NO^+ (v = 0 \rightarrow 4) + i\text{-}C_4H_{10} \rightarrow HNO + C_4H_9^+$$

$$C_3H_4^+(*;v) + NH_3 \rightarrow C_3h_3 + NH_4^+$$

(* from allene, propyne, cyclopropene)

$$NH_3^+(v) + H_2O \rightarrow NH_4^+ + OH^{91}$$

$$CH_4^+(v) + CH_4 \rightarrow CH_5^+ + CH_3^{92}$$

Clearly, the total energy content is not the determining kinetic factor for these H atom transfers. A merged-beam study of $D_2^+ + N \rightarrow D + DN^+$ over the range of rke from ~0.005 to 10 eV showed[93] a net conversion of internal to translational energy at initial kinetic energies less than 0.9 eV, and a reverse flow at higher rke's. For NH_3^+ (ν_2 with $v = 0 \rightarrow 11$) + $NH_3 \rightarrow NH_2 + NH_4^+$ the relative cross section *decreases* with increasing vibrational energy of the reactant ion, and this trend is independent of the draw-out voltage: $\sigma(E_v)/\sigma(v = 0)$ falls from unity to 0.4 for V (0 → 1.5 eV).[91] For more complex reactants, in which randomization in long-lived complexes is presumed to be most readily attained, the cross sections increase with decreasing vibrational energy. This is most marked in[94]

$$C_4H_8^+(v) + C_4H_8 \rightarrow \{C_8H_{16}+\}^{(v)} \rightarrow C_7H_{13}^+ + CH_3$$

In general one may anticipate that reactions which are strongly exoergic (energy release during the early stages of the encounter serves to force the product ion–molecule pairs apart) lead to short lifetimes and high relative translational energies.

Exoergic reactions wherein an *atom* migrates from a vibrationally excited molecule to an ion are characterized by dramatic increases in cross section with vibrational energy content for rke's in the thermal range:[95]

$$N_2(v) + O^+ \rightarrow N + NO^+ \quad k(v = 2)/k(0,1) \approx 40$$

$$k(6\text{–}11)/k(0,1) \approx 350$$

For the rke ≈ 9 eV the relative enhancement due to vibrational excitation is considerably diminished.[96] The rate constants for the three reactions, $O^+ + O_2 \rightarrow O_2^+ + O$, $O^+ + N_2 \rightarrow NO^+ + N$, and $O^+ + NO \rightarrow NO^+ + O$, are small at room temperature (20, 1.5, and 0.8 × 10^{-12} cm^3 $molecule^{-1}$ s^{-1}, respectively) *but increase* by as much as three orders of magnitude with increasing rke, over the range 0.04–5 eV.[97] Raising the vibrational temperature of $N_2(v)$ from 300 to 6000 K increases the branching ratio (α/β) from 0.69 to 0.82, for

$$N_2(v) + He^+ \xrightarrow{(\alpha)} N_2^+ + He$$

$$N_2(v) + He^+ \xrightarrow{(\beta)} N^+ + N + He$$

but has little effect on the overall rate coefficient.[95] In contrast, the cross section increases with v for $H_2(v) + NH_3^+ \rightarrow H + NH_4^+$.[98]

The transfer rate of a charged atom in an *endoergic* reaction from a vibrationally excited molecule ion appears to be substantially augmented by vibrational excitation.[99]

$$H_2^+(v) + He(Ne) \rightarrow H + HeH^+(NeH^+)$$

These cross sections have a threshold at $v = 3$ ($v = 2$ for Ne) at zero rke; at higher v's there is no rke threshold, and σ rises rapidly with v. The dependence the cross section on total energy for $v = 0$–5 is illustrated in Figure 5. When the rke exceeds 18 eV, σ becomes almost independent of v. Since a reasonably good potential energy surface is available for HeH_2^+ system, trajectory calculations on the effectiveness of reagent vibration ($v = 0$ to 5) proved instructive.[100] The computed cross sections do reproduce the experimentally derived energy dependence. A similar increase with v (4–10) has been observed[101] for

$$O_2^+(a^4\Pi_u,v) + O_2 \rightarrow O + O_3^+$$

An example of an endoergic ion–molecule reaction in which (via intermediate complex formation) translational energy is efficiently converted to internal energy, at low rke, is: $C^+ + D_2 \rightarrow CD^+ + D$.[102] The cross section declines sharply at the threshold (0.42 eV), passes through a broad maximum, and decreases to zero at about 22 eV. Thus it appears that at the higher energy the reaction switches from intermediate complex formation to an impact type collision.

The above citations comprise a small sample of a growing group of ion–molecule reactions for which the search for a unique $\kappa(E;E^*)$ function may not be meaningful.

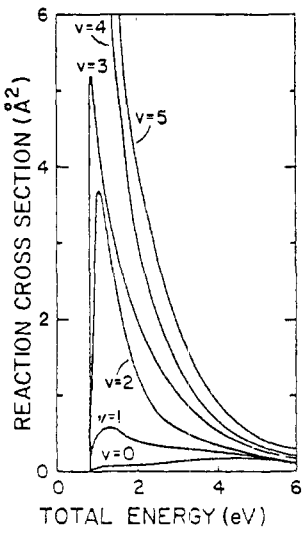

Figure 5. Dependence of the reaction cross sections for $H_2^+(v)$ + He → HeH^+ + H[ΔE° = +0.8 eV] on the total available energy, for selected vibrational excitation (cf. R. B. Bernstein, *Isr. J. Chem.*, **9**, 615 (1971), and ref 105, Figure 1.4).

C. Sensitivity of Rate Parameters to Translation, Rotation, and Orientation

The ideal experiments wherein one measures for each pair of reactants a large number of state-to-state cross sections for elastic, inelastic, and reactive collisions are difficult to perform, costly, and enormously time consuming. In addition, were such data available they would challenge the ingenuity of the compiler for presenting the essential conclusions in a manner which is both detailed yet comprehensible. Of course, the results of currently performed extensive trajectory calculations for systems which incorporate a relatively small number of reactant atoms simulate these ideal experiments, and the results are presented in the form of bar graphs and/or smoothed functional representations for final state distributions. The triangular contour graphs introduced by Polanyi for summarizing classical trajectory calculations[103] convey in an effective manner the disposal of energy in P space, for specified initial conditions in R space (thermal distribution; specific rotational or vibrational excitation, etc.), or vice versa. A particularly interesting pair of such graphs is shown in Figure 6. Obviously translation, rotation, and vibration are interlocked by the dynamic constraints imposed by the potential energy surface. Nevertheless, it is interesting to review selected experiments which demonstrate sensitivity of reactive cross sections to rke of the collisions, and to the rotational excitation of the reactants; additionally, corresponding inferences (via detailed balance considerations) can be developed from the observed partition of exothermicity into the translational and rotational energy sinks of the products. An argument is presented in section IV, as a basic postulate, that at a specified total energy (from a single E shell) a reaction follows a path of maximum entropy gain when all states react with equal a priori probability. In the following we are concerned with systems which relax but not necessarily along maximum entropy paths.

1. *Total Kinetic Energy (Center of Mass Coordinates)*

In discussing experiments on the effects of rke of the reactants on the state of the products it is useful to differentiate between *collision* dynamics and reaction dynamics. The former concerns the shape of the collision orbit for a pair of bodies during their approach and recession from the small volume wherein interesting chemical transformations can occur. With few exceptions such problems are adequately treated via classical mechanics and a central force field, i.e., an interaction potential which depends only on the instantaneous separation

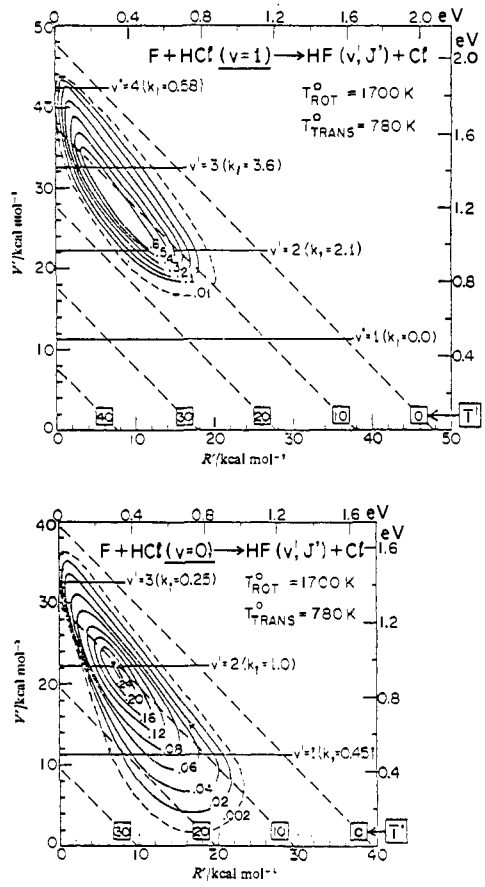

Figure 6. Triangle graphs which summarize the disposal of energy in the products [F + HCl(v = 0, 1) → HF (v',J') + Cl] (ref 214). The classical trajectory calculations lead to a continuum of magnitudes, shown by the contours which connect equal values for the unidirectional rate constant; these must be assigned to the nearest quantized (v' and J') level. The dashed (−45°) lines permit interpolation for the residual translational energy.

(r) of their centers of mass. *Reaction* dynamics refers to the complex motion executed by all the atoms over the duration of the collision (when the reactants reside within a sphere of radius approximately 2–3 times the sum of the viscosity radii of the pairs). This is a much more difficult problem which requires a quantum mechanical solution on a multidimensional potential surface; however, it is generally approximated by a classical mechanics solution on an approximate surface. In the usual trajectory calculations a minimum of computer time is allocated to the *collision* regime, so as to emphasize the *reaction* regime.

For a pair of point particles the well-known equations of motion completely chart the collision orbit for elastic encounters;[104] the effective potential $V_{eff}(r) = V(r) + \frac{1}{2}\mu g^2(b^2/r^2)$ incorporates the centrifugal barrier, which arises from the orbital angular momentum (μbg). Note that in molecular beam experiments, while one can specify the magnitude of g (i.e., rke) by velocity selection and by setting the angle of incidence of the beams, b is not susceptible to experimental control. For encounters between rotating molecules which have finite extension, the conservation condition applies to the *sum* of the components of angular momentum of rotation which lie in the plane of the collision orbit and the orbital angular momentum. The chore of unscrambling state-to-state cross sections from scattered product intensities of crossed beam experiments, even for resolved angles and beam velocities, is therefore an involved undertaking, particularly for inelastic and reactive collisions.[105]

There are many exoergic reactions which have no threshold; then the cross section decreases with increasing rke. Thus for

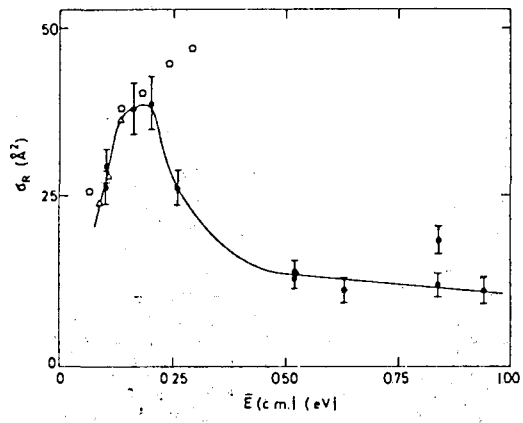

Figure 7. Total reactive cross section vs. rke of the reactants for K + $CH_3I \rightarrow KI + CH_3$: ● (ref 111), derived from direct integration of reactive differential cross sections; □, indirect values from angular distribution of (nonreactive) scattered K.

singly charged ion–molecule encounters, where $V(r) \propto r^{-4}$ (attractive potential), $\sigma_{R\rightarrow P} \propto (1/2\mu g)^{-1/2}$. For neutral–neutral collisions this dependence is shown by alkali atoms and diatoms reacting with the halogens.[106] Product ions are generated with very little rke, and except for the pair ($K_2 + I_2$) the products are exclusively $M^+ + M^+X^- + Y^-$.[107] However, when halogen atoms are abstracted by alkaline metal atoms from the halogen acids or from alkyl halides, the cross sections start at zero and rise with increasing rke.[108] Cross sections for the exothermic reactions, K + SF_6, CCl_4, and $SnCl_4$, appear to be independent of rke but sensitive to the stretching vibrations of the halides.[109] In the fluorine transfer reactions, K + CsF, RbF, the total scattering cross sections ($\sigma_{nonreact} + \sigma_{react}$) are large (≈100 Å²) for $3 \leq E_{rke} \leq 8$ kcal mol⁻¹. The ratio (σ_r/σ_{total}) is small and increases with rke for CsF (1.8 kcal endoergic); in contrast, it is close to 1/2 and decreases slightly with rke for RbF (1.5 kcal exoergic).[110] The cross section of the exoergic reactions, Cl + $Br_2 \rightarrow ClBr + Br$, increases with rke, 11 Å² at 6.8 kcal/mol, and 14 Å² at 14.7 kcal/mole.[308]

All endoergic reactions have thresholds, and their magnitudes depend on the state of internal excitation of the reactants. For simple systems, at the threshold (E_{tr}'), the cross section for each product state is concave upwards with $\sigma \propto (1 - E_{tr}'/E_{tr})^s$, where s = 1–3. The total reactive cross section rises to a maximum, levels off, and declines as new product channels are opened; an interesting example [K + CH_3I] is illustrated in Figure 7.[111] The unit exponent (s = 1) applies to a spherical interaction potential. The separation at the turnaround point (r_m) for the collision is determined by the impact parameter and the total kinetic energy in the center of mass coordinates,

$$1/2\mu g^2 = V(r_m) + (1/2\mu g^2)(b^2/r_m^2) \qquad (21)$$

If one specifies a *range* for reaction, r^*, such that at larger distances no reaction occurs [this is equivalent to setting $V(r_m)$ = 0 for $r_m > r^*$], and if the potential for reaction is known for all $r_m \leq r^*$, then the maximum impact parameter at which reaction occurs is $b^* = r^*[1 - V(r_m')/1/2\mu g^2]^{1/2}$. The reaction cross section is:

$$\sigma_{R\rightarrow P} = \pi(b^*)^2 = \pi(r^*)^2\,[1 - E_{tr}'/1/2\mu g^2] \qquad (22)$$

On this basis $\sigma_{R\rightarrow P} = 0$ for $1/2\mu g^2 < E_{tr}'$, and s = 1. Note that in Figure 7 the peak at 4 kcal/mol is followed by a slow decline at higher rke; this suggest that the impact-type collisions penetrate deeply enough to sense an attractive chemical well for $r_m < r^*$.[112] Thus, the indicated *overall* spherical potential is

$$V(r) = \epsilon_1 - \frac{(\epsilon_1 - \epsilon_2)(r^*)^2}{r^2}, \text{ for } r \leq r^* \qquad (23)$$

with ϵ_1 = 4.2 kcal mol⁻¹; ϵ_2 = 1.0 kcal mol⁻¹; r^* = 0.45 nm. When the attacking atom is Rb, scattering data suggest that the maximum in the reactive cross section lies below 0.12 eV; the integrated σ_r then decreases with rke, reaching a minimum at ≈0.9 eV, and rises slightly with further increase.[113] The threshold for the simplest of all reactions, $D + H_2 \rightarrow DH + H$, was found to be 0.33 ± 0.02 eV; σ(rke) is slightly concave (to 0.55 eV).[114] Redpath and Menzinger[115] found an appreciable upward curvature over the range $4 < E_{tr} \leq 9$ kcal/mol for the chemiluminescent reaction:

$$NO(^2\Pi_{3/2}) + O_2(^1A_1) \rightarrow NO_2'(^2B) + O_2(^3\Sigma_g^-)$$

Tang et al.[116] measured chemiluminescent reaction cross sections for $B + N_2O \rightarrow BO^* + N_2$ (σ increased by a factor of 10 over 1 < rke < 4 eV) and $Ho + N_2O \rightarrow HoO^* + N_2$ (σ increased by a factor of 2); within experimental error $s \approx 1$.

Attempts to drive highly endoergic reactions via supersonic molecular beams generally failed even though in the center of mass coordinates the rke greatly exceeded the previously established activation energies. This is not unexpected when no long-lived complex is produced, since one anticipates a low efficiency for conversion of large chunks of kinetic to vibrational energy in a single event. The cross sections for dissociation of TlCl via hard collisions are small (0.01 Å² at 6 eV[117]). The most striking example is the negative result obtained by Anderson and Jaffee[118] for the reaction: HI(seeded supersonic beam) + DI → HD + 2I. The cross section for HD production was less than their sensitivity limit (≈0.01 Å²) even for rke up to 113 kcal mol⁻¹. The reaction $H + F_2 \rightarrow HF^\dagger + F$ has a low activation energy. With the "arrested relaxation" technique, Polanyi et al.[119] found that as the mean reagent translational energy was increased (H atoms from a tungsten oven, up to 2800 K), the excess (above threshold) energy was channelled into product translation + rotation; the peak in the product vibrational excitation shifted from $v' = 6$ to $v' = 5$. These results are in agreement with predictions based on semiclassical trajectory calculations. For the complementary reaction, $F + H_2 \rightarrow HF^\dagger + H$, the large recoil velocities of the hydrogen atoms could be measured via their Doppler shifted fluorescence excited by Lyman α radiation.[120]

The functional dependence of the cross section on the total kinetic energy can also be derived, by applying detailed balance analysis to the reverse reaction, from measured kinetic energy disposal in the products. Translational energy releases from exoergic reactions were measured for a few systems via molecular beams, and (for about eight reactions) were inferred from energy balance considerations in "arrested relaxation techniques". On an a priori basis, if one assumed equal probability that the nascent product species terminate in any state compatible with a total energy content of the collision pair, then, since the translational modes have the highest density of states, followed by rotation, while the vibrational modes have the lowest densities, one would anticipate that the sequence in the partitioning of energy releases follows the same order. Indeed, this is illustrated by the reaction: Cs + $SF_6 \rightarrow CsF(v) + SF_5$. Herschbach and co-workers[121] found that all three modes have comparable Boltzmann temperatures, in accordance with the statistical model, and thus concluded that a relatively long-lived intermediate complex was formed (T_{tr} = 1190 ± 150 K; T_{rot} = 1050 ± 200 K; T_v = 1120 ± 90 K]. The schematic representation is

$$SF_6 + Cs \rightarrow \{SF_6 \cdot Cs\} \rightarrow \{F_5S \cdots FCs\} \rightarrow SF_5 + CsF(v)$$

An interesting contrast in kinetic energy disposal is presented by the pair: $K + I_2 \rightarrow KI + I$ (Figure 8a) vs. $K + CH_3I \rightarrow KI + CH_3$ (Figure 8b). The effect of reagent translation on product internal energy distribution in $Al + O_2 \rightarrow AlO^+ + O$ was investigated by Pasternack and Dagdigian.[309]

In the deactivation of $Hg(^3P_2)$ by various colliders,[24a] the functional form $\sigma \propto 1 - [V(r^*)/E_{tr}]$ was found satisfactory.

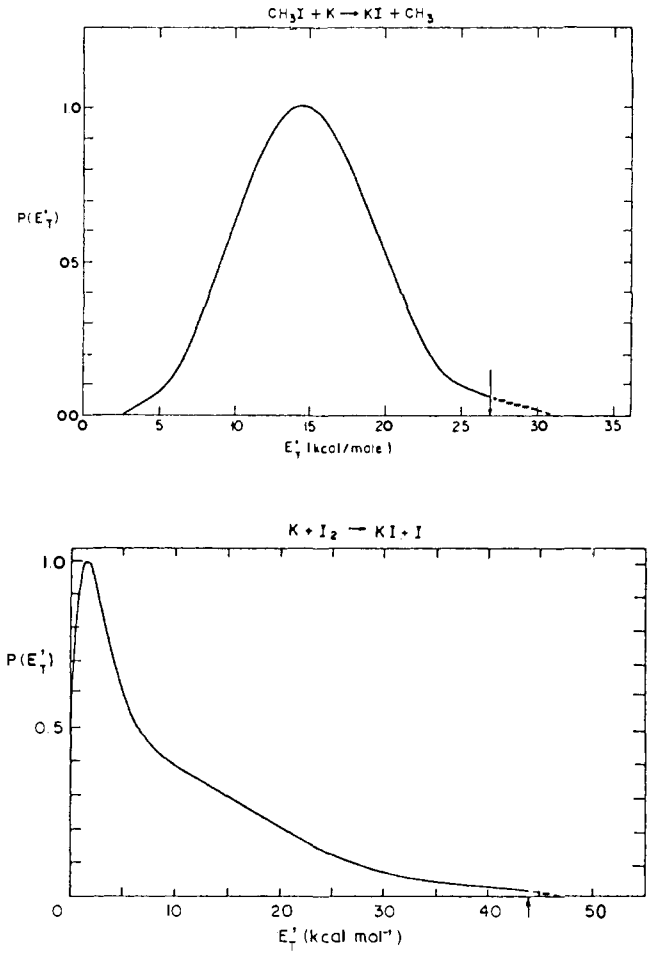

Figure 8. Comparison of *product* translational energies: (a) K + CH_3I → KI + CH_3; (b) K + I_2 → KI + I [cf. A. M. Rulis and R. B. Bernstein, *J. Chem. Phys.*, **57**, 5497 (1972), and ref 105, Figure 4.24; K. T. Gillen, A. M. Rulis, and R. B. Bernstein, *J. Chem. Phys.*, **54**, 2831 (1971), and ref 105, Figure 6.16].

However, with NO, the initial energy dependence and final state distribution were shown to be highly nonstatistical. The measured dependence of a branching ratio on rke for an electronic energy transfer was somewhat higher than that predicted on the basis of the corresponding Franck–Condon (F–C) factors.[122]

$$Ar(^3P_{2,0}) + N_2(X^1\Sigma_g^+,\ v = 0) \rightarrow Ar(^1S_0) + N_2(C^3\Pi_u;\ v' = 0, 1, 2, 3)$$

For rke's over the range 0.08–0.20 eV, $\sigma(v' = 0)/\sigma(v' = 1) = 3.5 \pm 0.2$. However, from previous measurements the indications were that at rke ≈0.03 eV this ratio was about 5. The anticipated value based on F–C factors is a constant at 1.9. The suspicion is that the relative cross section decreases with rke and approaches 1.9 at large values.

2. Available Rotational Energy

As indicated in the preceding section, the selective utilization of rotational energy for augmenting R → P conversions is circumscribed by the restrictions that the total angular momentum be conserved in every event. In A + BC → AB + C reactions, the rotational state of the diatomic product is therefore sensitively dependent on the masses of the reagents and on the impact parameter.[123] Most of the current information on rotational energy utilization is derived from studies of rotational energy disposal, either from scattered intensities of crossed beams or from fluorescence measurements under "arrested relaxation" conditions. The rotational state populations for the systems Rb + Br_2, Rb + HBr, Cs + CH_3I, and Cs + CCl_4 were determined[108] by passing the scattered beams of the alkyl halide products through a quadrupole electric field analyzer. The exoergicities of reactions with the halogen acids are modest (4.2–8.6 kcal mol^{-1}) and the fraction of that which appeared as rotation in the products ranged from 11 to 31%. The exoergicities for reactions with Br_2, CH_3I, and CCl_4 are large (37–50 kcal mol^{-1}) but only 2–5 kcal mol^{-1} was channeled into rotation; 80–90% of the exoergicity appeared as vibrational excitation of the alkali halide.

The technique of "arrested relaxation"[124] has provided interesting data on the distribution of products among vibrational–rotational states in highly exoergic reactions, and by inference the optimum distributions for the corresponding reverse reactions. The reactants (for example, H + Cl_2 → $HCl^\dagger$ + Cl) are injected for rapid mixing into a large low-pressure vessel, such that the nascent products suffer few if any collisions prior to radiating ($HCl^\dagger$ → HCl + $h\nu$). The distribution of product molecules among the various vibrational–rotational states can be estimated from the recorded intensities of the chemiluminescence spectrum. The results of these experiments are summarized in Table II. The most direct study of the effect of reagent rotational excitation on product energy distribution was presented by Douglas and Polanyi[125] for F + $H_2(v = 0;J)$ → $HF(v',J')$ + H. Control of the initial rotational states of the hydrogen was achieved by using normal H_2 at 77 and 209 K, and *p*-H_2 at the same two temperatures. Channeling of reaction exoergicity into vibration was somewhat higher for the reactants in $J = 0$, 2 (70 and 69%, respectively) compared with $J = 1$ (67%). These mean fractional allocations of exoergicity to product distributions are not reproduced by four different classical trajectory calculations, all of which predict a monotonic decrease with increasing J. This may indicate the presence of incorrect features in the potential energy surfaces which were used for these trajectories. The effectiveness of rotational energy of the CsF molecule upon its reactivity with K was measured in crossed molecular beams, over a range of rke 3–6 kcal/mol.[126] The reactive branching fraction was previously determined for a rotationally thermalized CsF beam.[110] At a given total energy, rotational excitation is significantly less efficient than hard collisions in promoting reactive decay of the intermediate complex $(CsFK)^\dagger$. In the reaction between H atoms and NO_2 (→OH + NO) in crossed molecular beams,[127] the relative populations of OH in various rotational states were measured for $v = 0$ and $v = 1$. High degrees of rotational excitations were observed; the recorded distribution was analyzed on the basis of a surprisal function, as discussed in the section IV.

Earlier investigators found unexpected rotational distributions in electronically excited products. Brenner and Carrington[128] recorded the chemiluminescence spectrum of $CH(A^2\Delta;v = 0)$ generated in the reaction between C_2H_2 and O; these experiments were carried out at reagent pressures of 0.1 to 8.5 Torr in an excess of N_2, Ar, or He. The spectra indicated a rotational state population which was a superposition of two Boltzmann distributions, one at 1200–1400 K (presumably the nascent products) and another at the temperature of the reactor, due to relaxation by the ambient gas after 10–30 collisions. The rotation–vibrational distribution of $CN(X^3\Sigma^+)$, produced by photolysis of ClCN at $\lambda \geq 160$ nm, was monitored by laser induced fluorescence.[129] The extent of collisional relaxation during the interval between production and reradiation was controlled by the total pressure and the delay between the photolyzing flash and the laser pulse. At a pressure of 0.07 Torr and a delay of 2 μs, the recorded distribution had an population peak at $J \approx 66$–70; after 25 μs rotational relaxation was complete.

3. Reactions between Oriented Molecules

In section I we called attention to the distinction between the dynamics of a reaction, as executed by closely coupled atoms during an R → P conversion, and the corresponding (*s*–*s*) graph for the process. The large body of qualitative and quantitative kinetic data on the effects of substituents on type reactions in-

TABLE II. Energy Partition in Nascent Products[a]

Reaction	Available energy (kcal/mole)	$\langle f_v \rangle$	$\langle f_J \rangle$	$\langle f_{tr} \rangle$	Vibrational state distribution
$H + F_2 = HF^{\dagger} + F$	106	~0.5			$k_1 = 0.2$ $k_2 = 0.3$ $k_3 = 0.5$ $k_4 = 0.65$ $k_5 = 1.00$ $k_6 = 0.95$
$H + Cl_2 = HCl^{\dagger} + Cl$	48.5	0.39	0.07	0.54	$k_1 = 0.28$ $k_2 = 1.00$ $k_3 = 0.92$ $k_4 = 0.08$ $k_5 < 0.08$
$D + Cl_2 = DCl^{\dagger} + Cl$	49.6	0.40	0.10	0.50	$k_1 = 0.1$ $k_2 = 0.37$ $k_3 = 1.00$ $k_4 = 0.88$ $k_5 = 0.27$ $k_6 = 0.05$
$H + Br_2 = HBr^{\dagger} + Br$	43.7	0.56	0.05	0.39	$k_1 < 0.1$ $k_2 = 0.19$ $k_3 = 0.89$ $k_4 = 1.00$ $k_5 = 0.23$
$D + Br_2 = DBr^{\dagger} + Br$	51 (rs)[d]	——0.69——		0.31	
$D + I_2 = DI^{\dagger} + I$	44 (rs)	——0.72——		0.28	
$D + IBr = \begin{cases} DBr^{\dagger} + I, \\ DI^{\dagger} + Br \end{cases}$	54 (rs)	——0.72——		0.28	
	38 (rs)	——0.68——		0.32	
$D + ICl = DI^{\dagger} + Cl$	30 (rs)	——0.76——		0.24	
$H + ICl = HCl^{\dagger} + I$[b]	55.8	0.6	0.2	0.2	Bimodal rotational distribution ($h/I = 4.6$) $k_1 = 0.30$ $k_2 = 0.63$ $k_3 = 0.79$ $k_4 = 0.81$ $k_5 = 0.96$ $k_6 = 1.00$ $k_7 = 0.75$
$H + F_2O = HF^{\dagger} + FO$	~93	≥0.32			$k_1 = 1.1$ $k_2 = 1.4$ $k_3 = 1.00$ $k_4 = 0.71$ $k_5 = 0.45$ $k_6 = 0.22$
$H + Cl_2O = HCl^{\dagger} + ClO$	~70	>0.30			$k_1 = 0.3$ $k_2 = 0.9$ $k_3 = 1.00$ $k_4 = 0.4$ $k_5 = 0.1$
$H + Cl_2S = HCl^{\dagger} + ClS$	~48	>0.35			$k_1 = 1.0$ $k_2 = 1.6$ $k_3 = 1.00$ $k_4 = 0.4$ $k_5 = 0.1$
$H + Cl_2S_2 = HCl^{\dagger} + ClS_2$	~51	>0.36			$k_2 = 0.80$ $k_3 = 1.00$ $k_4 = 0.92$ $k_5 = 0.40$
$H + BrCl + \begin{cases} HCl^{\dagger} + Br \\ HBr^{\dagger} + Cl \end{cases}$	53	0.55	0.09	0.36	$k_1 = 0.13$ $k_2 = 0.36$ $k_3 = 0.85$
	33	0.58	0.12	0.30	$k_4 = 1.00$ $k_5 = 0.79$ $k_6 = 0.30$ $k_1 = 0.27$ $k_2 = 0.45$ $k_3 = 1.00$ $k_4 = 0.45$
$H + O_3 = OH^{\dagger} + O_2$[c]	77.1	0.90	≈0.03		$^2\Pi_{3/2,1/2}$ spin states equal population $k_{\leq 6} \simeq 0$ $k_9 = \max$ $k_{10} = 0$ <7% of E_{101} remains in O_2
$H + NO_2 = OH^{\dagger} + NO$[c]	31	0.3–0.5	0.2–0.3		Fluorescence from $v' = 3, 2, 1$
$H + ClNO = HCl^{\dagger} + NO$[b]	68.5	0.5	0.07		$k_3 = 0.82$ $k_4 = 0.96$ $k_5 = 1.00$ $k_6 = 0.48$ $k_7 = 0.10$
$F + H_2 = HF^{\dagger} + H$	34.7	0.66	0.081	0.26	$k_1 = 0.31$ $k_2 = 1.00$ $k_3 = 0.48$
$F + D_2 = DF^{\dagger} + D$	34.4	0.66	0.076	0.27	$k_1 \approx 0.3$ $k_2 < 0.7$ $k_3 = 1.00$ $k_4 = 0.72$
$F + HCl = HF^{\dagger} + Cl$	~35				$k_1 \sim 0.7$ $k_2 = 1.00$ $k_3 \sim 0.15$
$Cl + HI = HCl^{\dagger} + I$	33.9	0.70	0.13	0.17	$k_1 = 0.18$ $k_2 = 0.32$ $k_3 = 1.00$ $k_4 = 0.74$
$Cl + DI = DCl^{\dagger} + I$	34.0	0.71	0.14	0.15	$k_1 \sim 0.08$ $k_2 = 0.12$ $k_3 = 0.33$ $k_4 = 0.68$ $k_5 = 1.00$ $k_6 = 0.05$
$Cl + HBr = HCl^{\dagger} + Br$	~17	†(obsd)			
$Br + HI = HBr^{\dagger} + I$	~18	†(obsd)			

[a] T. Carrington and J. C. Polanyi, *Chem. Kinet. (MTP Int. Ser.)*, **9** (1972). [b] M. A. Nazar, J. C. Polanyi, and W. J. Skrlac, *Chem. Phys. Lett.*, **29**, 473 (1974); see also *Faraday Discuss. Chem. Soc.*, No. 62, 319 (1977). [c] J. C. Polanyi and J. J. Sloan, *Int. J. Chem. Kinet., Symp. 1*, 51 (1975). [d] rs = reactive scattering.

directly led to the discovery of specific features in the corresponding potential energy surfaces. These are often expressed in geometric terms and assigned to selected orientations in the T structures. This is the basis for the concept of favorable vs. unfavorable "steric" factors. One recent example is the analysis of the stereochemical consequences of correlated rotations of "molecular propellers" as expounded by Mislow.[130] Chemists also refer to more or less favorable directions of approach in bimolecular encounters. The supporting evidence is derived mostly from reactions in solutions, and curiously no role is assigned to the solvent unless it participates directly in the reaction, nor is the influence of *solvent packing* considered, although such an effect is unavoidable in condensed phases. There is still a third sense in which "orientations" is used—the directing effect of substituents attached to the substrate, on the relative fractions of several possible products which are generated, for example, the free radicals additions to olefins.[131] This is due to an energetic factor, that is, the control of the shape of the potential energy surface by the specific substituents.

For gaseous reactions there are very few experiments wherein the mutual orientations of the reacting molecules enter explicitly in the discussion. Kinetic data obtained at moderate or high pressures are casually interpreted by introducing an arbitrary (p) factor; this accounts for those measured cross sections which are less than the kinetic theory (viscosity) derived values. Clearly, discussion of orientation effects has meaning only when the duration of a collision (i.e., the time during which the colliding pair remains within a sphere of radius approximately two collision diameters of each other) is significantly less than the rotational period of the lighter molecule, or of the internal rotation of any group close to the reaction site. In computational modeling of bimolecular events careful examination of both reactive and inelastic trajectories may indicate that the probability for reaction or for energy transfer is orientation dependent.

However, the few examples which have been published demonstrate that the collision process is dynamically complex, such that a variety of mutual orientations *are imposed on the reactants* during collision.[38] One could argue that while the relative orientation of the approaching molecules at large separation predetermines the portion of phase space which is swept out by the collision event, the relative orientation at closest approach, and hence in the T region, generally will be set by the shape of the potential energy surface. Possibly more significant factors than the mutual orientation are the rotational angular momenta of the pair and the impact parameter.

Study of reactive collisions in crossed "oriented" molecular beams provides the possibility for ascertaining whether selectivity of initial orientations is a crucial factor. Such experiments are difficult to perform because of the low signal levels available when one selects the reagents on the basis of their rotational state ($J;m$), vibrational state (v) as well as rke. However, the experiments which have been performed proved most interesting.[132] Partial selection of molecular orientations of symmetric rotators in molecular geams was achieved with inhomogeneous hexapole electric fields (CH_3I, t-BuI, $CHCl_3$, and CF_3I). These were then crossed with a beam of potassium atoms and the product intensities (KI;KCl) were measured as a function of scattering angle. For the alkyl iodides a significantly higher intensity was recorded for orientations with the I atom closest to the potassium, compared with orientations when the R group pointed toward the metal. However, for the latter orientations the reactive cross section was not zero. There was no difference between the head/tail encounters of K with $CHCl_3$, while CF_3I showed a larger reactivity for orientation with the CF_3 end directed toward K. In none of these was the scattering indicative of a long-lived complex. Preliminary results of trajectory calculations for (Rb + CH_3I) in oriented crossed beams,[133] in which a six-particle potential was used, were not entirely satisfactory. Bunker and co-workers searched for a surface which reproduced the main observed features, including the scattering angle distribution and the head/tail reactivity ratio. They tested over 30 surfaces and at last found one which appeared to account for most but not all of the data. An extended review of scattering from oriented molecules, covering experimental procedures, data, and interpretations was prepared by Reuss.[134]

At this stage one may conclude that steric factors are indeed significant, but molecular interactions are more complex than those deduced from the ball–stick models. The question whether directional attractive or repulsive forces between a colliding pair reorients the approaching molecules so as to facilitate (or hinder) reaction cannot be answered by experiment. Classical trajectories for some systems indicate that such reorientations do occur.[135,136] In solid matrices, at low temperatures (20 K), molecules in particular orientations do show preferential reactivity.[310]

D. Vibration Energy Pools

In the preceding sections we discussed the characteristic times associated with several types of transitions undertaken by the representative points for a molecular event, in its random-walk through phase space. That these transitions are strictly random, in that the probability for the occurrence of any specified event is entirely independent of the preceding or following events, is an assumption of considerable significance. Except when intramolecular energy flow occurs, the driving forces for this wandering of the representative point are molecular collisions, and the probabilities for the various types of jumps which can occur are controlled by the potential energy surface for the interacting pairs of molecules. A reasonable but unproven postulate is that, subject to total energy and momentum conservation, small hops are more likely than large ones. When one applies this to an (s–s) conversion he is merely restating an old dictum: the states which most probably precede or immediately follow transition states are similar in structure and in energy partition to the T states. This postulate provides the clue for the inadequacy of the purely statistical treatment in which the probability for an R → P conversion is merely dependent on $(E - E^*)_R$; it does suggest that a weighting function, such as was incorporated in eq 16 and 19, is required to provide for parameters which are missing in the statistical formulation but would appear as a consequence of a completely dynamical calculation.

Consider now the typical three-center reaction

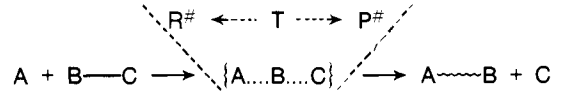

wherein the displacement of C is substantially exoergic and requires a low $E'_{\rightarrow}$. The states of R# which most frequently feed into T have relatively little translational and vibrational energy when measured from ground level of (A + BC). This applies to T and by symmetry to P#, i.e., when C is still close to AB. Thus, on their separating there is little kinetic energy in their center of mass coordinates. However, relative to the ground state of the product system (AB + C) these products are energized; consequently this energy must be incorporated in AB as vibrational excitation. Qualitatively, one concludes that the highest probability path which accounts for energy partition in the products is low rke and high vibrational content. It follows that for the reverse endoergic process (displacement of A by C) the T states of highest probability incorporate little rke of the participating species (AB + C) and the large $E'_{\leftarrow}$ must be comprised of vibrational energy in AB. Thus, vibrational excitation is of little use for the left to right conversion but is particularly effective for the right to left transition. This argument is not novel. An early discussion of energy distribution among reagents and products for three-center reactions was given by Polanyi,[137] and for four-center metatheses by Bauer and Resler.[138] In the following paragraphs we summarize experimental results for many reactions which were investigated under single collisions conditions (molecular beams or arrested relaxation techniques). During the past 5 years this work has been documented and analyzed in detail by prolific reviewers.[139]

1. *Abstraction and Displacement Reactions with H, X, or M Atoms*

As a class, the reactions of the hydrogen halides have received the most attention because the vibrational energy content of the products can be ascertained from their chemiluminescence in the infrared (indeed, many of these reactions generate chemically lasing media), and the vibrational energy content of the reactants can be controlled with the available lasers. From Table III of bond dissociation energies[140] one may readily select combinations of (atom + diatom) for which an abstraction step is substantially exoergic, and thus likely to produce vibrationally excited diatomic products. For $H_2 + X \rightarrow HX^{\dagger} + H$ (X limited to F and CN) the nascent product contains a substantial portion of the total available energy as vibration (50–70%) (Table II). Furthermore, within the vibrational energy pool the population distribution among the states is *inverted*; i.e., more nascent products are channeled into higher v states than into the lower ones. Reactions which generate $HF^{\dagger}$ are utilized for efficient chemically powered lasers since high inversion ratios are thus generated and the $v \rightarrow (v - 1)$ transition matrix elements are substantial.[141] The report by Perry and Polanyi[142] illustrates the currently attainable selectivity in measuring state-to-state rate constants via arrested relaxation for the four reactions: F + H_2 (D_2;HD). In the products the mean fractions of the available energy which appears as vibration are 0.66, 0.67, 0.59, and 0.63. The corresponding fractions for rotational excitation are 0.083,

TABLE III. Approximate Bond Dissociation Energies[140] (For Estimating Exoergicities in Atom Transfer Reactions)

	CN	F	Cl	Br	I	H
CN	143					129
F	[ ]	37.0				135
Cl	(105)	59.5	57.3			102.3
Br	(91)	67.2	51.6	45.5		86.6
I	(81)	66.4	49.7	41.9	35.6	70.4
H						103.2
Li		137	111	100	83	
K		117	101	90.5	78	
Cs		120	104	99.5	80	
Ba		(136)	(111)	98	97	
Cl_3C		106	70	50		90
H_3C	119	(108)	81	67	54	102.7
F_5S		(78)				

TABLE IV. RH + F → HF(v,J) + R[151a]

Reagent	Highest level v	Highest level J	R–H bond energy	Bond energy plus threshold energy	% E_v
$(CH_3)_2O$	3	10	93.3	98.7^{+2}_{-5}	45
					36
$(CH_3)_2S$	3	12		96.3^{+2}_{-5}	49
					40
$(CH_3)_3N$	3	8		100.6^{+2}_{-5}	57
					49
H_2O	1	10	119.2	121.4^{+2}_{-5}	64
					32
H_2O_2	4	10	89.5	89.0^{+2}_{-5}	52
					44
H_2S	4	7	91 ± 1	91.7^{+2}_{-5}	57
					48
NH_3	2	9	104 ± 2	109.9^{+2}_{-5}	50–61
					36–46
N_2H_4	(5)		76 ± 2	85^{+5}_{-12}	(~30)
					(~20)
PH_3	5	11	80	78.2^{+4}_{-5}	49
					45
CH_4	3	4	103 ± 2	103.4^{+2}_{-5}	58
					55
C_2H_6	3	8	98.2	101.0^{+2}_{-5}	63
					60
SiH_4	4	12	(80)	86.8^{+4}_{-5}	49–55
					44–50

0.076, 0.125, 0.066. [Note that while it is convenient to list and discuss *mean* values for energy partition among the vibrational rotational and translational energy pools, the distributions among the individual states have been determined[143] and provide checks for theoretical analyses.] Variation of the temperature of the reactants from 77 to 1316 K, shows that enhanced reagent translation results in enhanced product translation plus rotation.

Lasing by $HCN^{\dagger}$ has been demonstrated[144] but this system has not yet been incorporated into practical devices. Concurrently, halogen atom abstractions of the type $H + Y_2 \rightarrow HY^{\dagger} + Y$ (Y = F, Cl, Br, I) have been extensively studied. Also, vibrationally excited products which are either totally or partially inverted are produced in the displacement: $X + HY \rightarrow HX^{\dagger} + Y$ (provided the atomic number of X is less than the atomic number of Y[145]). However, studies of the displacement of CN by F and of the heavier halogens by CN have yet to be reported. Douglas et al.[146] estimated (from the depletion of chemiluminescence) the effects of controlling reactant energy on specific state rate parameters, for three endoergic ($v = 0$) reactions: HCl($v = 1$–4) + Br; HF($v = 1$–6) + Cl; HF($v = 1$–6) + Br. $\kappa_{endo}(v)$ exhibited a threshold at the vibrational level for which $\mathcal{E}_{vib} \approx E^*$; for $\mathcal{E}_{vib} > E^*$ the major path for depletion of the excited reactant is H atom transfer rather than deexcitation. This work is an experimental confirmation of classical trajectory predictions that in endoergic reactions, vibrational excitation is efficiently utilized for crossing the activation barrier.

TABLE V. Relative Vibrational Populations [RH + F → HF(v) + R][151b]

Substrate	Nascent (corrected) distribution v = 1	v = 2	v = 3	v = 4
CH_4	0.22	0.65	0.13	
C_2H_6	0.119	0.521	0.363	
$C(CH_3)_4$	0.166	0.708	0.132	
$C_6H_5CH_3$	0.281	0.391	0.309	0.027
o-$C_6H_4(CH_3)_2$			0.309	0.027
p-$C_6H_4(CH_3)_2$			0.309	0.027
1,3,5-$C_6H_3(CH_3)_3$			0.309	0.027
1,3,5-$C_6D_3(CH_3)_3$	0.170	0.359	0.430	0.047
C_6H_6	0.689	0.311		
CH_3CN	0.387	0.330	0.283	
C_6H_5OH	0.680	0.242	0.065	0.013

For the essentially thermoneutral reaction:

$$H + DCl(HCl) \xrightarrow{k_a} HD(H_2) + Cl,$$

and for

$$DCl + H \xrightarrow{k_d} D + HCl$$

there are confusing experimental results and contradictory calculations; hence it merits brief mention. Of special interest is the effect of controlled vibrational excitation of the halogen acid in augmenting these rates (see next section). For the *abstraction* path, the forward and reverse reactions were investigated in a discharge flow apparatus attached to an EPR spectrometer, to follow atom concentrations. The 1968 results which indicated that the ratio of $(k_a/k_{-a}) \approx (2\text{–}3)K_{eq(a)}$ has now been rectified.[147] It appears that the atomic Cl reacted with the HCl on the walls, probably to generate HCl_2, which confused the stoichiometry. For the *displacement* reaction, there appears to be a difference of several orders of magnitude in the reported measured preexponential factors of k_d. Molecular beam data ($A \approx 10^{13}$ [148]) are in conflict with photochemical experiments ($A \approx 10^{10}$). The larger value is supported by trajectory calculations for the H_2Cl system, with $k_a > k_d$.[149] Recent extended calculations by Dunning[150] for colinear states show a barrier of ≈ 8 kcal/mol for abstraction (H · · ·H · · · Cl) and ≈25 kcal/mol for exchange (H · · · Cl · · · H). The abstraction of H(D) atoms by F and Cl from hydrogen bearing species [F + HR → $HF^{\ddagger}$ + R] has been extensively investigated.[151] The spectrum of R's covered is shown in Tables IV and V. For several cases the partition of energy in the HF is illustrated in Figure 9.

Moehlmann and McDonald[152] estimated (from arrested-relaxation infrared–chemiluminescence spectra) the partition of energy in the products generated by F atom *abstraction* of hydrogens from several olefinic and aromatic substrates. Their data indicate that approximately 40% of the exothermicity appears as vibrational excitation of the $HF^{(v)}$, with the $v = 1$ state most likely to be populated. Of special interest were their estimates of the relative cross sections for *substitution* vs. *abstraction*, based on the recorded emission by the monosubstituted fluorides. Their results are summarized in Table VI. Note that the ratio of cross sections for substitution vs. abstraction can be large; for instance, it is 14 for a symmetrical dichloroethylene and 3 for monobromobenzene. One is directed to the intriguing question as to the partition of exothermicity between rke of the fragments [$RF^{\dagger}$ + (H;CH_3;X)] and the internal energy of the $RF^{\dagger}$ residue. These investigators later repeated the F substitution reactions[153,154] wherein they compared the observed vibrational

TABLE VI. Abstraction vs. Substitution [F + RH → HF† + R and → FR + H][152]

Substrate	(Abstraction) Relative populations $v = 1$	$v = 2$	$v = 3$	f_v	Ratio of cross sections: substitution to abstraction
Ethylene	0.44	0.32	0.02	0.38	3
Propene[a]	0.33	0.32	0.17	0.33	0.2
Vinyl chloride	0.40	0.36	0.04	0.41	4
Vinyl bromide	0.37	0.38	0.07	0.44	2
gem-Dichloroethylene	0.49	0.24	0.03	0.35	14
cis-Dichloroethylene	0.43	0.31	0.04	0.38	7
Benzene	0.42	0.30	0.07	0.41	3
o-Xylene	0.43	0.26	0.09	0.40	<0.2
o-Chlorotoluene	0.43	0.26	0.09	0.40	<0.2

[a] Propene: $v = 4$ attained 0.02.

TABLE VII. Characteristics of the Fluorine Substitution Reactions[154]

	Reaction	Density of states in products[a]	$\langle E_{tr} \rangle$,[b] kcal mol^{-1}	Exit channel barrier	Translational energy distribution	Complex lifetime, s	Vibrational energy distribution
I.	F + C_2H_3–H	10	4	Yes	Nonstatistical	$>5 \times 10^{-12}$	Nonstatistical
	F + C_2H_3–CH_3	550	14	Yes	Nonstatistical		
II.	F + C_6H_5–H	2×10^4	7	Yes	Nonstatistical	$>5 \times 10^{-12}$	Statistical
	F + C_6H_5–CH_3	3×10^6	14				
III.	F + C_2H_3–Cl	1.2×10^5	25	No	Statistical	$>5 \times 10^{-12}$	Statistical
	F + C_2H_3–Br	4×10^6	40				
IV.	F + C_6H_5–Cl	2.3×10^9	25	No	Statistical	$>5 \times 10^{-12}$	Statistical
	F + C_6H_5–Br	1.0×10^{12}	40				

[a] Number of vibrational states in a 1 cm^{-1} wavenumber interval. [b] Average product internal energy = (available energy) − (average recoil energy).

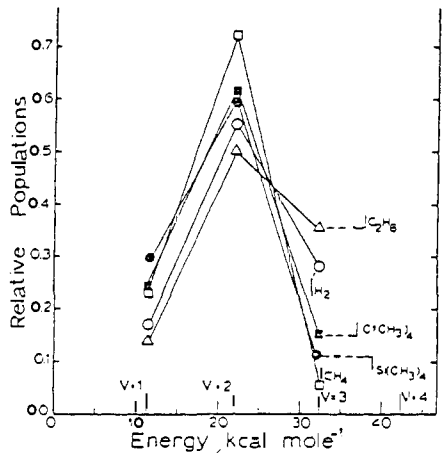

Figure 9. Relative vibrational populations from F + RH → HF(v') + R. Abstracted from D. W. Setser and H. W. Chang, *J. Chem. Phys.*, **58**, 2298 (1973).

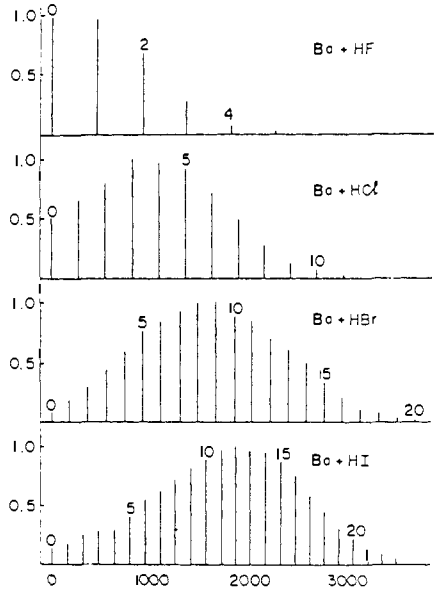

Figure 10. Distribution of BaX vibrational states from Ba + HX → BaX(v') + H (ref 158a).

energy distributions in various substituted olefinic and aromatic compounds with those which would be obtained had the products exhibited statistical partitioning of energy. Nonstatistical distributions were found only for the olefinic substrates, in which F replaced H or CH_3. For displaced Cl, Br, and for all the aromatic substrates, statistical vibrational distributions were generated; see Table VII.

Farrar and Lee[155] examined the production of chemically activated $C_2H_4F^‡$ in crossed beams of ethylene and F atoms. From the observed symmetric angular distribution of product species they concluded that the addition complexes had lifetimes of several rotational periods, and from the recoil velocity distributions deduced that ≈50% of the total available energy appeared in rke of the product species (H + H_2C=CHF). Similar results were obtained for

$$F + C_4H_8 \rightarrow \begin{cases} C_4H_7F + H \\ C_3H_5F + CH_3 \end{cases}$$

The latter case is of particular interest, for if one considers the products of the decomposition of the nascent $C_3H_8F^‡$ there is sufficiently rapid redistribution of energy for the weaker bonds to break even through they are far removed from the site of initial excitation; however, recoil energies were found to be much higher than those predicted had statistical redistribution occurred during the lifetime of the transient complex.

Chlorine and bromine substitutions in four vinyl bromides showed both statistical and nonstatistical behavior.[156] These reactions have large cross sections, 20–35 Å; the product translational energy distribution for (Cl + H_2C=$CHCH_2Br$ → $ClCH_2CH$=CH_2 + Br) was markedly nonstatistical. In three other cases (quoted in ref 154 and 155) the populations in one par-

TABLE VIII. Cross Sections and Energy Disposal[158a]

Reaction	Exoergicity, eV	$\langle E_v \rangle$/eV	$\langle E_J \rangle$/eV	$\langle f_v \rangle$	$\langle f_J \rangle$	$\langle f_{tr} \rangle$	Rel σ (scatt chamber)
Ba + HF	0.55	0.06	0.07	0.12	0.13	0.75	0.12
Ba + HCl	0.48	0.13	0.09	0.28	0.18	0.54	0.60
Ba + DCl	0.42	0.12	0.09	0.29	0.20	0.51	0.40
Ba + HBr	0.61	0.22		0.36			(1.00)
Ba + HI	1.26	0.22		0.18			0.67

ticular vibrational mode of the products appear to be highly enhanced.

There are several interesting interhalogen *displacement* reactions which are exoergic; these were investigated in crossed molecular beams.[155b,157] From velocity analysis it appears that the exothermicity is largely channeled into vibrational excitation. Two of the cases studied [Cl + Br_2; Br + I_2] have modest exoergicities. Experiments with F as the attacking atom would illustrate the effect of mass and the larger exoergicity.

Another sequence of *abstraction* reactions, where the attacking atom is an alkali or an alkaline earth metal, was studied by recording the intensity of scattered metal atoms by the halogens, halogen acids, and alkyl halides. Reference to the lower half of Table III provides estimates of the large exoergicities which are involved. A detailed analysis of product state distributions from the reaction Ba + HX → $BaX^{\dagger}$ + H was presented by Zare and co-workers;[158] it is illustrated in Figure 10. The observed disposal of exothermicity is summarized in Table VIII. Less detailed data on energy partition in the alkali metal bromides of K, Rb, Cs (M + Br_2 → $MBr^{\dagger}$ + Br) were mentioned in the previous section; between 81 and 90% of the available energy appears as vibrational excitation. For the reactions HF (v = 1–5) + Na → NaF + H, and HCl (v = 1–4) + Na → NaCl + H, Blackwell et al.[159] found a strong dependence of the rate on the vibrational state of the reagent for excitation above the threshold (the corresponding ΔE_0's are +13.5 and +6.2). This is indicative of a potential energy surface with the crest in the exit valley. Pasternack and Dagdigian[160] reported their preliminary studies of the reaction between M + BrCN (M = Ca, Sr, Ba). They also used laser-induced fluorescence to analyze the product states. The dominant pathway is the production of the monocyanide, with relatively little (or none) of the bromide. The fluorescence lifetimes of the MCN's were determined but not the partition of exothermicity. Schmidt et al.[161] studied the abstraction of Cl atoms from CCl_4 by Ba (→ $BaCl^{\dagger}$ + CCl_3) in a crossed beam experiment. Energy disposal of the product species was determined from the intensity of laser-induced fluorescence. The fraction of exothermicity which appeared in vibration was 0.75 ± 0.3, in rotation 0.04 ± 0.02. The vibrational state populations in the BaCl is narrow, with the maximum appearing at v = 43. In the reaction Ba + CF_3I → BaI^{+} + CF_3, the vibrational state distribution is bimodal, with peaks at $v \approx 27$ and 47. Two reaction paths are indicated.[311] Finally, Behrens and co-workers[162] found from recoil velocity spectra of products from crossed beams of Li with $SnCl_4$, PCl_3, and SF_6, that the reaction proceeded through a long-lived complex, with energy equipartitioning in a loose transition state.

2. Elimination Reactions

Highly energized alkyl halides (molecules or radicals) have been prepared via half a dozen routes. When sufficiently excited the substrates dehydrohalogenate, either through a three-center (α–α) or a four-center (α–β) transition state. The results of early kinetic investigations of (α–β) eliminations which were thermally induced are accounted for by RRKM theory. The objective of several recent studies was to establish empirical procedures for estimating activation energies; these are well documented[163] as are the experimental excursions to the high-temperature range utilizing shock tube techniques. In the present context, the significant questions revolve around the partition of the product olefins between cis and trans structures, the distribution of energy between the eliminated HX and the organic residue, and the disposal of excitation energy within each of the products.

Consider first (α–α) eliminations. In variously substituted ethanes this channel competes with the (α–β) channel when the threshold for the former is lowered by 1,1-dihalogen substitution. Then the nascent organic residue is a carbene, which rearranges preferentially to a cis olefin. The case of 1,1,2-trifluoroethane was analyzed in detail by Holmes et al.[164] The highly energized ethane resulted from the recombination of CH_2F with CDF_2 radicals which were generated during photolysis of mixtures of 1,3-difluoroacetone and 1,1,3,3-tetrafluoroacetone-d_2.

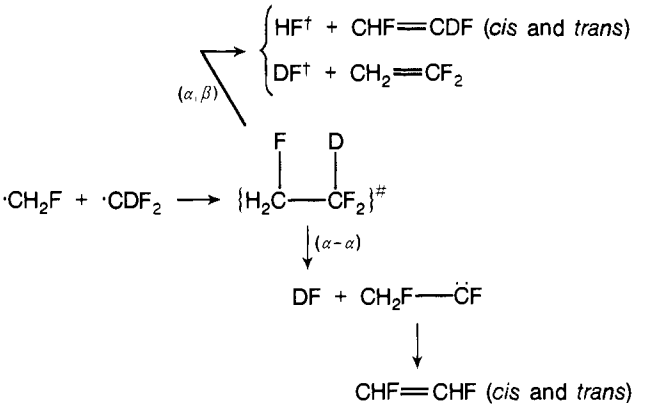

It appears that 78% of the available energy (which is 77 kcal/mol) is released in the olefin fragment for the (α–α) channel. In $\{CH_2Cl\text{–}CDCl_2\}^{\#}$ the internal energy distribution appears to be consistent with statistical partitioning of the excess energy. These disposal patterns contrast with (α–β) eliminations wherein the energy is channeled into translation and rotation of the products, and into vibrational energy of the $HX^{\dagger}$.

Holmes and Setser[165] estimated the redistribution of energy in the products resulting from the insertion of $^1CH_2$ into a C–H bond in chlorocyclobutane, followed by a four-center HCl elimination. If not collisionally stabilized the three highly excited methylchlorocyclobutanes (≈109 kcal/mol) undergo ring rupture to produce ethylene and propylene, or eliminate HCl to generate vibrationally excited methylcyclobutane. The latter is sufficiently energized to isomerize into substituted pentadienes. From the observed product distribution, the known activation energy for HCl elimination, and the reported fraction of available energy which appears as vibration in the ejected HX, these authors concluded that ≈30% of the total energy appears as *rke* or as rotational energy of the products; i.e., ≈57% is retained in the olefin fragment.

Gleaves and McDonald[166] recorded the infrared chemiluminescence from chemically activated halocarbonyls generated by $O(^3P)$ addition to the corresponding olefins. In the two cases

studied the elimination site is displaced from the newly formed bonds by one and three C–C bonds, respectively. They found that the vibrational state distribution of the ejected $HCl^{\dagger}$ was the same when oxygen was added either to 3-chlorocyclohexene or to 5-chloro-1-pentene. This indicated that the excess energy in the adduct was randomized in a time less than is required for reaccumulation of the activation energy at the four-center elimination site, independent of the molecular geometries. However, the $HCl^{(v)}$ distribution is highly nonstatistical ($N_2 > N_1$): the relative populations ($N_2 = 1$) are $N_1 = 0.83$; 0.94; $N_3 = 0.60$; $N_4 = 0.20$; $N_5 = 0.05$.

The addition or insertion of $O(^3P)$ atoms followed by $HF^{\dagger}$ (four-center) eliminations was also reported by Lin.[167] CHF and HCF_2 radicals were produced by successive photodetachment of Cl atoms from $HCFCl_2$ or HCF_2Cl (or of bromine atoms from $HCFBr_2$). Then, insertion following by elimination produced HF lasers.

$$O(^3P) + \begin{cases} CHF \rightarrow \{HFCO\}^{\#} \rightarrow HF^{\dagger} + CO \\ CHF_2 \rightarrow \{HF_2CO\}^{\#} \rightarrow HF^{\dagger} + FCO \end{cases}$$

$$\Delta H^{\circ} = -181 \text{ kcal/mol}$$

$$\Delta H^{\circ} = -103 \text{ kcal/mol}$$

The vibrational energy distributions in nascent $HF^{\dagger}$ from $CH_3CF_3^{\#}$ [$\leftarrow CF_3 + CH_3$] and from $CH_2CF_2^{\#}$ [$\leftarrow CH_2CF_2 + Hg^*(6^3P_1)$] were studied by Clough et al.[168] in a fast flow system. From the chemiactivated $CH_3CF_3^{\#}$, the elimination of $HF^{(v)}$ with $v = 1 \rightarrow 4$ was observed. The upper value corresponds closely to the activation energy for the reverse step: $CH_2CF_2 + HF \rightarrow CH_3CF_3^{\#}$. Thus, it appears that of the 72 kcal/mol which the radical pair, $H_3C\cdot\cdot CF_3$, incorporates (measured from $CH_2CF_2 + HF$ level), 30 kcal was statistically distributed prior to the $HF^{\dagger}$ elimination. They found that $\kappa(v)/\kappa(v = 1) = 0.43$ for $v = 2$, 0.13 for $v = 3$, 0.033 for $v = 4$. Analysis of the energy partition in $CH_2CF_2^{\#}$ produced by the ϵ–ϵ transfer from $Hg(6^3P_1)$ rests on the assumption that all of the 112 kcal ($^3P_1$–$^1S_0$) was transferred to electronic plus vibrational energy of the olefin. The observed relative rates of production of the excited $HF^{(v)}$ are $\kappa(v)/\kappa(v = 1) = 0.40$ for $v = 2$, 0.21 for $v = 3$, and 0.072 for $v = 4$. Here also, the distribution is accounted for by assuming that the vibrational excitation is a consequence of energy release during the displacement of $HF^{\dagger}$ from the HC≡CF residue.

Hydrogen or deuterium fluoride elimination lasers from highly energized species, produced by radical recombination, were first reported by Pimentel and co-workers;[169] stimulated emissions were recorded for $v = 1 \rightarrow 0$ and $v = 2 \rightarrow 1$, but no $v = 3 \rightarrow 2$ was detected. Also, HF, HCl, HBr laser emissions were observed upon photoexcitation of a variety of substituted olefins; these were summarized by Berry.[139d] The experimental observations suggest the sequence: selective excitation of the substituted olefin to a vibronic state, $^1(\pi,\pi^*)$, which rapidly decays ($\approx 10^{-13}$ s) by direct predissociation to products in their ground electronic state. However, the populations of $HX^{(v)}$ are nonstatistical (i.e., they are inverted).

It is worth noting that chemically activated fluoroalkanes can be prepared via chain fluorination[170]

$$F_2 = 2F$$

$$F + C_2H_6 \longrightarrow HF^{\dagger} + C_2H_5$$

$$C_2H_5 + F_2 \longrightarrow C_2H_5F^{\#} + F$$

$$C_2H_5F^{\#} \longrightarrow C_2H_4 + HF^{\dagger}$$

The exothermicity of the last step is 69.4 kcal/mol; this is more than that required for HF elimination; i.e., a substantial part of the exothermicity of the addition of F to the ethyl radical is retained as vibrational energy in $C_2H_5F^{\#}$. The application of detailed balance arguments to the reverse (HX insertion) reaction suggests that laser augmented addition of $HX^{(v)}$ to substituted olefins should occur at or somewhat above room temperature.

3. Other Insertion and Elimination Reactions

The production of vibrationally excited diatoms in highly exothermic reactions was first demonstrated by Norrish and co-workers in the mid-1950's and reviewed by Basco and Norrish[171]

$$XO_2 \xrightarrow[(h\nu)]{UV} XO + O \ (X \equiv Cl, N, O)$$

$$O + XO_2 \rightarrow O_2^{(v)} + XO, \text{ etc.}$$

Here attention is directed to the recent experiments wherein it was demonstrated that highly nonstatistical vibrational state populations were produced in many cases, sufficient to initiate stimulated emission of characteristic radiations. Perhaps the most dramatic case is the attack of CS_2 by oxygen atoms. The initial stripping of one sulfur atom ($\rightarrow CS + SO$) is followed by $CS + O \rightarrow CO^{\dagger} + S$ ($\Delta H^{\circ} = -85.1$ kcal mol^{-1}), generating a high level of vibrational excitation in the carbon monoxide. Emissions from $v = 18$ have been observed, and a low-pressure flame laser has been demonstrated.[172] The maximum population of $CO^{(v)}$ appears at $v = 12$. However, there is substantial disagreement among several investigators as to the relative nascent populations in the $v \leqq 6$ range. Kelly[173] suggested that these differences can be reconciled if one assumes that the various experimental configurations produced differing contributions of excited CO via: $CS_2 \rightarrow CO^{\dagger} + S_2$. Hudgens et al.[174] studied in a molecular beam experiment the reaction between $O(^3P)$ and CS_2 and CS, utilizing the technique of arrested relaxation of infrared chemiluminescence. Indeed, they found that the reaction proposed by Kelly does generate vibrationally excited CO. A similar but considerably less efficient laser can be made utilizing the reaction between oxygen atoms and C_3O_2.[175] A partially inverted CO population is probably generated by:

$$C_3O_2 \xrightarrow{\text{discharge}} C_2O + CO$$

$$O_2 \xrightarrow{\text{discharge}} 2O$$

$$C_2O + O \rightarrow CO^{\dagger} + CO \quad \Delta H^{\circ} = -160 \text{ kcal/mol}$$

Stricker and Bauer found that the net low gain is due to absorption (within the lasing medium) of CO radiation by the C_2O and C_3O_2 species. In the spin-forbidden reaction

$$O(^3P) + C_3O_2(^1\Sigma_g^+) \rightarrow 3CO(X^1\Sigma^+) \quad \Delta H^{\circ} = -115 \text{ kcal/mol}$$

the three CO's leave with about 16% of the total available energy, in a near-statistical population distribution.[176] A list of other reactions which lead to inverted or partially inverted CO populations is given in Table IX, assembled by Lin.[177] In the attack of COS by $O(^3P)$ and $O(^1D)$ Shortridge and Lin[178] found that of the total available energy only 11% for ^3P and 4% for ^1D are channeled into vibration of the CO; the maximum population appears in the $v = 0$ state.

A very interesting application of a carefully controlled CO probe laser permitted Lin and co-workers to diagnose the dynamics of the reaction of $O(^3P)$ atoms with allene, methylacetylene, and 1-(2-)butyne.[179] With allene, the $CO^{(v)}$ generated has a vibrational temperature of 5100 ± 100 K, compared to 2400 ± 200 K for that from methylacetylene. The mean vibrational energy contents of the $CO^{\dagger}$ were found to be 6.8, 2.3, 1.0, and 1.1 kcal/mol, respectively, in good agreement with predictions based on a statistical model; i.e., the energy appears to be randomized in the transition states. The distribution of $CO^{\dagger}$ resulting from the two reactions:

TABLE IX. Chemiexcitation of CO and HF Lasers[177] [a]

Pumping process	$-\Delta H^\circ$, kcal/mol	Transitions (Δv)
I. Bimolecular reactions		
a. $O(^3P) + CS \rightarrow CO + S$	85	(14,13) → (3,2)
$O(^1D) + CN \rightarrow CO + N(^2D)$	64	(13,12) → (5,4)
$O(^3P) + CN \rightarrow CO + N(^4S)$	74	(13,12) → (5,4)
$O(^3P) + CH \rightarrow CO + H$	176	(18,17) → (3,2)
$O(^3P) + CSe \rightarrow CO + Se$	118	(18,17) → (7,6)
$O(^3P) + CF \rightarrow CO + F$	129	(14,13) → (2,1)
b. $O(^3P) + C_3O_2 \rightarrow 3CO$	115	(11,10) → (7,6)
$O(^1D) + C_3O_2 \rightarrow 3CO$	160	(13,12) → (5,4)
$O(^3P) + C_2H_2 \rightarrow 2CO + 2H$	122	(13,12) → (12,11)
$O(^3P) + CH_2 \rightarrow CO + 2H$	75	(9,8) → (5,4)
$CH + O_2 \rightarrow CO + OH$	159	(14,13) → (2,1)
$CH + NO \rightarrow CO + NH$	105	(6,5) → (3,2)
c. $O + CHF \rightarrow HF + CO$	181	
$O + CHF_2 \rightarrow HF + FCO$	103	
$O + CH_2F \rightarrow HF + HCO$	114	
II. Photodissociation reactions		
$OCS + h\nu\ (\lambda \geq 165\ nm) \rightarrow CO + S$		(13,12) → (7,6)
$CH_2CO + h\nu\ (\lambda \geq 165\ nm) \rightarrow CO + CH_2$		(8,7) → (4,3)

[a] M. C. Lin, *Int. J. Chem. Kinet.*, **5**, 173 (1973).

$$^{(1,3)}CH_2 + O_2 \xrightarrow{(1)} \cdots\cdots \rightarrow HCOOH^\dagger \rightarrow CO^{(v)} + H_2O$$

$$CH_2 + CO_2 \xrightarrow{(2)} \left[H_2C\!-\!C(=O)\!-\!O \text{ (cyclic)} \right] \rightarrow CO^{(w)} + H_2CO$$

was investigated by Hsu and Lin,[180] who found values for $v \leq 13$ and $w \leq 4$. In reaction 2 the vibrational population was close to that expected for randomization in the $[H_2COCO]$ long-lived intermediate. A similar calculation for (1) predicted a hotter distribution than that observed, suggesting that it is produced via several channels. The addition of $O(^3P)$ to cyclooctene[181] produces a biradical intermediate, with 20–40 kcal/mol of vibrational energy. Intersystem crossing ($T_1 \rightarrow S_0$) and a very rapid internal H-atom transfer generate cyclooctanone with 118 kcal of excitation, but with an estimated lifetime of ≈65 s. From its IR emission spectrum the authors concluded that in this large molecule all the vibrational modes (of widely different character) were populated according to their statistical weights.

Mixtures of H_2 and O_3 when flash photolyzed in a laser cavity emitted stimulated IR radiation, which was identified as P_1 transitions of $v = 3 \rightarrow 2$, $2 \rightarrow 1$ and $1 \rightarrow 0$ of $OH^{(v)}$.[182] There are two pumping reactions:

$$O(^1D) + H_2 \rightarrow H + OH^\dagger \text{ and } H + O_3 \rightarrow OH^\dagger + O_2$$

Jensen[183] summarized the current status of IR laser emissions derived from metal–atom oxidation reactions. The metallic vapors were generated by exploding wires in atmospheres of the oxidizers $[O_2, F_2, NF_3]$.

The final citation pertains to the vibrational energy distribution produced in NO during the reaction of $N(^4S)$ with molecular oxygen.[184] Upon correcting for the v–v quenching of the nascent population of $NO^\dagger$ by the excess O_2, the authors concluded that 24% of the NO molecules were produced in level $v = 2$ (which degraded to $v = 2 \leftrightarrow 7$); the nascent populations in $v = 3 \rightarrow 7$ were respectively 16, 25, 23, 70, and 5%.

4. *Photodissociation and Recombination Reactions*

It is not surprising that products of molecular fragmentation are often generated with substantial energy content when dissociation is a consequence of excitation to an electronic state which is well above a bond dissociation energy. The series XCN (X = Cl, Br, I, CN) is a current favorite. The state distributions of the product CN ($X^2\Sigma^+$) were determined from its laser-induced fluorescence spectra.[185] Of special interest in the present context are the results reported by Kawasaki et al.[186] on the partition of energy in the photodissociation of molecular beams of four aryl halides. The average translational energy of the fragments ranged from 17.4 to 11 kcal/mol and was independent of the frequency of the light absorbed. The authors propose that the electronic but not the vibrational energy was transferred to the carbon–halogen bond, and that 5–10 vibrational quanta were excited in the aromatic rings by the repulsive force of the departing halogen atoms.

The vibrational energy content of $HCl^\dagger$ produced by photoelimination from various chloroethylenes is highly nonstatistical; indeed, flash-photolyzed mixtures of chloroethylene and argon (1/100 at 50 Torr) with $\lambda > 1550$ Å are lasing media.[139d,197] Dissociation of CF_2Cl_2 and CF_2Br_2 can be induced by short duration pulses of a focused CO_2 laser beam. Under collision-free conditions the $CF_2(X)$ fragments were found to be vibrationally excited.[188] Their state distributions, as measured by recording the UV laser excited fluorescence spectra, correspond to vibrational temperatures 790 K for CF_2Br_2 and 1050 K for CF_2Cl_2.

A number of atom–atom and atom–diatom recombination reactions (assisted by a third body) were observed to generate association products in excited vibrational states, as anticipated in all formulations of diatom recombination theory. Chen and co-workers[189] recently found a case where the exoergicity (~15 kcal/mol) was channeled into the chaperone molecule:

$$F + O_2 + HF \rightarrow FO_2 + HF(v = 1)$$

Finally, in the associative electron detachment reaction

$$O^- + CO \rightarrow CO_2^\dagger + e^-$$

Bierbaum et al.[190] confirmed that most of the exothermicity (≈92 kcal/mol) remained in the molecular product (as suggested by the low translational energies observed for e^-) by recording strong IR emissions at 4.3 μm, when they injected CO into a stream carrying O^- ions.

E. IR Laser-Induced Reactions

1. *On Distinguishing Vibration-Specific from Thermal Effects*

The current development of state-specific analytical techniques, in which lasers and electronic data processing procedures are playing dominant roles, have opened new vistas to kineticists in their exploration of nascent population distributions. The experimental results show that many "simple reactions" generate a wide range of distributions; for a significant fraction the nascent products are not partitioned statistically. It is plausible to postulate that in an exoergic reaction the nascent P# distribution reflects that present in the T states, which in turn reflects the distribution in the R# states. Detailed balance considerations provide a parallel argument for the reverse process (endoergic). In the following paragraphs we have briefly summarized the reported experiments in which selectively excited vibrational states were utilized.

Consider first the challenge which well-designed experiments must meet. Suppose a procedure is available for selectively exciting a particular mode in one of the reactants of a bimolecular process to a high overtone vibration. [This is not a trivial task, even when precisely tuned high-powered lasers are available, because the everpresent vibrational anharmonicity takes the absorbing species out of resonance. But it can also be achieved in a variety of other ways: by controlled electron impact; by excitation to a higher electronic state and relaxation to high vibrational levels in the ground state; by prereaction which generates species in excited vibrational state, etc.] One must now measure the reactive cross sections for a sample thus

prepared, and compare it with those of a sample in complete statistical equilibrium at the temperature which characterizes the translational and rotational degrees of motion. At this point there appear both practical and conceptual problems. First, such an experiment must be performed under conditions where the half-time for reaction ($\approx\tau_\ell$ or $1/k[X]$) is significantly less than that for v–R–T equilibration ($\tau_{i\to j}$). Otherwise, the energy injected into vibrations will merely raise the temperature of the mixture and the augmented rate will be a consequence of thermal heating. This can be managed by careful experimental design, i.e., perform the reaction at low pressures, use diluents which transfer energy to the walls as rapidly as vibrationally energy is absorbed by the reactant, etc. Every kineticist is also aware that careful design is required to minimize confusion of the primary step, which may be selectively augmented, with subsequent steps in chain reactions, and to correct for heterogeneous effects produced at the walls and by reactive impurities. Obviously, experiments with molecular beams under "single collision" conditions are inherently free from these limitations.

Second, were the reaction rate accelerated by vibrational excitation exactly to the extent which would be accomplished by the same amount of energy injected into rotation and/or translation, the experiment would demonstrate that a *single* energy pool provides an adequate description of the process; i.e., all regions of phase space in E layers, at and above E*, are strongly coupled. It is therefore necessary to *compare* the relative cross sections for various modes of energy injection, not merely to demonstrate that laser irradiation augments rates. In turn this raises the next question: if the intramolecular redistribution time (τ_r) is comparable or somewhat slower than the reaction half-time, then a full description requires the use of several vibrational energy pools, each associated with a specific mode.

During the past decade many papers appeared wherein the authors claim to have demonstrated *vibrationally enhanced* reaction rates induced by absorption of IR radiation. If their sole evidence was that their derived product distribution (in complex reactions) differed in some measure from what was obtained under strictly thermal conditions, the argument is invalid. Product distributions generated by complex mechanisms depend sensitively on the presence of heterogeneous components, and on the temperature profile in the reactor, both spatial and temporal. With laser radiation this is rarely known even with modest precision. The following is a partial list of sufficient (but not necessary) criteria for proposing that specific vibrational excitation was effective: (a) demonstrate isotopic specificity; (b) demonstrate conversion of only *one* component (the absorbing species), in a mixture in which other species can undergo parallel reactions with closely equal activation energies under thermal conditions; (c) suppose a reactant (or a pair of reactants) follows two or more reaction paths with different rates (if specific vibrational excitation, corrected for different *high power* absorption coefficients, accelerate the two routes by different amounts, it follows that specificity of excitation had been retained); (d) drive the system out of equilibrium, in a direction opposed to that which it would follow due to a rise in temperature; (e) time resolve the production of reaction products with a resolution comparable to the mean collision time, and demonstrated these differ from thermally driven cases. (f) For reactions driven by *single* photon absorption, substantially different augmented rates developed by different portions of a single absorption band (corrected for absorption coefficient) indicate specificity. This criterion breaks down for multiple photon absorption since the mean high power absorption coefficients can differ substantially for closely adjacent spectral intervals.

Obviously the demonstration of enhancement of vibrational excitation is more direct for diatomic and triatomic species than for polyatomic reactants. In the following selected summary, references to "strange" results which were obtained under thermal or mixed thermal-vibration-specific conditions are not included.[312] The reader is directed to several reviews: Berry;[191] Birely and Lyman;[192] Aldridge et al.;[193] Kimel and Speiser;[194] Smith;[195] and Wolfrum.[196] First let us dispose of two interesting reports which involve electronic as well as vibrational excitation for simple molecules. The data reported by Whitson et al.[184] on the reaction $N(^4S) + O_2 \rightarrow NO(v = 2\rightarrow 7) + O$ were mentioned in the preceding section. Electronically excited NO_2 oxidizes CO at room temperature;[197] the relative photoaugmented bimolecular rate constants increased by a factor of 10 when the irradiating wavelength was changed from 600 to 450 nm. The rate constant under thermal excitation is[198]

$$k_b = 10^{12.1} \exp(-27\,600/RT)\ \text{mol}^{-1}\ \text{cm}^3\ \text{s}^{-1} \text{ for } T > 1000\ \text{K}$$

$$= 10^{11.8} \exp(-27\,700/RT)\ \text{mol}^{-1}\ \text{cm}^3\ \text{s}^{-1} \quad \text{for low } T\text{'s}$$

Attempts by Karl and Bauer (1974, unpublished) to induce this reaction at room temperature by irradiating mixtures of NO_2 + CO with a cw HF laser (≈200 mW absorbed by ≈5 Torr equimolar NO_2/CO) were not successful.

Balykin et al.[199] utilized Ar^+ ion laser coincidences with I_2, to study selected ortho–para conversions. The former absorbs the 514.5 nm line while the latter absorbs 501.7 nm. They found irradiation conditions under which photopredissociation of the ortho molecule generated atoms (quantum yield from the $B^3\Pi_{o+u}$ state was $\approx 10^{-5}$) which associated with a para molecule to generate transient I_3 complexes. Dissociation, with equal probability, to the ortho and para forms led to a net conversion of the latter to the former. In the presence of 2-hexene, the (electronically) selectively excited I_2 molecules, either the ortho or para forms, added directly via a bimolecular process, while the unexcited species did not, thus leaving substantially enhanced mole fractions of the unexcited form. This contrasts with the thermally induced addition, which follows a radical chain mechanism, so that no selectivity can be established.

2. Excited Diatoms

Table X is a partial list of reported infrared laser augmented reactions of diatomic reagents. Since these have have been extensively discussed during the past two years brief comments on several reactions (in sequence, as listed) will suffice. In many of these experiments the diagnostic was the infrared fluorescence of the excited diatom. Its decay is a consequence of many factors, of which the reaction of interest is only one; hence, consider in addition to the indicated reaction, v–R–T quenching, diffusion, reactions with impurities, and reaction (heterogeneously) on the cell walls. Failure to unscramble these factors in every case led to ambiguous estimates of the augmentation factors.

The metathesis reaction $H_2^{(v)} + D_2 = 2HD$ (and by symmetry, $D_2^{(v)} + H_2 = 2HD$) differs from the others in the first group in several important respects.[203] The measured activation energy (shock tube technique[203b]) for the thermal reaction is about 40 kcal/mol. However, via stimulated Raman excitation of H_2[1] and subsequent "ladder climbing" to $v \geq 4$, which can undergo an exchange reaction, a sufficient population is developed to generate detectable HD (mass spectrum), even though the translational and rotational distributions remain at room temperature. The fact that all theoretical calculations of potential energy surfaces for 4 H atoms, for selected T structures, show barriers above 110 kcal/mol poses a dilemma which awaits resolution. In the laser-induced exchange, $HF^{(v)} + D_2 \rightleftarrows HD + HF$,[210] the reaction mixture could not be maintained at room temperature; indeed, in the illuminated core of the reaction cell temperatures in the range of 1100–1300 K were generated. Careful unfolding of the extent of conversion as affected by laser power, total pressure, and composition led to a classical rate

TABLE X. Laser Augmented Reaction Rates (Diatomics)

Excited Species	Reagent	Product	ΔH°_{300} (kcal/mol)	$k_{thermal}$ Log A	$k_{thermal}$ E_a	Comments	Ref
$H_2^{(v)}$	H′	HH′	0		7.6	$\kappa(1)/\kappa(0) \sim 1.5 \times 10^3$	200
[$E_{v=1}$	F	HF†	−32.6		2.1	E_{trans} more effective than E_{vib}	
11.9 kcal]	Cl	HCl	+1.2		5.5	$\kappa(1)/\kappa(0) \sim 40$ (interp. not clear-cut)	201
	Br	HBr	+16.7		19.7	$\kappa(1)/\kappa(0) \sim 7 \times 10^2$	
	O	OH	+1.9	−10.57	9.4	Negative results suggest E_v not effective; sensitivity ≈50%	202
	D_2	2HD		−10.5	≈40	Exchange measurable for $v \geq 4$	203
$OH^{(v)}$	O	O_2	−16.6			$\kappa(1)/\kappa(0) \approx 2$–3	204,205
[$E_{v=1}$	Cl	HCl†	−0.9			Reagent vibration is preferentially channeled into product vibration	206
10.2 kcal]	H_2	H_2O	−14.7		5.1	$\{\kappa(2); \kappa(1)\}/\kappa(0) \leq 2$	205
	HBr	H_2O	−31.0		≤0.8	$\kappa(1)/\kappa(0) = 9$	204
	CO	CO_2	−18.5		(0 → 8)	Augmentation suggested, but not clear-cut	205
	CH_4	H_2O	−14.7		3.4	$\kappa(1)/\kappa(0) \leq 4$	205
	O_3	$HO_2 + O_2$	−38.0			$\kappa(9)/\kappa(0) \approx 10^3$	207
		$H + 2O_2$	+8.7			$\kappa(4)/\kappa(0) \approx 10^{2.7}$	208
		$OH + O_2 + O$	+25.4				
$HF^{(v)}$	H	H_2	+32.4			$\kappa(1)/\kappa(0) = 5 \times 10^6$; $\kappa(3)/\kappa(2) = 3 \times 10^6$	209
[$E_{v=1}$	Cl,Br	HCl,HBr				Enhanced rates for vib excitation ($v = 1 \rightarrow 6$)	146
8.3 kcal]	D_2	DF + HD				Equipartition best accounts for data	210
	Na	NaF	+13.5			Substantial enhancement ($v = 1 \rightarrow 5$)	159
	Ba	BaF†				Product retains 64% of reactant E_v	158b
$HCl^{(v)}$	H′	H′Cl	0		>20		150
[$E_{v=1}$		H′H	−1.1	−10.8	3.5	$\kappa(1)/\kappa(0) \approx 1$	211;212
8.2 kcal]	D_2	DCl + HD			8	No exchange obsd for HCl ($v = 6$)	213
	F	HF†	−32.7		1.0	E_{trans} more effective than E_{vib}; v enhances rate (ΔE_v reactants channels into ΔE_v product)	214
	Cl′	HCl′	0	6.6		Exchange vs. deexcitation have not been unscrambled	215
	Br	HBr	+15.18		>16	$\kappa(2)/\kappa(0) \approx 10^{10}$; ^{35}Cl selective; $\kappa(4)/\kappa(2) \simeq 10$	216
	O	OH	+0.9	−11.1	6.3	$\kappa(3)/\kappa(2) = 3.6$ $\kappa(1)/\kappa(0) = 300 \pm 100$	217
	Na	NaCl	+6.2			Substantial enhancement ($v = 1 \rightarrow 4$)	159
	K	KCl	+0.96			$\kappa(1)/\kappa(0) \approx 100$ [E_v approx. 10× more effective E_{tr}]	218
	C_4H_8	$(CH_3)_3CCl$				HCl ($v = 6$) add at room temperature	219
$HBr^{(v)}$	Br′	HBr′	0			Quasi-classical Monte Carlo calculations	220
	H	H_2				Vib excitation enhance both abstraction and exchange	
	I	HI	+16.2			$\kappa(2 + 3)/\kappa(0 + 1) \simeq 10^9$	221
$CN^{(v)}$	$O(^3P)$	$CO^\dagger + N(^4S)$	−73.9			Cross section slightly increases with v = 1–6	222
		$CO^\dagger + N(^2D)$	−18.7			Cross section decreases with v	
	$O_2(^3\Sigma^-)$	NCO	−4			$\kappa(v + 1)/\kappa(v) = 0.8$ for $0 < v < 7$	222
	CH_4	$HCN + CH_3$	−15.2	−11	1.7	$\kappa(1\text{–}4)/\kappa(0) \approx 2.3$	223
	C_2H_2	products			≈0	$\kappa(1\text{–}4)/\kappa(0) \simeq 2$	223
	C_2H_4					$\kappa(1\text{–}5)/\kappa(0) \simeq 5$	
$CO^{(v)}$	S	CS	+80.5			$\kappa(v + 1)/\kappa(v) \approx 10^4$ for $6 < v < 14$	224
$NO^{(v)}$	O_3	$NO_2(^2B)$				$\kappa(1)/\kappa(0) = 5.7$	225
		$NO_2(^2A_1)$	−47.7			$\kappa(1) > \kappa(0)$; independent $\kappa(1)$ cannot be extracted	

expression for a reaction with four active square terms:

$$d[HD]/dt = k^\ddagger[HF]_0[D_2]_0$$

$$k^\ddagger = Z(E^*/RT)^{s-1}\Gamma^{-1}(s)\exp(-E^*/RT)$$

with $s \approx 2$, $E^* \approx 55$ kcal/mol; Γ (gamma function).

The dependence of product state distribution on the extent of excitation of the reagent, in

$$OH\ (v \leq 9) + Cl = O + HCl(v' \leq 11)$$

was investigated by Blackwell, Polanyi, and Sloan.[206] With the prereaction, $H + O_3 \rightarrow OH(v = 6\text{–}9) + O_2$, high v levels were populated; using $H + NO_2 \rightarrow OH(v = 1\text{–}3) + NO$, the OH† was produced in low vibrational levels. The course of reaction with chlorine atoms was ascertained from the depletion of OH† chemiluminescence, and the corresponding growth of emission from HCl†. Their data demonstrated that vibrational excitation of the reagent was *preferentially* converted to vibrational excitation of the product (Figure 11).

Between $HCl^{(v)}$ and H three processes can occur: v–R–T re-

TABLE XI. IR Laser Augmented Reaction Rates (Small Polyatomics)

Excited Species	Reagent	Products	$\Delta H°_{300}$, kcal/mol	$k_{thermal}$ Log A	E_a	Augmented rates Comments	Ref
$O_3^\dagger$ (001)	$O_2(^1\Delta_g)$	$2O_2 + O$	1.4			$k(001)/k(000) = 38$	228
	$NO(X^2\Pi)$	$NO_2(\bar{B}^2B_2)$				$k(001)/k(000) = 5.6$	228,229
	NO	$NO_2(\bar{A}^2B_1)$	−4.8	−12.15	2.33	$k(001)/k(000) = 5.6$	228
	NO	$NO_2(\bar{X}^2A_1)$	−47.6	−11.90	4.18	$k(001)/k(000)$ { 17.1 / 9.5	230
	$SO(X^3\Sigma_g^-)$	$SO_2(\bar{X}^1A_1)$	1−106.6	−11.60	2.1		
		$(\bar{a}^3B_1)$	−33.0	(−13.3)	3.9	$k(010)/k(000) = 2.5$	231
		$(\bar{A}^1B_1)$	−22.0	−12.77	4.2		
$N_2O(0n0)$	Ba	BaO				$\sigma(0n0)/\sigma(000) \sim 4$–5	233
	Sm	SmO				Vib enhanced for low rke only (<5 kcal/mol)	234
OCS	O	SO + CO				$k^\ddagger/k(0) \cong 1$	235
C_2H_4	O	CH_3 + CHO					
CH_3F	D	DF + CH_3	−26			No significant enhancement for ($2\nu_3$; ν_1; ν_4)	236
CH_3F	Cl_2	CH_2FCl + HCl	−23			Enhancement via	237
CH_3F	Br	CH_2F				Vibrational excitation	238
CH_3Br	Cl					indicated	239
N_2F_4		$2NF_2$	+20			Augmented dissociation rate	240

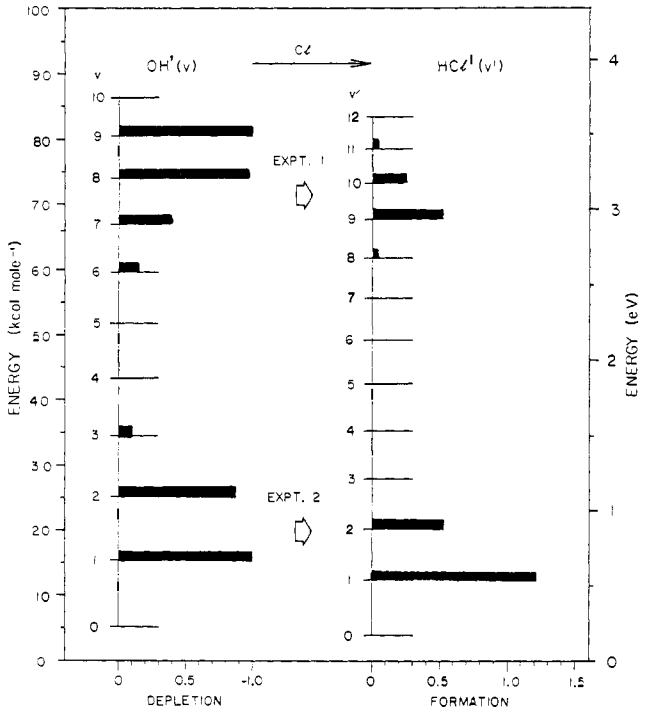

Figure 11. Correlation of vibrational energy distribution in the product with initial excitation of reactant: $OH^\dagger(v) + Cl \rightarrow O + HCl^\dagger(v')$.

laxation, at which the atomic species are particularly effective, H-atom abstraction, and H-atom exchange. Because of discrepancies between several experiments for the $v = 0$ state, and difficulty in unscrambling these processes, further study of this system is indicated.[150] The two papers by Brooks and coworkers[218a,b] are complementary. The abstraction step, K + HCl → KCl + H, is endoergic for the $v = 0$ state. With crossed molecular beams they demonstrated that excitation to ($v = 1$) increased the reactive cross section by about two orders of magnitude. Later they investigated the dependence of the cross section on the *rke* of the colliding pair, covering the range 2.1–12.1 kcal/mol (center of mass coordinates). It was evident that an equivalent amount of translational energy was not as effective as vibrational excitation for accelerating this reaction. In their analysis, the authors were careful to decouple the statistical from the dynamical factors.

Vibrationally excited $CN(X^2\Sigma^+, v)$ was produced by photolyzing C_2N_2, and their state distribution monitored by time-resolved infrared laser absorption spectroscopy.[222] In spite of the fact that a single vibrational quantum exceeds the reported activation energy for attack by oxygen atoms, excitation to $v \leqq 6$ has little effect on the rate constant. At $v = 7$, a second channel is opened: $O(^3P) + CN(X^2\Sigma^+, v = 7) \rightarrow C(^3P) + NO(^2\Pi)$ and the rate of disappearance of $CN^{(v=7)}$ exceeds that for $v = 6$. In contrast, the rate of reaction of CN[$v = 1 \rightarrow 7$] with O_2 *decreases* with increasing v. The last entry in Table X is of particular interest.[225] That vibrational excitation of the NO facilitates transfer of an oxygen atom from O_3 to the excited species was not generally anticipated; this suggests that the collision complex has a sufficiently long lifetime to permit energy transfer, but with a low probability since the augmentation factors are about equal for [$NO(v = 1) + O_3$] as for [$NO(v = 0) + O_3(001)$], while the energy content of the former is about twice that of the latter pair.

3. *Excited Small Polyatomics (Table XI)*

The discovery of the laser-augmented rate for ($O_3^\dagger$ + NO) by Gordon and Lin,[226] which they observed through the enhanced chemiluminescence of the ^2B states of NO_2, precipitated a flood of research activity which is still continuing. A concensus has been reached that all the vibrations of ozone are involved, not merely the initially excited (001), but there remain differences between investigators as to the detailed interpretation of the experimental observations. The dark reaction was investigated by Clough and Thrush.[227] Gordon and co-workers[232] recently determined the temperature dependence of the laser-induced chemiluminescence of $NO_2(^2B_{1,2})$ and found an "activation energy" which is 1.33 ± 0.10 kcal/mol less than that for the dark reaction (4.18 kcal/mol). That is, 44% of the vibrational content of the $O_3(001)$ was utilized in the activation process; the preexponential factor was essentially unaltered. However, Cool and Hui[229c] found that there was a small reduction in the preexponential factor, as well as a decrease in the effective activation energy due to laser excitation.

Wolfrum and Kneba[236] found no enhancement of the slow reaction D + $CH_3F \rightarrow$ DF + CH_3 upon vibrational excitation of the methyl fluoride ($\nu_1, \nu_4; 2\nu_3$), even though that state is above the activation barrier. Qualitatively, this is in agreement with calculations on model potential energy surfaces. In their study of the laser induced reaction between $CH_3F^\dagger$ and Cl_2 [C–F stretch at 1050 cm^{-1} strongly absorbs the P(20) line of the 9.6-μ CO_2 laser], Earl and Ronn[237] utilized laser pulses greater than 100 MW/cm^2 and up to 800 MW/cm^2, at which 20% conversions were noted. The reaction sequence under these high flux

conditions (10^{19} photons for 3×10^{13} molecules) is unknown; indeed, the most logical mechanism is neither of the two they proposed. The next two reactions listed in the table were carried out under cleaner conditions. Mixtures of CH_3F and Br_2 (0.07 Torr, 100 °C) were exposed simultaneously to 10 W at the P(20) line, and to a mercury vapor lamp which photolyzed the Br_2.[238] The following chain reaction was initiated:

$$Br + CH_3F^{\dagger} \rightarrow HBr + CH_2F$$

$$CH_2F + Br_2 \rightarrow CH_2FBr + Br$$

A threefold increase over the thermal rate was observed under conditions where the estimated maximum temperature rise was quite small. Manuccia, Clark, and Lory[239] found ($^{79}Br/^{81}Br$) selectivity in the laser augmented reaction of $H_3CBr^{\dagger} + Cl$, the latter generated by a microwave discharge in a flowing (Cl_2 + Ar) mixture prior to passage into the reaction cell. The mechanism is parallel to that given by the Russian workers. With R(14) of the 10.6-μ CO_2 band and the reactor at −100 °C, ^{79}Br in the CH_2BrCl product was enriched by 3%; with P(10) the product was enriched in ^{81}Br. The successful design of this experiment illustrates the necessity for taking into consideration the several time scales for concurrent processes. Clearly isotopic selectivity is destroyed when fast near-resonant v–v transfer excites the nonabsorbing species. However, pressures were adjusted so that collisional deactivation was somewhat faster than near-resonant energy transfer for the nonabsorbing molecules. In contrast, the steady-state population of the absorbing species was established by balancing collisional deactivation with laser excitation (i.e., used a high laser flux).

4. Laser-Augmented Rates for Large Molecules

Interest in "laser-induced chemistry" (LIC) is currently growing at an exponential rate. Experiments with gaseous absorbers are most often performed at pressures ranging from 10^{-1} to 10^2 Torr. The reactants are exposed to short pulses (≈200 ns) of focused CO_2 laser radiation, either free running or line selected, at 10^7–10^8 W cm^{-2}. Generally, fragmentation occurs, but occasionally intramolecular isomerizations are also observed. The experimental design focuses on selection of types of conversion which are of special interest; hopefully, these could be controlled by choice of irradiating frequency, reactant pressure, and the presence of a radical scavenger. A growing fraction of reports cover studies of LIC under collision-free conditions. While the literature is already extensive, the current high level of activity mitigates against the preparation of a coherent summary and no such attempt is made here. However, for classifying chemical conversions on the basis of whether they involve single vs. multiple energy pools, it is instructive to consider several types of LIC processes. Obviously, for conversions resulting from excitation to electronic states via visible or UV radiation the use of lasers introduces no *principles* which differ from those developed by photochemists during the past half century. The distinctive features involve higher specificity in state selection (monochromaticity), and higher levels of excitation made possible by the brilliance of laser sources. In assessing these developments one should not overlook the tremendous impact of novel detection and data logging devices on the variety of experimental designs now available in the area of photochemistry. An additional feature of high brilliance sources is the possibility of studying nonlinear optical processes.

The most novel aspect of LIC involves vibrational excitation within the ground electronic state. Since $v \rightarrow R,T$ relaxation for large molecules is generally fast, separation of thermal from vibration-specific effects is often difficult to demonstrate. The criteria listed in section III.E.1 must be applied. When τ_ℓ is longer than $\tau_{i \rightarrow j}$, the system is *thermalized*, so that conventional thermodynamic constraints apply. Nevertheless "unexpected chemistry" may appear because one can generate large temperature gradients in reaction cells and permit rapid quenching of reactions under strictly homogeneous conditions. One can also generate periodic thermal cycling in the reacting mixture. The significance of such temperature–time sequences has been generally overlooked, and the consequent unexpected product distributions tend to be ascribed to "specific" excitations, even when the experiments were performed in the 10^2 Torr pressure regime.[241] Inspection of streamline flows and temperature profiles, set up at steady state, due to convection generated by heating of the central core in a vertical cell (while the walls are maintained near room temperature), should make one hesitate to claim that the product distributions in such experiments, were they *thermalized*, would match what one would observe in a conventionally heated reactor. The reader is directed to Figure 12 which illustrates the complex temperature–time history of a sample under typical laser irradiation, in the high-pressure regime ($p > 5$ Torr).

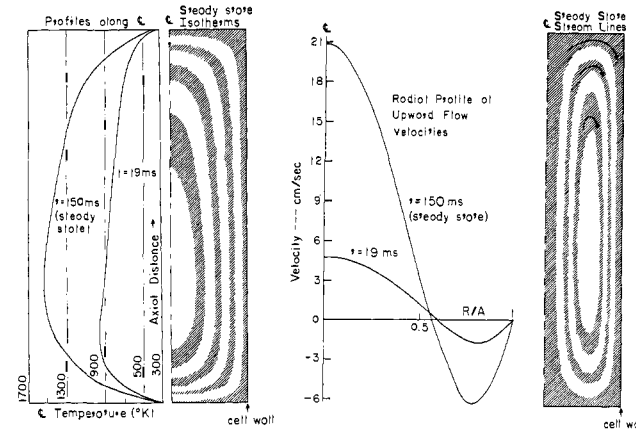

Figure 12. Temperature profiles and convective circulation (calculated for incompressible flow) in a vertical cell, irradiated with a coaxial laser beam. The cell is 1 cm in diameter and 2.5 cm long, filled with 5 Torr of SF_6 and 95 Torr of Ar. The program was run assuming an exponential decaying function for 10 W in (at the bottom) and 5 W out (at the top). The laser beam was assumed to have a Gaussian shape of the form $\exp(-R/A)$. The walls and windows were maintained at 300 K. This system attained *steady state* in about 125 ms, the time to reach one-half of the steady-state heat balance ($\dot{Q}_{in} \approx \dot{Q}_{out}$) in about 10 ms. The left diagram shows the isotherms (concentric cylinders) attained in 150 ms, and the temperature distribution along the center line at 19 and 150 ms from the instant the beam was turned on. The right diagram shows the streamline flow developed at 150 ms and the dependence of vertical flow velocity on radius. *Precaution:* The mean temperatures estimated from the extent of conversions of selected reactons indicate that the calculated temperatures are overestimated owing to the assumption of incompressibility of the fluid. Calculations which take into account density changes generated by the temperature profiles (compressible flow) are very difficult to make. Qualitatively, substantial radial flow would be induced so as to mix the material along the central streamline (which is at high temperature) with the colder material in the surrounding cylinders and thus reduce the effective temperature. (calculations performed by John Schuster and W. O. McLean, Department of Thermal Engineering, Cornell University).

When the system is not thermalized one may roughly categorize three distinct levels of excitation.

$E^{\dagger}$: at this extreme, molecules absorb a few quanta such that their internal dynamics is still represented by a normal mode approximation. In the absence of external perturbations, such as molecular collisions or very strong electric fields, no energy redistribution occurs. Three atom encounters, A + $BC^{\dagger}$, belong to this group. Another example in this category is the highly specific, self-scavenging reaction of trifluorophosphine adduct of borane.[49,242] The mechanism proposed is:

$$H_3B{:}PF_3 \rightleftarrows H_3B + PF_3 \quad \text{(fast)}$$

$$H_3B + H_3BPF_3^{\dagger}(3\nu_3) \rightarrow B_2H_6 + PF_3$$

$E^{\ddagger}$: This is an intermediate case, where the energy content

TABLE XII. LIC Which Involve Bimolecular Reactions[a]

Absorbing species	Reagent	Irradiating laser	Products	Comments	Ref
Cl_2CS	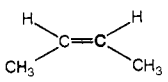	λ 4705.5 λ 4657.9	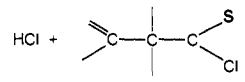	[ε excitation] reagent $p \approx 1$ Torr, quantum yield ≈ 0.5, $^{35}Cl/^{37}Cl$ selective	244
ICl	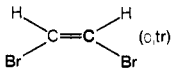	CW dye λ 5145	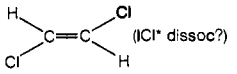	[ε excitation] trans isomer enriched ^{37}Cl	245
N_2F_4 SF_6	H_2	CO_2(10.6 μ) pulse	Chemiluminescence (Uv, vis, IR)	Light pulses initiate explosive reaction	246
SF_6	SiH_4	CO_2 (10.6 μ) pulse	S_2^* ($B^3\Sigma_u^- \rightarrow X^3\Sigma_g^-$) SiF_4; HF	Residual SF_6 enriched in $^{34}SF_6$	243
H_3CBr	Cl	CO_2 (CW laser)	$HCl + H_2CBr'$	Isotopically selective for Br (79/81)	239
$O_2(X^3\Sigma_g^-)$	$C_2(CH_3)_4$ olefins	dye--- intracavity	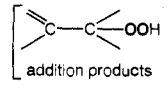	[ε excitation] Selective production of hydroperoxide	247

[a] We did not list processes in which a second reagent was added merely to serve as a scavenger of the primary dissociation fragments produced by MΦP.

is below the critical energy for reaction but considerably above the range for the application of normal modes. The partition of energy between vibrations of various symmetries and vib-internal rot is significant. Such molecules react only when involved in bimolecular processes but in the absence of a considerable amount of excitation (via the absorbed laser radiation) there would be no significant reaction. There are very few members in this group (Table XII). Most of the currently reported investigations are in the last group. When excitation attains such levels that the absorbing species react rapidly prior to an encounter with a second reagent, then the system is in the novel regime of multiphoton processes (MΦP).

E^*: At this extreme the molecules absorb *coherently* considerably more than the critical energy (E^*) required for dissociation or isomerization. Even though the phase of the vibrational mode is initially locked onto the laser radiation field, because of the presence of a very high density of states ($\geq 10^8$ cm^{-1}) above the level of the fourth or fifth vibrational harmonic, the injected vibrational energy is rapidly randomized with a characteristic time $\tau_r \leq 10^{-9}$ s. Above E^* each level of excitation has a characteristic lifetime (τ_ℓ) which depends on ($E^* - E^*$).[48] The statistical theory, which requires only knowledge of the density of energy states for the various branching ratios, satisfactorily accounts for the observed product distributions.[45c] What is generally lacking is knowledge of the population distribution among the excited states. Thus, the various type of experiments may be characterized as follows:

Conventional kinetics	$\tau_r < \tau_{v,v} < \tau_{v,RT} < \tau_\ell(\tau_{bl})$
LIC—lethal regime ($E^* - E'$) collision-free case	$\tau_r(\tau_{vvl}) < \tau_\ell < \tau_{v,v} < \tau_{v,RT}$
LIC—sublethal [$E^\ddagger \approx {}^2/_3 E'$]	$\tau_r(\tau_{vvl}) < \tau_{bl} < \tau_{v,v} < \tau_{v,RT}$
LIC—n.m. regime [$E^\dagger \approx 3$–$6\ h\nu$]	$\tau_{bl} < \tau_{vvl} < \tau_{v,v} < \tau_{v,RT} < \tau_r$

The specificity demonstrated by the trifluorophosphine decomposition[49] is a strong argument that at low vibrational excitations the energy remains highly localized. Consider the following facts:

(a) The band pumped by the 10.6-μ CO_2 laser is nominally assigned to the symmetric stretching of the PF_3, whereas the B–P bond is broken.

(b) The efficiency for decomposition depends sensitively on which of the CO_2 rotational lines is used. Energetically they are practically identical.

(c) For the same power input, and very nearly equal high power beam absorption coefficients, the extent of decomposition of D_3BPF_3 is ≈30% greater than that of H_3BPF_3.

(d) There appears to be no difference in decomposition rates of $H_3{}^{10}BPF_3$ and $H_3{}^{11}BPF_3$, whereas there is a significant $^{10}/_{11}$ isotope effect of D_3BPF_3.

(e) These observations are in direct accord with the calculated mean amplitudes for the B–P separation, on the assumption that a normal mode analysis is applicable up through the third harmonic.

For intermediate levels of excitation no experiments have yet been successfully designed to test the extent of intramolecular energy flow. However, there are several computer simulations of classical models which provide some insight into this question (section IV). The fact that isotopic selectivity can be achieved merely demonstrates that under carefully controlled conditions some bimolecular conversions occur more rapidly than *v–v* energy transfer, even in the presence of high concentrations of atomic and molecular fragments. This is illustrated by the explosive reaction between SF_6 and SiH_4, initiated by single pulse of a CO_2 laser.[243] There is a threshold for this process. A minimum of ≈7 J must be deposited within 1 μs at a total gaseous pressure of 10 Torr. The spectral and temporal distribution of emitted chemiluminescence depends sensitively on the fuel to oxidizer ratio and on the pulse energy. The principal emission is due to $S_2(B^3\Sigma_u^- \rightarrow X^3\Sigma_g^-)$; and in the upper electronic state vibrational temperatures range from 3000 to 13 000 K. The luminosity peaks sharply at $p(SiH_4)/p(SF_6) = 1.0 \pm 0.05$. On each side of the maximum of the emission vs. composition curve, at ratios of 0.95 and 1.22 for a 12-J pulse, the *residual* SF_6 is enriched in the ^{34}S isotope. The observed fractionation factors at these compositions are 8 ± 2. The separation between the two sharply peaked optimum compositions increases with increasing pulsed energy (Figure 13).

The discovery of MΦP at E^*, being a truly novel phenomenon, has generated an extensive literature during the past three years, covering theoretical analyses,[248–250] computer modeling,[251] and laboratory studies conducted with a variety of gases, in flow reactors at low pressures and in crossed molecular beams. The experimental parameters have now been fairly well established: one must work in a "collision-free" regime, wherein a sufficient number of photons are deposited in a time less than the mean time between molecular collisions; the optimum frequency of the incident radiation for MΦP is shifted somewhat to the low side of the optical absorption maximum; the extent of conversion scales with the total energy deposited, rather than with the flux; experimentally there appears to be a threshold but the level for various absorbers is still being debated.[252] The development of a unified theory for the absorption process has not faired as well.

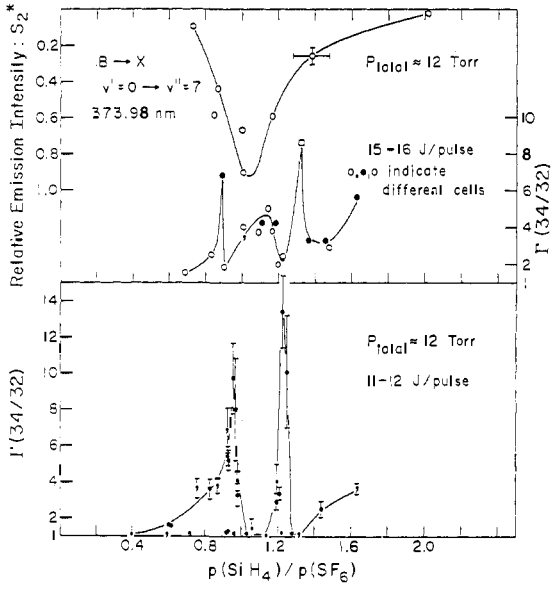

Figure 13. Dependence of chemiluminescent intensity and isotope enrichment factor on fuel/oxidizer ratio: $\Gamma \equiv (^{34}S/^{32}S)$ in residual $SF_6/(^{34}S/^{32}S)$ in reference cell

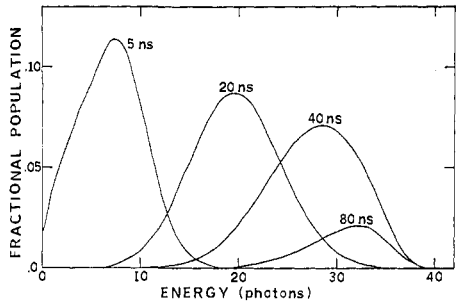

Figure 14. The population distribution in SF_6 at various times, calculated for a 100-ns, 200-MW/cm^2 rectangular laser pulse excitation. Initially only the ground level is populated, but the laser excitation, being a stochastic process, soon distributes the population over many levels. As time goes on, the population is continuously pumped up and the distribution curve shifts to higher energies. Correspondingly, the average excitation energy, $\langle n \rangle h\nu$, also increases with time. At $t \sim 30$ ns, the high-energy tail of the distribution curve clearly extends beyond the dissociation level. As the laser excitation drives the population distribution upward, the dissociation yield increases. Above E_0 the depletion of state populations is dominated by the dissociation rate. This accounts for the abrupt cutoff at about $n = 40$.

Both quantum and classical formulations have been presented based on models which seem trivially simple compared to the molecules tested in the laboratory. A central feature of the absorption process is the retention of coherence between the molecular vibrations and the radiation field. The quantum mechanical problem requires formulation of the absorption process as the time evolution of the molecule-incident field complex, to deduced probabilities for transition from the ground vibrational state to various excited states. This is difficult to do for coupled anharmonic oscillators which are embedded in a potential function appropriate for real molecules.

The significant difference between the lethal laser excitation and thermal excitation in conventional unimolecular rate studies appears in the state distribution of populations from which reactions occur. Both types involve the same molecular τ_r's and τ_ℓ's. This was analyzed by Grant.[251b] To emphasize their point we reproduced one of their computed curves (Figure 14), which shows the population distribution at various times produced by a 100-ns rectangular pulse at 200 MW cm^{-2}. This is based on a phenomenological model for the multiphoton dissociation of SF_6.

TABLE XIII. Bimolecular Reactions (gas phase) Which Show Arrhenius Graph Curvature (abstracted from ref 253b)

Reaction[d]	T range kilodegrees (Kelvin)	(Low T) E_a/R, kcal/deg	(High T) E_a/R, kcal/deg
$H + CH_4 \rightarrow H_2 + CH_3$	0.4–2.0	6.0	7.5[a]
$H + C_2H_6 \rightarrow H_2 + C_2H_5$	0.4–1.4	4.0	7.5
$H + HBr \rightarrow H_2 + Br$	0.3–2.0	0	1.5
$O + H_2 \rightarrow OH + H$	0.4–2.0	5.0	7.0
$O + CO_2 \rightarrow CO + O_2$	1.2–4.5	15.0	30.0
$OH + CO \rightarrow CO_2 + H$[c]	0.2–2.5	0	4.0
$OH + H_2 \rightarrow H_2O + H$	0.3–1.8	2.0	3.5
$OH + OH \rightarrow H_2O + O$	0.3–2.0	4.0	3.5
$OH + CH_4 \rightarrow H_2O + CH_3$	0.2–2.0	2.0	5.0
$CH_3 + C_2H_6 \rightarrow CH_4 + C_2H_5$	0.4–1.4	6.0	15.0
$CO + NO_2 \rightarrow CO_2 + NO$	0.5–1.4	15.0	20.0
$Al + CO_2 \rightarrow AlO + CO$	0.3–1.9	2.6	~30[b]

[a] Illustrative data by J. C. Biordi, J. F. Papp, and C. P. Lazzara, *J. Chem. Phys.*, **61**, 741 (1974). [b] A. Fontijn and W. Felder, *ibid.*, **67**, 1561 (1977). [c] W. C. Gardiner, D. B. Olson, and J. N. White, *Chem. Phys. Lett.*, **53**, 134 (1978). [d] The reaction $Cl + CH_4 \rightarrow HCl + CH_3$ [e] shows non-Arrhenius behavior (communication from F. Kaufman). [e] M. S. Zahniser, B. M. Berquist, and F. Kaufman, *Int. J. Chem. Kinet.*, **10**, 15 (1978).

The challenge of MΦP is clear. Diagnostic techniques are needed for measuring vibrational state distributions in the upper levels with nanosecond time resolution. Dynamically realistic models of coupled anharmonic oscillators must be analyzed so as to provide appropriate descriptions of the transition of intramolecular motions from one applicable to orthogonal normal modes at low excitation, to the complete washing out of the localized (spiked) distributions at very high levels of excitation. Nevertheless, while the information developed to date based on LIC is incomplete, there is sufficient evidence that in many reactions the pre-T and post-T distributions are not statistical; that is, several energy pools must be considered to provide an adequate description of the sequence of (*s–s*) transformations.

F. Do Conventional Kinetic Experiments Indicate Multiple Energy Pools?

1. Nonlinear Arrhenius Graphs

The striking nonstatistical population distributions, which were found for the nascent products from highly exoergic reactions and the variously augmented rates experimentally observed when some reagents were pumped by specific IR laser radiation, were recognized only after "state-selective" preparative and analytical techniques were developed. The question whether under such highly nonequilibrium conditions the *apparent* activation energy is quantitatively related to the conventionally measured activation energy is hardly pertinent. However, if one performs experiments under conditions which depart measurably but not extensively from a Boltzmann distribution (indeed, to a greater or lesser extent this is the case for all kinetics experiments, except for rates derived from spectral line shapes at equilibrium; refer to the Appendix), the quantitative features of the temperature coefficient of the rate constants for elementary steps do prove to be informative. When data became available over large enough temperatures ranges, for several apparently straightforward reactions, the Arrhenius plots were found to be nonlinear, well outside the limits of experimental error[253] (Table XIII). To account for the observed ln k vs. $1/T$ plots, on the basis of eq 14 one has the choice of either modifying the $\kappa(E;E^*)$ or the $\mathbf{P}(E;T)$ functions.

The hope that one could deduce $\kappa(E;E^*)$ from eq 14, via a Laplace transform, using the observed T dependence of $\kappa(T;E^*)$, is doomed to disappointment. First, to obtain an inversion which is sufficiently informative the experimental function must be known with very high precision over an extended temperature

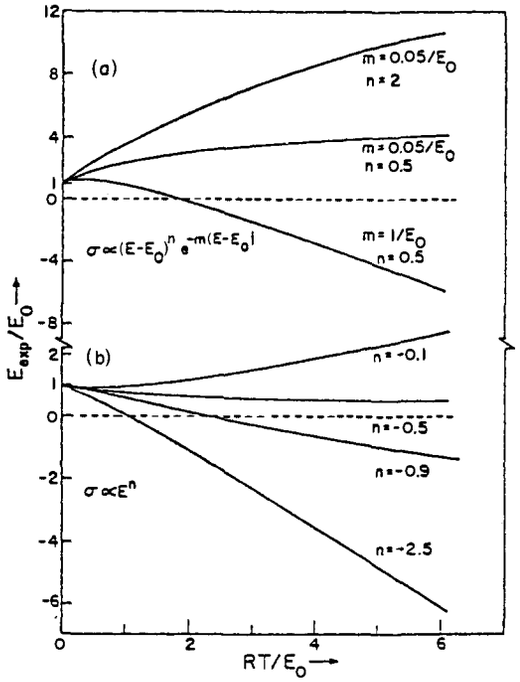

Figure 15. Variation of the Arrhenius slope with the reduced temperature for assumed threshold shape functions (ref 255).

range, so as to provide a significantly sensitive measure of the integrand. (Note the parallel situation for the attempted Laplace inversion to determine the density of energy states.[254]) Second, in view of the possibility that eq 16 may provide a better description, it is a strong assumption to place the entire onus of the departure of $\kappa(T)$ from the accustomed Arrhenius form upon the functional dependence of $\kappa(E)$. Even so, one is merely deferring the problem. Molecular dynamics must be invoked to account for whatever form is deduced for $\kappa(E;E^*)$. Nonetheless, it is interesting to note briefly several reports covering this approach. Since a Laplace inversion is not practical, LeRoy[255] and Menzinger and Wolfgang[256] tested, by direct integration over a Boltzmann distribution, a variety of functional forms for $\kappa(E;E^*)$ [they prefer to use the cross section $E\cdot\sigma(E;E^*)$]. Indeed, they clearly illustrated the sensitivity of the local slopes of log ln κ vs. $1/T$ curves to the shape of $\sigma(E)$ at the threshold. However, one may well question whether a close correspondence between an observed $k(T;E^*)$ and one of the curves shown in Figure 15 unambiguously implies the corresponding $\kappa(E;E^*)$. Inspection of eq 16 suggests a plethora of situations which could lead to curvature of Arrhenius plots. An illustration of the effect of enhanced rate due to vibrational excitation (for a hypothetical two level case) on the overall rate was presented by Polanyi and Schreiber.[257] Clearly, in the absence of additional information the unfolding of the product of the cross section and distribution functions generally is not unique. The direct approach is to study experimentally highly perturbed but known non-Boltzmann distributions. Even then the results will not be as clear-cut as are investigations with state-selected reagents.

2. Diatom Dissociations

The most direct procedure for calculating a phenomenological rate constant, as was indicated above, is to insert state specific transition probabilities into a master equation and to solve for the time evolution of populations (eq 12), treating each significant state as an independent species. Extensive applications of this approach have been published relative to dissociation of diatomic molecules; the objective was to account for the universal observation that the experimentally derived activation energies were 10–30 kcal/mol less than the corresponding spectroscopic values.[258] Here the focus was not on curvature of Arrhenius plots

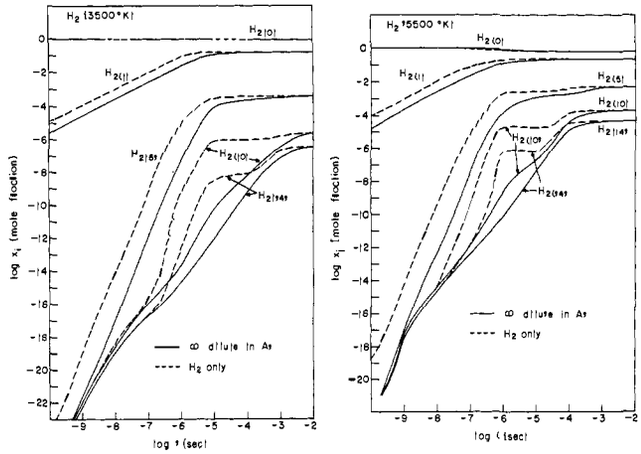

Figure 16. Computed vibrational state populations in a dissociating diatomic gas. Note the plateaus which extend from $\approx 10^{-6}$ to $\approx 10^{-4}$ s, at levels *below* the Boltzmann values. Under nondissociating conditions vibrational relaxation occurs in ≈ 1 μs (ref 57).

(they are straight lines within substantial experimental errors) but on the magnitudes of their slopes. The cause was ascribed to "depletion" of the upper vibrational states below their Boltzmann level, to the effects of the centrifugal barrier, and to the decrease in the three-body recombination rate probability with rising temperature.[259] In our opinion, even though "the depletion factor" alone is not sufficient to account for the observed difference in $(D_0^0 - E_a)$ for all diatoms and for many triatomic species, it must be taken into consideration for cases wherein the population of states immediately below the critical ones are controlled by both inelastic nonreactive collisions and by reactive collisions. This is crucial during early times in all reactions, when the rate of return from the product states *is* considerably slower than the rate of depletion of the reactant states, as is obviously the case for:

$$X_2^{(v-1)} + M \rightleftarrows X_2^{(v)} + M \underset{\text{fast; } v \text{ close to upper limit}}{\overset{\text{slow (3-body)}}{\rightleftarrows}} 2X + M$$

The calculated time evolution of the vibrational state populations in H_2 (highly diluted in Ar or in pure H_2) at two temperatures is shown in Figure 16.[57] Note the sequential leveling-off of vibrational state populations in the time domain $(10^{-7}$–$10^{-4})$ s, at magnitudes well below equilibrium, even though the major effect of vibrational relaxation appears at $\approx 10^{-7}$ s. This clearly illustrates the perturbing effect of dissociation on the upper state populations prior to establishing *chemical* equilibrium due to three-body recombination, when the concentration of H atoms becomes large enough.

Analogous significant perturbations of Boltzmann distributions can occur in other reactions, for example, in the homogeneous $H_2 + D_2 = 2HD$ exchange, and in similar metatheses. In their reinvestigation of this reaction, Lifshitz and Frenklach[203b] found that after correcting their observed HD conversions for possible contributions from three-center displacements ($H + D_2 \rightarrow HD + D$), there remained a substantial bimolecular component, for which the rate constant is:

$$k_b = 10^{14.1\pm0.8} \exp\left[-\frac{(38 \pm 5) \times 10^3}{RT}\right] \text{mol}^{-1}\ \text{cm}^3\ \text{s}^{-1}$$

The possibility exists that the low activation energy is a consequence of depletion of $v \geqq 4$ states. The essential point is that depletion effects are not noticed where there is no prior knowledge or expectation of a "reasonable" activation energy.

IV. Comments on Theory

In chemical kinetics one either measures the time variation

of state populations or of total species concentrations for a variety of system parameters, or, calculates state-to-state transition probabilities. Rate constants, cross sections, and activation energies are derived quantities, resting upon specific models. In the preceding sections a family of time scales was introduced to stress the operational features which characterize the evolution of reacting systems; these τ's apply either to averages over individual molecular events or to direct measurements of large assemblies of molecules. We compiled an abundance of experimental data and computational results which negate the simplistic postulates that: (a) for every elementary reaction, under *all* experimental conditions, there is a phenomenonlogical rate constant (or a unidirectional flux coefficient) which is a function of the temperature only; and that, (b) measured rate constants can be directly related to a dominant state-to-state transition probability.

Current theoretical developments support the conclusion that a model which is based on these assumptions is inadequate. To supplement conventional kinetics, there are two approaches: one which focuses on individual molecular events, and another which is concerned with departures of averaged quantities from predictions based on uniform phase space distributions.

A. Trajectory Calculations

Estimates of the relative effectiveness of nonrandom energy distributions, specifically associated with spikes localized in phase space, for controlling the rates of R → P conversions can be, and have been, most directly derived from extended trajectory computations. For reviews refer to Porter,[260] Thompson,[215b] Polanyi and Schreiber.[257] These were carried out roughly in parallel with experimental demonstrations of selective activation, but with very few exceptions, success was judged by how closely the computed results matched the published rates, often neglecting to ascertain whether experiments were actually performed under statistical equilibrium. In due course the distillation of much work led to the recognition that difficult problems remain to be solved. Note the following: (i) The unknown function of primary concern is the potential hypersurface, which orchestrates the paths followed by the atomic cores during collisions between molecules, and post-excitation. Not many potential functions for three-center systems are known with the required accuracy;[150,261-263] for larger molecular aggregates only semiempirical formulations are available, and these encompass a wide range of reliability.[39] A question of primary concern is the uniqueness of the function for electronically excited states, or for reactants with open-shell configurations, for which the low-lying electronic states are closely spaced [for example, $F(^2P_{3/2},^2P_{1/2}) + H_2(^1\Sigma_g^+;v,J)$].[264] (ii) Nagging questions remain with reference to the system dynamics—how to establish the correspondence between results based on classical trajectories and the quantum world of real molecules. There is ambiguity as to how to apportion branching ratios from the computer-generated continuous distributions into the quantized states. Serious efforts have been directed toward the solution of the Schrödinger equation for atom plus diatom collisions in 1, 2, and 3 dimensions.[53d,e] More general cases were reviewed recently.[265] The correlation of cross sections computed for different dimensionalities is not trivial. The "surprisal" (see below) for angular scattering, energy disposal, and impact parameter distributions is dimensionally invariant; hence systematics for interconverting reaction probabilities have been developed.[266] A satisfactory answer has yet to be given as to how one should treat the zeropoint energies of the participants in inelastic collisions, particularly for small energy transfers. Classically some energy is always transferred during a collision, whereas quantum mechanical molecules obey digital rules. (iii) There are ambiguities as to how to develop potential energy surfaces which are sufficiently accurate at van der Waals distances to permit calculation of energy transfer probabilities. This remains a difficult problem when more than three atoms are involved in molecular encounters.

A few illustrative results which are pertinent to our topic are briefly summarized below. Preston and Pack[267] tested two potential energy surfaces for the CO_2–Ar pair. On the basis of approximately 3×10^4 classical trajectories they obtained inelastic cross sections for *rotational energy transfer* which are in excellent agreement with molecular beam experiments,[268] and showed that large ΔJ transitions occur frequently. Quasiclassical calculations compare favorably with accurate quantum mechanical close coupling calculations for collisionally induced rotational transitions in N_2–Ar collisions, CO–He, OCS–H_2, etc.[269] Extended 3D calculations on the CO_2–rare gas system were made by Suzukawa[270] and for vibrational deexcitation of $CO_2^\dagger + H_2$ (D_2) by Sathyamurthy and Raff.[271] Below rke's of one electron volt translation ⇄ vibrational energy transfer is inefficient, the major process being translation ⇄ rotation. These calculations also reproduce quite well the molecular beam data. On the other hand, Buck and McGuire,[272] using a coupled state approximation for HCl–Ar collisions, found that with their surface they could not reproduce the experimental total cross sections for rotational transitions.[273]

Extensive studies of *vibrational relaxation* of diatomics via atomic collisions were undertaken for hydrogen and the hydrogen halides.[215b] Some of these proved particularly interesting in that collisional energy transfers occur with comparable efficiency via two mechanisms, nonreactive and exchanges. The possibility that atomic exchange reactions may prove particularly effective for vibrational relaxation in diatom collisions was proposed by Bauer and Tsang.[274] Thompson concluded[275] that for the four cases he explored [H_2 + I; H_2 + Cl; HCl + H; and HCl + Cl] the types of energy transfer which were predicted on the basis of his 3D quasiclassical calculations were very sensitive to the initial internal states of the diatom, so that general rules regarding relative probabilities for specific transfers could not be readily formulated.

Reactive collisions for three-body hydrogen–halogen systems were investigated in great detail via classical trajectories in 1-, 2-, and 3D, and under a variety of quantum mechanical approximations. The results of these computer explorations have been pitted against a large body of experimental work and found to be generally satisfactory, but this was accompanied by manipulation of parameters which characterized the potential energy surfaces. Porter et al.[54] showed that for their surfaces, which incorporated a single adjustable parameter, the dynamical effects resulting from momentum transfer required the reactions to proceed through excited vibrational states of the H_2 (D_2). The rates computed from rotationally averaged cross sections were substantially in agreement with the experimental data for a substantial range of temperatures. White and Thompson[220] investigated the effect of reactant vibration and rotation on energy transfer and on atom transfer rates for [H + HBr] and [Br + HBr]. In both systems atom exchange contributes significantly to energy relaxation, and excitation of the diatom increases the reaction rate coefficient. A summary of the Monte Carlo trajectories for the family $H + X_2 \rightarrow HX^{\ddagger} + X$, (X ≡ F, Cl, Br, and I) has recently been presented by Pattengill, Polanyi, and Schreiber.[276] The purpose of these calculations was to assess the reliability of a simple unadjusted LEPS potential energy surface. It did not lead to quantitative agreement with experiment but did demonstrate the general characteristics of such reactions with respect to the dynamical quantities for the products, that is, vibrational, rotational and scattering angular distributions.

A generalization which emerged from the Toronto school study of many trajectories for the A + BC family is that low barriers generally occur in the reactant valley; that is, the A · · · BC bond is substantially formed prior to release of C. Then the rke of the collision is more effective for inducing reactions

than is vibrational excitation. For substantially exothermic reactions the products are vibrationally excited. The converse holds for the reverse endothermic direction; that is, the high barriers appear in the product valley, and vibrational excitation is particularly effective for atom transfer. However, these conclusions are modulated by the dynamic factors which depend on the relative masses of the interacting particles and on the impact parameters of collision (for details refer to ref 257).

Quasiclassical trajectory calculations for reactive collisions have been reported for Cl + HBr and Cl + HI.[277] For the first reaction an average rate constant at 295 K of 30.2×10^{12} cm^3 mol^{-1} s^{-1} was obtained, compared to the experimental value of 4.5×10^{12}. For its *reverse*, the computed rate coefficient for Br + HCl ($v = 2$) also was a little over six times that found experimentally by Arnoldi et al.[216a] Similar checks were obtained for the distribution of vibrational product states of the $HCl^{(v')}$ [$N(v' = 2)/N(v' = 1) = 0.4$]. As expected, increasing the initial reactant vibrational energy shifts the product distribution to higher vibrational states. A variety of combinations of three-center encounters have been similarly analyzed.[278] Attention is called to Hijazi and Polanyi's[279] study of the magnitude and orientation of rotational momentum in (A + BC) exchange reactions. There are two sources of rotational excitation in the product (AB), the orbital angular momentum of the reactants, and repulsion between the products. The first is prominent when m_A, m_B are large while m_C is small; the second is significant when three conditions are fulfilled: substantial repulsive energy released on separation of the products; reaction occurs predominantly through a bent intermediate (A^BC); and $m_C > m_B$.

For symmetric systems both nonreactive collisions and atom exchange contribute to vibrational relaxation. The dynamics of collisions between H + H_2 ($1 \leq v \leq 4$) and D + D_2 ($1 \leq v \leq 4$) were investigated by Smith[280] via quasiclassical trajectory analysis on a Yates–Lester potential energy surface. Exchange is selectively enhanced by vibrational excitation, but the degree of selectivity diminishes as v is increased. Thompson[281] found for (Cl + Cl_2) and (I + I_2) that reactant vibration enhances the rate of atom exchange whether present in amounts either less than, or in excess of the energy barrier, provided the rke of the collisions is low; that is, the overall effect diminishes with increasing temperature. These results merit further study. Monte Carlo trajectory calculations of H_2 + Ar collisions show[282] that reagent vibrational excitation is very effective in promoting dissociation (as expected), that rotational energy is second most effective, while rke is least effective. Trajectories have also been computed for polyatomic reactions wherein large groups are "collapsed" so that they can be represented by a single mass point. Setser et al.[283] tested this approach for (F + HR) reactions on a LEPS surface, with the mass and other properties of the R unit adjusted to simulate the reaction of F with CH_4 and CH_3Br. They did find that approximately 60% of the exoergicity appears as vibrational energy of the HF. The specific case F + H–CH_3 → $HF^{\dagger}$ + CH_3 was studied in more detail by Gauss;[284] he used a LEPS surface with self-adjustable parameters to estimate the net thermal rate, which did agree with the experimental observations.

Relatively few quasi-classical trajectory calculations have been reported for the $A_2 + B_2 \rightarrow 2AB$ case. Thompson and McLaughlin[285] investigated the reaction dynamics of H_2 ($v = 0$, 2, 4, 6) + F_2 ($v = 0$ or 6), and looked for the wide variety of products which can thus be generated [H + F + HF (+6.5 kcal/mol); 2HF (−134.4 kcal/mol); F_2H + H (+5.4 kcal/mol); H_2F + F (+5.1 kcal/mol); F_2 + 2H (+109.4 kcal/mol); H_2 + 2F (+38.0 kcal/mol)]. While the major reaction products are (HF + H + F) and (2HF), they found that even for excited H_2 ($v = 2$) the cross sections for all of the product channels are small; the rke thresholds for reaction are quite high, but these do decrease with vibrational excitation. Overall it appears that the reaction H_2 ($v \geq 1$) + F_2 → H + HF + F proceeds at the sufficient rate to provide chain branching in the H_2/F_2 system, which leads to explosions. Classical trajectories were calculated for ($H_2 + I_2$) by Raff et al.[286] They concluded that the molecular mechanism is dynamically forbidden but that an atomic mechanism is allowed, via a loose H_2I complex. The results of this work has been questioned; a complete analysis of this mechanism awaits the development of a reliable surface for this four-atom system. The reaction dynamics on surfaces with "early" energy barriers for AB + CD → AC + BD, comparable to those for three atom cases, was discussed by Mok and Polanyi.[287] With regard to reagent excitation and disposal the four-center system showed features similar to the three-center case.

Classical trajectories were calculated for five- and six-center systems, relative to the rate of intramolecular vibrational energy redistribution as applied to unimolecular reactions. Of special interest are the studies of bond breaking in $HC{\equiv}CCl$,[65] for which computations are in accord with RRKM, and the internal reorientation in H_3CNC,[66] which is not. The unimolecular dissociation of ethane via C–C and C–H bond breaking was simulated by trajectory calculations on a well-coupled potential energy surface.[288] Lifetime distributions were obtained for both fragmentation channels at several excitation energies (180–240 kcal/mol). The trajectory results for different energization patterns do not agree with corresponding statistical predictions. Full trajectories for a six-center bimolecular reaction were calculated by Chapman and Bunker:[289] $CH_3 + H_2 \rightarrow CH_4 + H$, at rke ≈ 25 kcal/mol. Vibrations of H_2 *enhance*, while out-of-plane bending vibrations of the CH_3 *depress* the reaction cross section; excitation of the other vibrations in the methyl group have minor effects.

We have yet to develop appropriate descriptions of the state of excitation of large molecules, when their energy content is above that required to fill the first few harmonics of all the fundamentals. The conditions under which large and small molecules undergo optical dephasing following the absorption of resonant radiation were formulated by Orlowski et al.[290] The accuracy of the infinitesimal amplitude, weak coupling approximation was found to break down, even for triatomic harmonic systems, at energies above one-quarter of a bond dissociation energy, based on a classical dynamical analyses.[291] Classical trajectories were also used to study the flow of energy in energized five-atomic molecules: D_3CCl and D_3CH. McDonald and Marcus[292] calculated the vibrational spectrum for each mode of the activated molecule and for the product (CD_3). For excitation energies substantially above that required for dissociation, inspection of the trajectories showed large fluctuations in the energy within each mode vs. time; i.e., the energy flowed freely between modes on a time scale of ≈5 ps. Distribution of energy in the product was found to be random for a surface with no exit channel barrier, and where there was not strong intermode coupling. When barriers are present the distributions are nonrandom; also, for low levels of excitation (<1 eV) the trajectories show quasi-periodic structure, such that neighboring trajectories separate approximately linearly with time (nonergotic criterion), rather than exponentially (ergotic condition).[43,51b] The translational energy distribution for decomposition of highly energized complexes over a centrifugal barrier was studied via Monte Carlo simulations; these show that every complex formed does not have unit probability for decomposition, contrary to the usual RRKM assumption.[293]

One should inquire whether quasi-classical trajectory calculations accurately reflect the effects of reactant excitation and product energy disposal. A significant study is the comparison of predictions thus made, with quantum calculations for a specified potential energy surface. Two 3D calculations for hydrogen atom exchange in (H_2 + H) have been reported recently. Elkowitz and Wyatt[294] investigated this reaction on two surfaces and found that the cross sections, summed over rotational state transitions 0→1, 0→3, 0→5, · · · , have the same

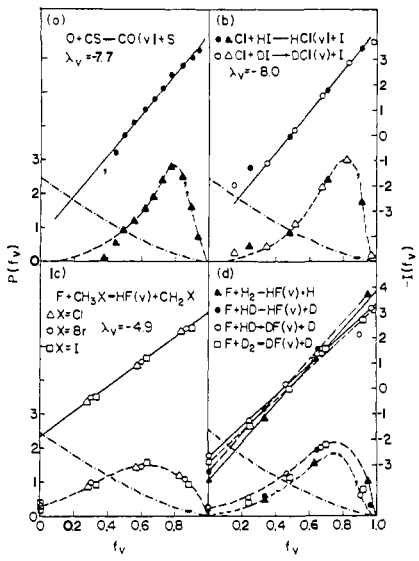

Figure 17. Typical surprisal plots (ref 300): ·-·-· indicate prior expectations; - - - - connects experimental points; — is the linear surprisal function.

translational energy threshold as that derived for the Porter–Karplus surface via classical trajectories; but, for rke > 0.35 eV the quantum mechanical cross section is ≈20% higher than the classical one. Conversely for the Yates–Lester–Liu surface the classical cross sections were approximately 15% higher. The functional dependence of cross sections on rke are very similar even though there are significant differences in the scattering functions. The four papers by Schatz and Kuppermann[53d] are extensive and informative. They also used the Porter–Karplus surface and found that the reactive cross sections show significant rotational angular momentum polarization, with $m_J = m_J' = 0$ transitions dominant for low reagent rotational quantum numbers. In contrast, the averaged rotational distribution can be fitted to a statistical temperature to a highly degree of accuracy. The integral cross sections have an effective threshold (total energy) of about 0.5 eV. Differences between the 3D and corresponding 1- and 2D results are largely interpreted as resulting from bending motions in the transition state. The best overall agreement between the reactive, integral, and differential cross sections, and the quasiclassical ones of Karplus, Porter, and Shavit appear at energies above the classical threshold. This leads to near equality of the quantum and quasi-classical thermal rate constants at 600 K, but at low temperatures the effects of tunneling become important so that the quantum rate is higher than the classical one by a factor of 2 at 300 K, and 18 at 200 K.

Exact quantum mechanical transition probabilities for the colinear reaction: $H + F_2(v = 0) \rightarrow HF(v' \leq 11) + F$ were described by Connor, Jakubetz, and Manz[295] and by Halavee and Shapiro[296] who used an approximate colinear quantum mechanical model. The former report that on an extended LEPS surface the calculated average cross sections, adjusted for 3D,[266] were in good agreement with the classical trajectory results, and with the experimental values, as well as with those reported by the second set of authors. The latter investigated 11 other hydrogen/halogen reactions and found good agreement with the experimental results.

From the above summary it follows that extensive computer modeling and laborious theoretical analyses provide the means for exploring three-center systems in detail, and with few exceptions deduce angular distributions for scattering, energy and atom transfer probabilities, the effects of reagent excitation, and energy partition in the products. Overall, the trajectory calculations agree well with experiment. However, broad generalizations which could be extended to more complex systems have not yet emerged. It is evident that while trajectory analysis has provided us with insight into the dynamical parameters which control individual collisions, the fine structure of these dynamical details depends sensitively on some features of the approximate surfaces used in the calculations. Also, insufficient attention has been devoted to the statistical aspects which are incorporated in all laboratory experiments.

B. The "Surprisal" Formulation for Nonrandom Systems

A general formulation is now available for describing systems which are not fully randomized. The primary targets of the principal innovators[297] were the nascent product distributions generated in highly exoergic reactions. This approach has the attractive feature of utilizing reduced variables in terms of which most distributions can be represented by linear functions, although they have widely different appearance when plotted as mole fraction vs. quantum number. For each type of energy sink, E_v, E_R, E_{tr}, such that for an isolated event (at a constant total energy) $E = E_v + E_R + E_{tr}$, introduce the parameter $f_i \equiv E_i/E$, i.e., the fraction of the energy which a product species has if it is generated in the specified state [for example, $f(v = 2) \equiv E(v = 2)/E$ measures the fraction of the available energy which is present in $v = 2$ for that event]. Designate the observed probability for such events (the fraction of the total which terminate in state i) for which the total available energy is E, by $P(E_i)$, and define the "surprisal":

$$I(f_i) \equiv -\ln [P(E_i)/P^0(E_i)] \tag{24}$$

Here $P^0(E_i)$ is the expected, or "prior", distribution which would result were deposition in all states equally probable. This function can be computed from the known spectroscopic states of the product species. Empirically, it was found that in all but a trivial number of cases for which nonrandom distributions were either observed in the laboratory or estimated from classical trajectory calculations, plots of the surprisal function vs. f_i were linear; i.e.

$$I(f_i) = \lambda^0 + \lambda_i f_i \tag{25}$$

Thus, each of the complex nonrandom distributions which characterize the nascent products from exoergic reactions can be fully represented by two parameters. Intuitively one anticipates that these parameters are alike for similar reactions; indeed, this has been demonstrated for $F + H_2$, D_2 and HD (Figure 17).

The following rationale for eq 25 was presented by Levine.[298] Since $k\Sigma_i P(E_i) \ln P(E_i)$ has the aspect of an entropy, he defined the *entropy deficiency* for the nascent distribution

$$\Delta S^d \equiv k\sum_i P(E_i) \ln [P(E_i)/P^0(E_i)] \tag{26}$$

This is a negative quantity and approaches zero when $P(E_i) \rightarrow P^0(E_i)$. To maximize this entropy deficiency subject to the condition that the probability function be normalized, and that the computed mean of $I(E_i)$ be equal to that observed [i.e., known first moment: $\langle I(E_i) \rangle \equiv \int_0^1 I(E_i)P(E_i)\,df_i$], use the conventional procedure with Lagrangian multipliers (λ^0, λ_i); this leads to

$$P(E_i) = P^0(E_i) \exp[-(\lambda^0 + \lambda_i f_i)] \tag{27}$$

(which is eq 24 and eq 25). One may hope that since the entropy deficiency depends on specific features of the potential energy surface, the magnitudes of the corresponding Lagrangian multipliers would be derivable from the parameters which characterize that surface. While such a priori correlations are being sought for simple cases, it is interesting to inspect the results of a variety of data reductions via the surprisal function, in the hope of uncovering *empirical* correlations for families of reactions. Here we encounter (as yet) an unresolved problem—for

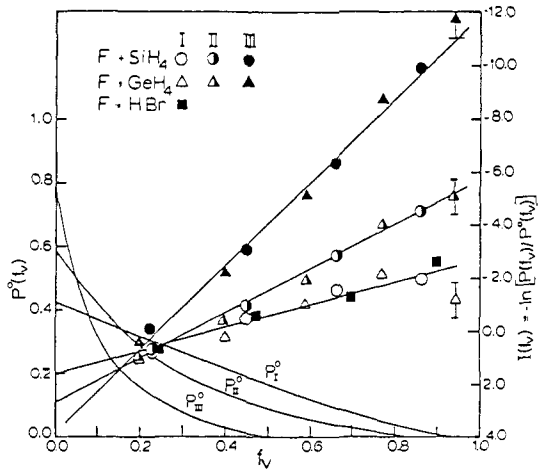

Figure 18. Surprisal plots for H-atom abstraction by F from three substrates, computed for models I, II, III (ref 151b).

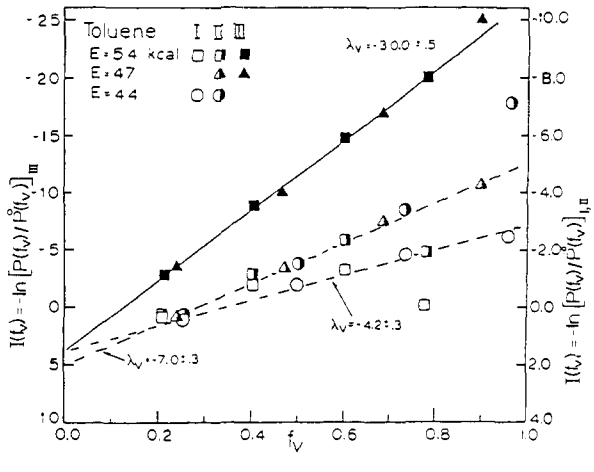

Figure 19. Surprisal plots for H-atom abstraction by F from toluene, computed for three models, and assuming a range of values for the available energy (ref 151b).

complex reactions the calculation of the prior distribution $P^0(E_i)$ may be ambiguous.

In their surprisal analysis of the HF† product vibrational energy partition which Bogan and Setser[151b] derived from chemiluminescence measurements for reactions F + HR, three models were tested for the computation of the prior distributions: (i) a three-body model, in which the polyatomic product was treated as a mass point; (ii) an extended three-body model, in which the polyatomic product was replaced by a finite size object, to include its three rotational degrees of freedom; (iii) a model which incorporated all vibrational and rotational modes of the radical. For calculating the density of states they followed the prescription of Kinsey.[70] The available energy was obtained from:

$$E = D_0^0(\text{H–F}) - D_0^0(\text{H–R}) + E_a + 3RT$$

All three "priors" led to linear surprisals vs. $f(v)$, as illustrated in Figure 18. Note, however, that slight adjustments had to be made in the choice of D_0^0(H–R) and E_a, since these quantities are not precisely known for all the HR's; the authors selected values which generated the best straight lines. The sensitivity of the Lagrangian parameters to the choice of E is illustrated in Figure 19, for the case of toluene. Levine pointed out[298] that λ_v has the aspect of a temperature; Setser's data show that its magnitude for complex products apparently depends on the assumptions introduced in calculating the $P^0(E_v)$ function.

In their study of the effect of localized energy accumulation on the rate of reaction Levine and Manz[72a,299] concluded that vibrational excitation can lead to various consequences. They considered 20 reactions for which either laboratory experiments or trajectory calculations showed effects due to selective energy deposition, and compared the "observed" rate constants with those expected on prior grounds, were all states at the specified total energy to react at the same rate [i.e., $\kappa(E)$ only]. Here they defined the surprisal function for vibrational excitation, assuming both rotation and translation were thermalized:

$$I(v|T) = -\ln [\kappa(v|T)/\kappa^0(v|T)] \qquad (28)$$

For highly endoergic processes, for which the mean excitation at the operating temperature is well below the endoergicity for the reaction, it appears that the increase in rate due to vibrational energy is larger than that expected on the basis of a comparable increase in thermalized (trans + rot) energy. The incremental enhancement per Δv is greater for excitation of the lower vibrational states. As the extent of excitation approaches the endoergicity of the reaction, the enhancement factor decreases. Thus, for mildly endoergic, thermoneutral and exoergic reactions the incremental increase in rate is usually less than that expected from statistical utilization of an equal amount of energy. This is illustrated in Figure 20.[300]

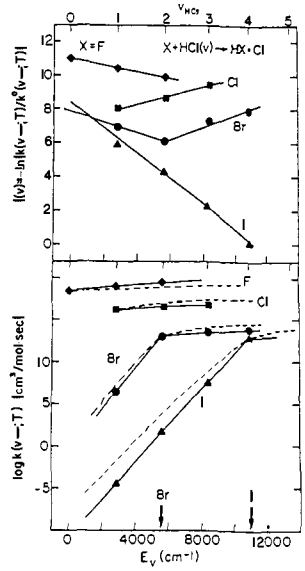

Figure 20. Comparison of rate constants for specific vibrational excitation X + HCl(v) → HX + Cl, and of the corresponding surprisal functions. The arrows indicate the magnitudes of $\mathcal{E}^*$ for X = Br and I [$\mathcal{E}^* = 0$ for Cl; $\mathcal{E}^* = -31$ kcal/mol for F] (cf. Figure 17).

Perry and Polanyi[301] undertook a surprisal analysis to estimate the branching ratio for the reaction: F + HD → HF†(v',J') + D vs. DF†(v',J') + H. The excited product distributions were obtained from chemiluminescent spectra; the predicted Γ(HF/HD) = 1.41 ± 0.18, is in excellent agreement with the measured value, 1.45. However, whereas classical trajectory calculations (on several surfaces) indicated that Γ should increase with increasing rotational excitation of HD, the opposite trend is given by the surprisal formulation. Polanyi et al.[214] called attention to H + $F_2(v = 4)$ → HF(v') + F, for which trajectory calculations show a bimodel distribution in v'. However, the linear relation (eq 27) is presumed to apply when $P^0(E_i)$ is computed, *subject to all the known constraints;* in general, ln [$P(E)/P^0(E)$] need not be monotomic.

The surprisal formulation is more than a convenient format for economically summarizing much information on nascent product distributions. It is a natural extension of statistical mechanics to systems which generate nonuniform distributions, and thus provides a rationale for the observed large variations in product state populations, and for the differing effects on reaction rates of specific reagent excitation. Its most attractive

features is that it provides a language for discussing averaged quantities for reactions under single collision conditions without imposing a detailed analysis of the individual events. For additional reviews, refer to ref 302 and 303.

V. Conclusions

In the above analysis of how energy accumulation and disposal affect the rates of chemical reactions we rediscovered several basic concepts. The conventional separation of phase space into reactant, transition, and product regions, while convenient, is arbitrary, since there is no intrinsic difference between transformations which we recognize as reactive encounters and those which are inelastic-nonreactive. In this connection it is helpful to consider the various time scales associated with *inter* and *intra* molecular energy transfer and structural rearrangement. Also, while all of kinetics can be divided into three parts [(i) computation of potential energy surfaces; (ii) obtaining solutions of the equations of motion on these surfaces, for representative sets of initial conditions; (iii) appropriately weighting the contributions of each type of scattering process to fit the experiments at hand], this partition is not entirely clear-cut, particularly for reactions which involve more than a few atoms; coupling to low-lying electronic states can occur.

All experiments, whether performed under "single collision" conditions or in the bulk, to a lesser or greater extent, involve averages over sets of initial states, as well as averages over the variety of paths which connect the reactant to the product spaces. Furthermore, in experiments with bulk reagents one cannot avoid using distributions over populations of initial states which are directly coupled to the chemical reactions, so that the conventional assumption of a Boltzmann function for the weighting distribution is always an approximation. In that sense all rates, except those measured at *chemical* equilibrium (for example, via spectral line shapes), are affected by the relative probabilities for transitions between states, both in the reactant and product spaces. However, at moderate gas densities and in solutions, the departure from Boltzmann distributions is small; the extent of departure is comparable to the ratio of cross sections for reactive to that for energy transfer processes, *for the states involved.* In the current upswell of gas-phase chemical kinetics, experimental conditions are deliberately chosen to permit the exploration of the reactivities of selected initial states, and of branching ratios into product states. These have provided considerable insight into "how molecules react".

The partition into reactant, transition, and product spaces is deeply imbedded in our language, and pursuit of the "structure of the T state" is accepted as a worthwhile goal. One conclusion which follows from the above discussion is that studies of highly excited reactant and product states should prove rewarding since these must be similar to the T states. Another conclusion: it may prove useful to consider "significant regions" in $R^\dagger$ and $P^\dagger$ spaces, so as to collapse the vast number of states into a smaller number of nearly homogeneous groups. A quantitative formulation of such an approach is given by the "surprisal". This function constitutes a useful framework for the correlation of much kinetic data recorded under single collision conditions. However, its extension to large molecules may prove ambiguous.

Finally, it is interesting to note that upon dividing kinetics into three types of problems, one finds that there remain computational but no conceptual difficulties with parts i and iii, but that is not the case for part ii, when moderately excited polyatomic molecules are involved. As yet a satisfactory description of the dynamics of such molecules is not available.

VI. Appendix

The most rudimentary model which illustrates the effect of *population depletion* on a reaction rate is the three-state system [A ⇄ B ⇄ C] wherein B is considered to be an excited form of A. Then, under steady-state conditions, eq 12 for the forward flux gives:

$$\left[\frac{d[C]}{dt}\right]_f = \kappa_2\left(\frac{\kappa_1}{\kappa_{-1}}\right)\left(1 - \frac{\kappa_2}{\kappa_{-1}} + \ldots\right)[A] \qquad (29)$$

Were the population of B maintained in statistical *equilibrium*, this flux would be $\kappa_2(\kappa_1/\kappa_{-1})$, since the rate controlling step is κ_2. Thus, the *steady state* rate of production of C is always less, by the factor of $(1 - \kappa_2/\kappa_{-1} + \ldots)$.

A more general analysis shows that whenever a *net* reaction occurs at a finite rate, departure from statistical equilibrium is always induced;[51c] the steady-state magnitude depends on the ratio of the *upper state* relaxation cross sections to those for the reactive cross sections. A simple but general model consists of an energy ascending set of states $(1, 2, \ldots, i)$ wherein transitions between adjacent states only are allowed $(\kappa_{i,i+1};\kappa_{i,i-1})$ as well as reaction from each of these to a common product state $(\kappa_{i,\alpha})$. Define $\beta_i \equiv n_i/n_i^e$, where n_i^e is the population state i would have (at any t) were the system in a Boltzmann distribution. When the ambient temperature is fixed, n_i^e is time dependent due to transitions $\kappa_{i,\alpha}$ and $\kappa_{\alpha,i}$. At $t = 0$, all states except α are filled to their equilibrium levels ($\beta_i = 1$). When one "turns-on" the reaction, the master equation for the evolution of the system is

$$\beta_i \frac{d \ln n_i}{dt} = -\kappa_{1,0}g(i)[\beta_i - \beta_{i-1}] + \kappa_{1,0}g(i + 1)\,\tilde{\omega}_{i+1}[\beta_{i+1} - \beta_i] - \kappa_{i,\alpha}\beta_i + \kappa_{\alpha,i}(n_\alpha/\beta_i) \qquad (30)$$

Here we defined $\kappa_{i,i-1} \equiv \kappa_{1,0}g(i)$; $\tilde{\omega}_{i+1} \equiv \exp[-(E_{i+1} - E_i)/RT]$. In the right member the second term is always smaller than the first and may be negligible except when the density of states is high; also at early times all but the third term are small, so that $n_i(t)$ initially declines as $\exp(-\kappa_{i,\alpha}t)$. However, except for the very unrealistic case when all the $\kappa_{i,\alpha}$'s are such as to maintain all β_i's equal, the first and second terms soon begin to grow. The direction is determined by the logical assumption that $\kappa_{i,\alpha} > \kappa_{i-1,\alpha}$; the higher states will be depleted more than the lower ones, and $\beta_i < \beta_{i-1}$. Note that for a high density of states the recovery rate is almost second order $[g(i + 1) \simeq g(i)$, and $\tilde{\omega}_{i+1}$ approaches unity]. The decline in β_i begins to level off *only when*

$$\kappa_{1,0}g(i)\{|\beta_i - \beta_{i-1}| - \tilde{\omega}_{(i+1)}|\beta_{i+1} - \beta_i|\} \to \kappa_{i,\alpha}\beta_i \qquad (31)$$

Thereafter β_i *continues to deviate from unity* $[\approx(1 - \kappa_{i,\alpha}/\kappa_{i,i-1} + \ldots)$ for a widely spaced set of states, when i is the lowest state for which there is significant reaction] until the accumulation of the products in the α state is high enough so that the reverse reaction rate becomes significant; i.e., the system approaches *chemical* equilibrium.

VII. Key to Symbols

- τ_c *mean* time between collisions for species of interest (1) encountering bath molecules (2) $\tau_c^{-1} = Z_{12}[2]$; [ ] designates: molecules cm^{-3}
- Z_{12} kinetic theory collision number for species 1 (use molecular diameters derived from gaseous viscosities), with species 2 at unit concentration; (s^{-1} molecule^{-1} cm^3) $Z_{12} = (2/\pi)^{1/2}(\mu_{12}/kT)^{3/2}(\pi b_{max}^2)$.
- b_{max} the largest impact parameter which leads to a "collision"
- $Z_{i\to j}$ survival factor, for molecules (1) in state i toward deexcitation ($\to j$) by collision with species 2; $Z_{i\to j} \equiv \tau_{i\to j}/\tau_c$

$\tau_{i\to j}$ directly measured relaxation time for deexcitation $[=Z_{i\to j}/Z_{12}[2]]$

$\tau_r(E) \approx \tau_r^*$ characteristic time for dispersal of a "localized" excitation—in the vicinity of the critical energy shell (very similar to $\tau_{i\to j}$ but restricted to motion within an E layer)

E^* threshold energy for an (*s–s*) transformation

$\tau_\ell(E)$ *mean* lifetime for an energized molecule, with $E_{total} \geq E^*$; restricted to motion within an E layer

$\tau_{v,vl}$ intramolecular vibrational energy transfer

$\tau_{v,v}$ intermolecular vibrational energy transfer

$\tau_{v,RT}$ vibration → rotation + translation All of these are induced by collisions and generally are longer than τ_c

$R^\dagger \to R^\# \cdot T \cdot P^\# \to P^\dagger$ sequence defined in Figure 3

$\mathbf{P}_{i\to j} \equiv Z_{i\to j}^{-1}$ transition probability, per collision, for the step $(i\to j)$ in species 1, induced by collision with 2

$\kappa(i,j)$ a "microscopic" rate parameter; $= \mathbf{P}_{i\to j}Z_{12}[2]$

λ_z sequence of reciprocal relaxation times for a coupled, first order, kinetic system; these are roots of a secular determinant; λ_0 is the smallest, nonzero, root.

$\kappa\begin{pmatrix} i,R \\ z,P \end{pmatrix}$ "microscopic" state-to-state rate parameter, similar to $\kappa(i,j)$ except that it indicates passage through the T region, from (i) in R, to (z) in P.

$\omega(\vec{p};q;E)$ effectiveness function for an $R^\dagger \to T$ transformation

rke;g *r*elative *k*inetic *e*nergy of a colliding pair, in their center of mass coordinates; its magnitude is g

b impact parameter for a binary collision

$\langle f(b,g)\rangle$ fraction of collisions with impact parameters between b and $b + db$, and rke between g and $(g + dg)$ which lead to reaction; $\langle f\rangle$ is averaged over the distribution of internal energies

$$\sigma(g) \equiv \int_0^\infty 2\pi b \langle f(b,g)\rangle \, db$$

total reaction cross-section

$$\kappa(g) = \left(\frac{2}{\pi}\right)^{1/2}\left(\frac{\mu_{12}}{kT}\right)^{3/2} g \cdot \sigma(g)$$

unidirectional rate parameter; in general $\kappa(E;E^*)$

$$\kappa(T) = \left(\frac{2}{\pi}\right)^{1/2}\left(\frac{\mu_{12}}{kT}\right)^{3/2} \cdot \int_0^\infty g^3 \exp\left\{-\frac{\mu_{12}g^2}{2kT}\right\} \sigma(g)\, dg$$

unidirectional, for Maxwellian distribution in rke.

$k(T)$ phenomenological rate constant

$\mathcal{E}^{th}$ threshold energy for reaction (from the lowest vibrational state), for an otherwise Boltzmannized system

Endo(exo)ergic vs. endo(exo)thermic best defined in Scheme I.

SCHEME I

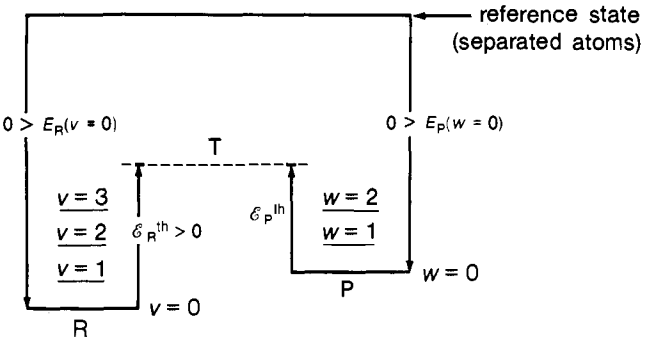

Endoergic when $\{E_P(w) - E_R(v)\} > 0$

Exoergic when $\{E_P(w) - E_R(v)\} < 0$

Endothermic when $\{\mathcal{E}_R^{th}(v) - \mathcal{E}_P^{th}(w)\} > 0$

Exothermic when $\{\mathcal{E}_R^{th}(v) - \mathcal{E}_P^{th}(w)\} < 0$

Acknowledgments. The author is grateful to the staff of the Los Alamos Scientific Laboratory for the hospitality extended to him during his sabbatic leave, when a major portion of this report was prepared. He is also indebted to Professors M. Goldstein, G. Hammes, and B. Widom (at Cornell) to to Drs. D. Breshears, J. Lyman, and D. Thompson (at LASL) for many stimulating discussions of basic concepts and data evaluation. He is specially grateful to several authors who sent him prepublication copies of their manuscripts and helpful comments regarding literature sources.

VIII. References and Notes

(1) B. Stevens, "Collisional Activation in Gases", Pergamon Press, Oxford, 1967, p 12.
(2) (a) C. B. Moore, *J. Chem. Phys.*, **43**, 2979 (1965); (b) P. Borrell, *Adv. Mol. Relaxation Processes*, 1, 69 (1968); (c) E. E. Nikitin, "Physical Chemistry—An Advanced Treatise", Vol. VI-A, W. Jost, Ed. Academic Press, New York, N.Y., 1974, Chapter 4; (d) R. C. Amme, *Adv. Chem. Phys.*, **28**, 171 (1975); (e) S. Ormonde, *Rev. Mod. Phys.*, **47**, 193 (1975).
(3) R. C. Millikan and D. R. White, *J. Chem. Phys.*, **39**, 3209 (1963).
(4) (a) J. D. Lambert and R. Salter, *Proc. R. Soc. London, Ser. A*, **253**, 277 (1959); (b) J. D. Lambert, *J. Chem. Soc., Faraday Trans. 2*, **68**, 364 (1972).
(5) (a) J. J. Hinchen, *J. Chem. Phys.*, **59**, 2224 (1973); (b) J. F. Bott and N. Cohen, *Ibid.*, **63**, 1518 (1975), for HCl; (c) D. C. Allen, T. J. Price, and C. J. S. M. Simpson, *Chem. Phys. Lett.*, **45**, 183 (1977), for CO_2.
(6) (a) M. A. Kwok and R. L. Wilkins, *J. Chem. Phys.*, **63**, 2453 (1975), measured vibrational energy transfer in HF(v) + HF, DF(v) + DF, and DF(v) + D_2 for $v = 1$–5; (b) J. F. Bott, *J. Chem. Phys.*, **65**, 4239 (1976); HF(v) + H_2(H_2,CO); $v = 1$–3; (c) P. R. Poole and I. W. M. Smith, *J. Chem. Soc., Faraday Trans. 2*, **73**, 1434 (1977).
(7) J. F. Bott and R. F. Heidner III, *J. Chem. Phys.*, **66**, 2878 (1977).
(8) C. E. Treanor, *J. Chem. Phys.*, **43**, 532 (1965).
(9) (a) G. P. Quigley and G. J. Wolga, *J. Chem. Phys.*, **63**, 5263 (1975); *Chem. Phys. Lett.*, **27**, 276 (1974); (b) I. W. M. Smith, *Acc. Chem. Res.*, **9**, 161 (1976); (c) R. G. Macdonald and C. B. Moore, *J. Chem. Phys.*, **65**, 5198 (1976); (d) G. A. West, R. E. Weston, Jr., and G. W. Flynn, *Ibid.*, **67**, 4873 (1977).
(10) B. Widom and S. H. Bauer, *J. Chem. Phys.*, **21**, 1670 (1953); (b) M. Buchwald and S. H. Bauer, *J. Phys. Chem.*, **76**, 3108 (1972).
(11) (a) J. K. Hancock and A. W. Saunders, Jr., *J. Chem. Phys.*, **65**, 1275 (1976); (b) H. K. Shin, *J. Am. Chem. Soc.*, **98**, 5765 (1976).
(12) (a) E. E. Nikitin and S. Ya. Umanski, *Faraday Discuss. Chem. Soc.*, No. 53, 1 (1972); (b) T. Hikida, S. Nakajime, T. Ichimura, and U. Mori, *J. Chem. Phys.*, **65**, 1317 (1976).
(13) K. Glänzer and J. Troe, *J. Chem. Phys.*, **63**, 4352 (1975); **65**, 4324 (1976).
(14) I. W. M. Smith in "Molecular Energy Transfer", R. D. Levine and J. Jortner, Ed; Wiley, New York, N.Y., 1976.
(15) (a) D. Secrest, *Annu. Rev. Phys. Chem.*, **24**, 379 (1973); (b) E. Weitz and G. Flynn, *Ibid.*, **25**, 275 (1974). (c) Annotated bibliographies; K. Takayanagi, *Adv. At. Mol. Phys.*, 1, 149 (1965); updated prepublication maniscript, Jan 1976.
(16) J. D. Kelley and R. L. Thommarson, *J. Chem. Phys.*, **66**, 1953 (1977).
(17) C. B. Moore, *Adv. Chem. Phys.* **23**, 41 (1973).
(18) P. F. Zittel and C. B. Moore, *J. Chem. Phys.*, **58**, 2922 (1973).
(19) (a) H. Matsui, E. L. Resler, Jr., and S. H. Bauer, *J. Chem. Phys.*, **63**, 4171 (1975); (b) W. S. Drozdoski et al., *Ibid.*, **65**, 1542 (1976).
(20) J. W. Suitor and W. C. Kirby, *Int. J. Chem. Kinet.*, **9**, 13 (1977).
(21) (a) R. C. Slater and G. W. Flynn, *J. Chem. Phys.*, **65**, 425 (1976); (b) D. R. Sieberg and G. W. Flynn, *Ibid.*, **64**, 4973 (1976).
(22) D. S. Y. Hsu and M. C. Lin, *Chem. Phys. Lett.*, **42**, 78 (1976).

(23) I. V. Hertel, H. Hoffmann, and K. A. Rost, *Chem. Phys. Lett.*, **47**, 163 (1977).
(24) (a) K. Liu and J. M. Parson, *J. Chem. Phys.*, **65**, 815 (1976). (b) For the reaction (rate constant at 300 K: 1.07×10^{-11} cm^3/s)

$$Hg(6^3P_2) + NO(X^2\Pi) \rightarrow Hg(6^1S_0) + NO(A^2\Sigma, v' = 0) \xrightarrow{h\nu} NO(X^2\Pi, v'' = 0\text{–}11)$$

refer to: H. F. Krause and S. Datz, *Chem. Phys. Lett.*, **41**, 339 (1976). (c) An extensive review has been prepared by A. B. Callear, "Physical Chemistry–An Advanced Treatise", H. Eyring et al., Ed., Academic Press, New York, N.Y., Chapter 10 in Vol VIB, 1975.
(25) S. R. J. Brueck and R. M. Oxgood, Jr., *Chem. Phys. Lett.*, **39**, 568 (1976).
(26) H. Dubost and R. Charneau, *Chem. Phys.*, **12**, 407 (1976).
(27) (a) F. Legay, "Vibrational Relaxation in Matrices, Chemical and Biological Applications of Lasers", Vol II, C. B. Moore, Ed., Academic Press, New York, N.Y., p 43; (b) R. M. Hochstrasser in "Molecular Energy Transfer", R. Levine and J. Jortner, Ed., Wiley, New York, N.Y., 1976, p 292; (c) A. Blumen, J. Manz, and V. Yakhot, *Chem. Phys.*, **26**, 287 (1977).
(28) (a) W. Kaiser and A. Laubereau, "Laser Spectroscopy", Proceeding of the 2nd International Conference, Megéve, France, 1976; "Tunable Lasers and Applications" (Leon Conference, Norway), A. Mooradian et al., Ed., Springer-Verlag, Berlin, 1976; (b) A. Laubereau and W. Kaiser, "Lasers in Physical Chemistry and Biophysics", Proceedings the 27th International Meeting, Societe de Chemie Physique, June 17–20 (1977).
(29) (a) R. T. Bailey in "Molecular Spectroscopy" (Specialist Periodical Report), Vol. 2, The Chemical Society, London, 1974; (b) R. R. Alfano et al., *Phys. Rev. Lett.*, **29**, 1655 (1972); *Opt. Commun.*, **18**, 193 (1976); (c) J. Schroeder et al., *J. Chem. Phys.*, **66**, 3215 (1977).
(30) D. W. Oxtoby and S. A. Rice, *Chem. Phys. Lett.*, **42**, 1 (1976).
(31) D. Chandler and L. R. Pratt, *J. Chem. Phys.*, **65**, 2925 (1976).
(32) G. E. Busch and P. M. Rentzepis, *Science*, **194**, 276 (1976); (b) R. M. Hochstrasser and A. C. Nelson, *Opt. Commun.*, **18**, 361 (1976); (c) K. B. Eisenthal, *Acc. Chem. Res.*, **8**, 118 (1975).
(33) V. M. Aras et al., *J. Chem. Soc., Faraday Trans. 1*, **73**, 1039 (1977).
(34) (a) D. C. Tardy and B. S. Rabinovitch, *Chem. Rev.*, **77**, 369 (1977); (b) S. C. Chan, B. S. Rabinovitch et al., *J. Phys. Chem.*, **74**, 3160 (1970); (c) P. J. Marcoux, E. E. Siefert, and D. W. Setser, *Int. J. Chem. Kinet.*, 7, 473 (1975).
(35) D. V. Sickman and O. K. Rice, *J. Chem. Phys.*, **4**, 608 (1936).
(36) P. J. Robinson and K. A. Holbrook, "Unimolecular Reactions", Wiley-Interscience, London, 1972.
(37) D. M. Golden, R. K. Solly, and S. W. Benson, *J. Phys. Chem.*, **75**, 1333 (1971).
(38) I. S. Wang and M. Karplus, *J. Am. Chem. Soc.*, **95**, 8160 (1973).
(39) (a) M. J. S. Dewar, *Science*, **187**, 1037 (1975); *Faraday Discuss. Chem. Soc.* No. 62, 197 (1977); (b) G. G. Balint-Kurti, *Adv. Chem. Phys.*, **30**, 137 (1975); (c) R. Hoffmann, *J. Am. Chem. Soc.*, **90**, 1475 (1968).
(40) R. P. Bell, *Trans. Faraday Soc.*, **66**, 2770 (1970).
(41) B. J. Zwolinski and H. Eyring, *J. Am. Chem. Soc.*, **69**, 2702 (1947). See also S. H. Lin and H. Eyring, *Annu. Rev. Phys. Chem.*, **25**, 39 (1974).
(42) D. L. Bunker and S. A. Jayich, *Chem. Phys.*, **13**, 129 (1976).
(43) S. A. Rice, *Discuss. Faraday Soc. Chem. Soc.*, No. 55, 114 (1973); (b) D. W. Oxtoby and S. A. Rice, *J. Chem. Phys.*, **65**, 1676 (1976); (c) S. A. Rice, "Excited States", Vol. 2, Academic Press, E. C. Lim, Ed., New York, N.Y., 1975, p 112 ff.
(44) P. Brumer and J. W. Duff, *J. Chem. Phys.*, **65**, 3566 (1976).
(45) (a) J. G. Black et al., *Phys. Rev. Lett.*, **38**, 1131 (1977); (b) D. S. Frankel, Jr., and T. J. Manuccia, *Chem. Phys. Lett.*, submitted for publication; (c) E. Yablonovitch, *Opt. Lett.*, 1, 87 (1977).
(46) J. N. Butler and G. B. Kistiakowsky, *J. Am. Chem. Soc.*, **82**, 759 (1960).
(47) J. F. Meagher, K. J. Chao, J. R. Barker, and B. S. Rabinovitch, *J. Phys. Chem.*, **78**, 2535 (1974).
(48) E. R. Grant et al., *Chem. Phys. Lett.*, **52**, 595 (1977).
(49) (a) K.-R. Chien and S. H. Bauer, *J. Phys. Chem.*, **80**, 1405 (1976); (b) S. H. Bauer and K.-R. Chien, *Chem. Phys. Lett.*, **45**, 529 (1977).
(50) J. O. Hirschfelder and E. Wigner, *J. Chem. Phys.*, **7**, 616 (1939).
(51) (a) N. B. Slater, "Theory of Unimolecular Reactions", Cornell University Press, Ithaca, New York, N.Y., 1959, (b) K. G. Kay, *J. Chem. Phys.*, **64**, 2112 (1975), presented a dynamical derivation of the RRKM expression for the decomposition rates of isolated molecules, and established the ranges of validity for the assumed statistical distribution of populations. (c) K. G. Kay, *J. Chem. Phys.*, **65**, 3813 (1976); (d) S. Ehrenson, *J. Am. Chem. Soc.*, **98**, 6081 (1976).
(52) The assignment of quantum numbers (v,J) classically computed end states is not unambiguous. A recent analysis has been presented by D. G. Truhler and J. W. Duff, *Chem. Phys. Lett.*, **36**, 551 (1975).
(53) (a) E. Bauer, *J. Chem. Phys.*, **23**, 1087 1955); (b) T. A. Dillon and J. C. Stephenson, *ibid.*, **58**, 2056, 3849 (1973); (c) W. H. Miller, *ibid.*, **62**, 1899 (1975); **63**, 1166 (1975); (d) A. Kuppermann et al., *ibid.*, **62**, 2502 (1975); **63**, 674, 685 (1975); 65, 4596, 4624, 4642, 4668 (1976); (e) H. Essen, G. D. Billing, and M. Baer, *Chem. Phys.*, **17**, 443 (1976).
(54) R. N. Porter, L. B. Sims, D. L. Thompson, and L. M. Raff, *J. Chem. Phys.*, **58**, 2855 (1973), did follow this prescription.
(55) (a) B. Widom, *Science*, **148**, 1555 (1965); (b) N. S. Snider, *J. Chem. Phys.*, **42**, 548 (1965); (c) D. Gutkowicz-Krusin, *Ibid.*, **67**, 2830 (1977).
(56) Abstracted from G. G. Hammes, "Principles of Chemical Kinetics", Academic Press, New York, N.Y., 1978.
(57) S. H. Bauer, D. Hilden, and P. Jeffers, *J. Phys. Chem.*, **80**, 922 (1976).
(58) S. H. Bauer, B. P. Yadava, and P. Jeffers, *J. Phys. Chem.*, **78**, 770 (1974).
(59) H. B. Rosenstock, M. B. Wallenstein, A. L. Warhaftig, and E. Eyring, *Proc. Nat. Acad. Sci.*, U.S.A., **38**, 667 (1952).
(60) B. Anlauer and Ch. Ottinger, *Z. Naturforsch., Teil A*, **27**, 293 (1972).
(61) P. J. Derrick and A. L. Burlingame, *Acc. Chem. Res.*, **7**, 328 (1974).
(62) (a) L. Melander, "Isotope Effects on Reaction Rates", Ronald Press, New York, N.Y., 1960; (b) ref 36, Chapter 9.
(63) (a) S. W. Benson and D. M. Golden, "Physical Chemistry–An Advanced Treatise", Vol. VII, H. Eyring, Ed., Academic Press, New York, N.Y., 1975, Chapter 2; (b) S. W. Benson, "Thermochemical Kinetics", 2nd ed, Wiley, New York, N.Y., 1976.
(64) D. L. Bunker, *J. Chem. Phys.*, **40**, 1946 (1964).
(65) W. L. Hase et al., *J. Chem. Phys.*, **64**, 651, 2256, 2442 (1976).
(66) D. L. Bunker, *Acc. Chem. Res.*, 7, 195 (1974).
(67) K. Evans, D. Heller, S. A. Rice, and R. Scheps, *Chem. Soc., Faraday Trans. 2*, **69**, 856 (1973).
(68) D. L. Bunker and W. L. Hase, *J. Chem. Phys.*, **59**, 4621 (1973).
(69) S. H. Bauer, *AGARD Conf. Proc.* No. 2 (Oslo, May, 1966), 1 (1967).
(70) J. L. Kinsey, *J. Chem. Phys.*, **54**, 1206 (1971).
(71) N. Davidson, "Statistical Mechanics," McGraw-Hill, New York, N.Y., 1962, p. 230 ff.
(72) (a) H. Kaplan, R. D. Levine, and J. Manz, *Chem. Phys.*, **12**, 447 (1976); (b) see also D. S. Perry, J. C. Polanyi, and C. W. Wilson, Jr., *Chem. Phys. Lett.*, **24**, 484 (1976).
(73) I. Koyano in "Comprehensive Chemical Kinetics", Vol. 18, C. H. Bamford and C. F. H. Tipper Ed., Elsevier, Amsterdam, 1976, Chapter 6.
(74) S. G. Lias and P. Ausloos, "Ion-Molecule Reactions", American Chemical Society, Washington, D.C., 1975.
(75) T. Baer, B. P. Tsai, and A. S. Werner, *J. Chem. Phys.*, **62**, 2497 (1975).
(76) J. L. Franklin, *Science*, **193**, 725 (1976).
(77) A. I. Ossinger and E. R. Weiner, *J. Chem. Phys.*, **65**, 2892 (1976).
(78) C. E. Klots, *J. Chem. Phys.*, **64**, 4269 (1976).
(79) (a) B. P. Tsai, A. S. Werner, and T. Baer, *J. Chem. Phys.*, **63**, 4384 (1975); (b) P. P. Dymerski and A. G. Harrison, *J. Phys. Chem.*, **80**, 2825 (1976).
(80) T. Baer, B. P. Tsai, D. Smith, and P. T. Murray, *J. Chem. Phys.*, **64**, 2460 (1976).
(81) A. S. Werner and T. Baer, *J. Chem. Phys.*, **62**, 2900 (1975).
(82) C. E. Klots, D. Mintz, and T. Baer, *J. Chem. Phys.*, **66**, 5100 (1977).
(83) A. D. Williamson and J. L. Beauchamp, *J. Chem. Phys.*, **65**, 3196 (1976).
(84) D. C. Carter, *J. Chem. Phys.*, **65**, 2584 (1976).
(85) D. M. Mintz and T. Baer, *J. Chem. Phys.*, **65**, 2407 (1976).
(86) (a) S. J. Riley and K. R. Wilson, *Faraday Discuss. Chem. Soc.*, No. 53, 132 (1972); (b) R. C. Dunbar and J. M. Kramer, *J. Chem. Phys.*, **58**, 1266 (1973).
(87) K. C. Kim, *J. Chem. Phys.*, **64**, 3003 (1976).
(88) (a) R. Stockbauer and M. G. Inghram, *J. Chem. Phys.*, **65**, 4081 (1976); (b) M. Riggin, R. Orth, and R. C. Dunbar, *Ibid.*, **65**, 3365 (1976).
(89) (a) K. Honma, K. Tanaka, I. Koyano, and I. Tanaka, *J. Chem. Phys.*, **65**, 678 (1976); (b) see also W. A. Chupka in "Ion-Molecule Reactions", Vol. 1, J. L. Franklin Ed., Plenum Press, New York, N.Y., 1972, Chapter III.
(90) W. A. Chupka, M. E. Russell, and K. M. Refaey, *J. Chem. Phys.*, **48**, 1518 (1968).
(91) W. A. Chupka and M. E. Russell, *J. Chem. Phys.*, **48**, 1527 (1968).
(92) W. A. Chupka and J. Berkowitz, *J. Chem. Phys.*, **54**, 4256 (1971).
(93) D. J. McClure, C. H. Douglas, and W. R. Gentry, *J. Chem. Phys.*, **66**, 2079 (1977).
(94) M. L. Gross and J. Norbeck, *J. Chem. Phys.*, **54**, 3651 (1971).
(95) A. L. Schmeltekopf, E. D. Ferguson, and F. C. Fehsenfeld, *J. Chem. Phys.*, **48**, 2966 (1968).
(96) R. H. Neynaber and G. D. Magnuson, *J. Chem. Phys.*, **58**, 4586 (1973).
(97) D. L. Albritton et al., *J. Chem. Phys.*, **66**, 410 (1977).
(98) F. C. Fehsenfeld et al., *J. Chem. Phys.*, **62**, 2001 (1975).
(99) (a) W. A. Chupka and M. E. Russell, *J. Chem. Phys.*, **49**, 5426 (1968); (b) J. A. Rutherford and D. A. Vroom, *Ibid.*, **58**, 4076 (1973).
(100) W. N. Whitton and P. J. Kuntz, *J. Chem. Phys.*, **64**, 3624 (1976).
(101) P. M. Dehmer and W. A. Chupka, *J. Chem. Phys.*, **62**, 2228 (1975).
(102) E. Lindemann et al., *J. Chem. Phys.*, **56**, 1003 (1972).
(103) J. C. Polanyi and D. C. Tardy, *J. Chem. Phys.*, **51**, 5717 (1969).
(104) J. O. Hirschfelder, C. F. Curtiss, and R. B. Bird, "Molecular Theory of Gases and Liquids", Wiley, New York, N.Y., 1954, pp 45–51.
(105) R. D. Levine and R. B. Bernstein, "Molecular Reaction Dynamics", Oxford University Press, New York, N.Y., 1974, pp 191–203.
(106) (a) R. Grice, *Adv. Chem. Phys.*, **30**, 247 (1974); (b) B. G. Gwenlock, C. A. Johnson, and J. E. Parker in ref 73, Chapter 4.
(107) E. W. Roth, B. P. Mathur, and G. P. Reck, *J. Chem. Phys.*, **65**, 2912 (1976).
(108) (a) J. P. Toennies in ref 2c, Vol. VIA, Chapter 5; (b) R. B. Bernstein and B. E. Wilcomb, *J. Chem. Phys.*, **67**, 5809 (1977).
(109) T. M. Sloane, S. Y. Tang, and J. Ross, *J. Chem. Phys.*, **57**, 2745 (1972).
(110) S. Stolte, A. E. Proctor, and R. B. Bernstein, *J. Chem. Phys.*, **65**, 4990 (1976).
(111) M. E. Gersh and R. B. Bernstein, *J. Chem. Phys.*, **55**, 4661 (1971).
(112) R. M. Harris and D. R. Herschbach, *Faraday Discuss. Chem. Soc.*, No. 55, 121 (1973).
(113) S. A. Pace, H. F. Fang, and R. B. Bernstein, *J. Chem. Phys.*, **66**, 3635 (1977).
(114) A. Kupperman and J. M. White, *J. Chem. Phys.*, **44**, 4352 (1966).
(115) A. E. Redpath and M. Menzinger, *J. Chem. Phys.*, **62**, 1987 (1975).
(116) S. P. Tang, N. G. Utterback, and J. F. Friichtenicht, *J. Chem. Phys.*, **64**, 3833 (1976).
(117) E. K. Parks and S. Wexler, *Chem. Phys. Lett.*, **10**, 245 (1971).
(118) S. B. Jaffee and J. B. Anderson, *J. Chem. Phys.*, **51**, 1057 (1969).
(119) (a) J. C. Polanyi, J. J. Sloan, and J. Wanner, *Chem. Phys.*, **13**, 1 (1976); (b) J. C. Polanyi and J. L. Schreiber, *Faraday Discuss., Chem. Soc.*, No. 62 (1977).

(120) D. E. Klimek and J. C. Polanyi, *Faraday Discuss. Chem. Soc.*, No. 62, 333 (1977).
(121) (a) S. J. Riley and D. R. Herschbach, *J. Chem. Phys.*, **58**, 27 (1973); (b) S. M. Freund et al., *ibid.*, **54**, 2510 (1971).
(122) A. N. Schweid, M. A. D. Fluendy, and E. E. Muschlitz, Jr., *Chem. Phys. Lett.*, **42**, 103 (1976).
(123) N. H. Hijazi and J. C. Polanyi, *Chem. Phys.*, 11, 1 (1975).
(124) (a) K. D. Aniauf et al., *J. Chem. Phys.*, **57**, 1561 (1972). (b) J. C. Polanyi and K. B. Woodall, *ibid.*, **57**, 1574 (1972).
(125) (a) D. J. Douglas and J. C. Polanyi, *Chem. Phys.*, **16**, 1 (1976); (b) P. L. Devries and T. F. George, *Chem. Phys. Lett.*, **43**, 391 (1976).
(126) S. Stolte, A. E. Proctor, W. M. Pope, and R. B. Bernstein, *J. Chem. Phys.*, **66**, 3468 (1977).
(127) (a) J. A. Silver et al., *J. Chem. Phys.*, **65**, 1811 (1976); (b) J. C. Polanyi and J. J. Sloan, *Int. J. Chem. Kinet.*, **7**, 51 (1975).
(128) W. Brenner and T. Carrington, *J. Chem. Phys.*, **46**, 7 (1967).
(129) M. Sabety-Dzvonik and R. Cody, *J. Chem. Phys.*, **64**, 4794 (1976).
(130) K. Mislow, *Acc. Chem. Res.*, **9**, 26 (1976).
(131) J. M. Tedder and J. C. Walton, *Acc. Chem. Res.*, **9**, 183 (1976).
(132) (a) P. R. Brooks, *Science*, **193**, 11 (1976); (b) R. J. Beuhler, Jr., R. B. Bernstein, and K. H. Kramer, *J. Am. Chem. Soc.*, **88**, 5331 (1966).
(133) D. L. Bunker and E. A. Goring-Simpson, *Faraday Discuss. Chem. Soc.*, No. 55, 93 (1973).
(134) J. Reuss, in *Adv. Chem. Phys.*, **30**, 389 (1975).
(135) (a) P. J. Kuntz, M. H. Mok, and J. C. Polanyi, *J. Chem. Phys.*, **50**, 4623, (1969); (b) P. M. Hieri, *ibid.*, **67**, 4665 (1977).
(136) V. H. Shui, J. P. Appleton, and J. C. Keck, *J. Chem. Phys.*, **56**, 4266 (1972), show the interesting ballet performed by the trio [H, Cl, Ar] during a successful association to produce HCl†.
(137) J. C. Polanyi, *J. Chem. Phys.*, **31**, 1338 (1959).
(138) S. H. Bauer and E. L. Resler, Jr., *Science*, **146**, 1045 (1964).
(139) (a) J. A. Kerr compiled extensive tables of rate constants for A + BC → AB + C reactions (atom and radical attack) under thermalized conditions: ref 73 Chapter 2. (b) A bibliography on the chemical kinetics of the hydrogen halides, including chemiexcitation and energy-transfer studies (1959–1973) was prepared by F. Westley, NBS Special Bulletin No. 392, U.S. Government Printing Office, Washington, D.C., 1974. (c) An extensive review on the production of excited states of simple molecules and of their reactivities (488 refs): I. W. M. Smith, *Adv. Chem. Phys.*, **28**, 1 (1975) Chapter 1. (d) M. J. Berry in ref 14.
(140) (a) V. I. Vedeneyev et al., "Bond Energies, Ionization Potentials and Electron Affinities" (Transl. *Scripta Tech. Lett.*), W. D. Price, Ed., Edward Arnold Publishing, London, 1966. (b) V. deB. Darment, "Bond Dissociation Energies", NSRDS-NBS No. 31, U.S. Government Printing Office, Washington, D.C., 1970. (c) "JANAF Thermochemical Tables", Dow Chemical Co., Midland, Mich.
(141) N. Cohen and J. F. Bott, "Handbook on Chemical Lasers", R. Gross and J. Bott, Ed., Wiley, New York, N.Y., 1976.
(142) D. S. Perry and J. C. Polanyi, *Chem. Phys.*, **12**, 419 (1976).
(143) (a) O. D. Krogh, D. K. Stone, and G. C. Pimentel, *J. Chem. Phys.*, **66**, 368 (1977). (b) Detailed experimental and theoretical treatment of H + XY → HX‡ + Y reactions: J. C. Polanyi and W. J. Skrlac, *Chem. Phys.*, submitted for publication.
(144) G. A. West and M. J. Berry, *Opt. Commun.*, **18**, 128, Abstr N8 (1976).
(145) S. H. Arnold et al., *Appl. Phys. Lett.*, **30**, 637 (1977).
(146) D. J. Douglas, J. C. Polanyi, and J. J. Sloan, *Chem. Phys.*, **13**, 15 (1976).
(147) (a) J. E. Spencer and G. P. Glass, *J. Chem. Phys.*, **79**, 2329 (1975); (b) P. F. Ambidge, J. N. Bradley and D. A. Whytock, *J. Chem. Soc., Faraday Trans. 1*, **72**, 2143 (1976).
(148) J. D. McDonald and D. R. Herschbach, *J. chem. Phys.*, **62**, 4740 (1975).
(149) (a) D. L. Thompson, H. H. Suzukawa, and L. M. Raff, *J. Chem. Phys.*, **64**, 2269 (1976); (b) R. F. Heidner, III, and J. F. Bott, *ibid.*, **64**, 2267 (1976).
(150) (a) T. Dunning, Jr., *J. Chem. Phys.*, **66**, 2752 (1977); (b) P. Botschwina and W. Meyer, *ibid.*, **67**, 2390 (1977), calculated the barrier height for H' + BrH exchange; (c) Remeasurement of the activation energy for Cl + H_2 → HCl + H was reported by J. H. Lee, et al., *J. Chem. Soc., Faraday Trans. 1*, **73**, 1530 (1977).
(151) (a) D. W. Setser and coworkers, *J. Chem., Phys.*, **58**, 2298, 2310 (1973); (b) D. J. Bogan and D. W. Setser, *ibid.*, **64**, 586 (1976); and Symposium Series on "Kinetics and Dynamics of Fluorine Containing Free Radicals", J. W. Root Ed., American Chemical Society, Washington, D.C., 1977. (c) D. W. Setser et al., *J. Phys. Chem.*, **81**, 888, 898 (1977).
(152) J. G. Moehimann and J. D. McDonald, *J. Chem. Phys.*, **62**, 3061 (1975).
(153) J. G. Moehimann and J. D. McDonald, *J. Chem. Phys.*, **62**, 3052 (1975).
(154) J. F. Durana and J. D. McDonald, *J. Chem. Phys.*, **64**, 2518 (1976).
(155) (a) J. M. Farrar and Y. T. Lee, *J. Chem. Phys.*, **65**, 1414 (1976); (b) J. M. Farrar and Y. T. Lee, Symposium Series on "Fluorine Chemistry", American Chemical Society, Washington, D.C., 1977; (c) J. M. Parsons et al., *Faraday Discuss. Chem. Soc.* No. 55, 344 (1973).
(156) J. T. Cheung et al., *Faraday Discuss. Chem. Soc.* No. 55, 377 (1973).
(157) J. B. Cross and N. C. Blais, *J. Chem. Phys.*, **52**, 3580 (1970), and references therein to previous publications.
(158) (a) H. W. Cruse, P. J. Dagdigian, and R. N. Zare, *Faraday Discuss. Chem. Soc.*, No. 55, 277 (1973); (b) J. G. Pruett and R. N. Zare, *J. Chem. Phys.*, **64**, 1774 (1976) (Ba + HF).
(159) B. A. Blackwell, J. C. Polanyi, and J. J. Sloan, *Faraday Discuss. Chem. Soc.*, No. 62, 147 (1977).
(160) L. Pasternack and P. J. Dagdigian, *J. Chem. Phys.*, **65**, 1320 (1976).
(161) W. Schmidt, A. Siegel, and A. Schultz, *Chem. Phys.*, **16**, 161 (1976).
(162) R. Behrens, Jr., R. R. Herm, and C. M. Sholeen, *J. Chem. Phys.*, **65**, 4791 (1976).
(163) (a) E. Tschuikow-Roux and K. A. Maitman, *Int. J. Chem. Kinet.*, **7**, 363 (1975); (b) K. R. Maitman, E. Tschuikow-Roux, and K-H. Jung, *J. Phys. Chem.*, **78**, 1035 (1974); (c) P. Cadman, A. W. Kirk, and A. F. Trotman-Dickson, *J. Chem. Soc., Faraday Trans. 1* **72**, 996 (1976).
(164) B. E. Holmes, D. W. Setser, and G. O. Pritchard, *Int. J. Chem. Kinet.*, **8**, 215 (1976).
(165) B. E. Holmes and D. W. Setser, *J. Phys. Chem.*, **79**, 1320 (1975).
(166) J. T. Gleaves and J. D. McDonald, *J. Chem. Phys.*, **62**, 1582 (1975).
(167) M. C. Lin, *Int. J. Chem. Kinet.*, **5**, 173 (1973).
(168) P. N. Clough, J. C. Polanyi, and R. T. Taguchi, *Can. J. Chem.*, **48**, 2919 (1970).
(169) (a) M. J. Berry and G. C. Pimentel, *J. Chem. Phys.*, **49**, 5190 (1968); (b) E. Cuellar, J. H. Parker, and G. C. Pimentel, *ibid.*, **61**, 422 (1974).
(170) P. Cadman, A. W. Kirk, and A. F. Trotman-Dickson, *J. Chem. Soc., Faraday Trans. 1*, **72**, 1027, 1428 (1976).
(171) N. Basco and R. G/ W. Norrish, *Can. J. Chem.*, **38**, 1769 (1960).
(172) (a) H. S. Pilloff, S. K. Searles, and N. Djeu, *Appl. Phys. Lett.*, **19**, 9 (1971); (b) S. K. Searles and N. Djeu, *Chem. Phys. Lett.*, **12**, 52 (1971); (c) A. A. Vetter and F. C. C. Culick, *J. Chem. Phys.*, **67**, 2304 (1977).
(173) J. D. Kelly, *Chem. Phys. Lett.*, **41**, 7 (1976).
(174) J. W. Hudgens, J. T. Gleaves, and J. D. McDonald, *J. Chem. Phys.*, **64**, 2528 (1976).
(175) (a) M. C. Lin and S. H. Bauer, *Chem. Phys. Lett.*, **7**, 223 (1970); (b) J. Stricker and S. H. Bauer, as yet unpublished data on vibrational state distribution for CO†, 1977.
(176) D. S. Y. Hsu and M. C. Lin, *J. Chem. Phys.*, submitted for publication.
(177) (a) M. C. Lin, *J. Chem. Phys.*, **61**, 1835 (1974); (b) R. G. Shortridge and M. C. Lin, *J. Phys. Chem.*, **78**, 1451 (1974).
(178) R. G. Shortridge and M. C. Lin, *Chem. Phys. Lett.*, **35**, 146 (1975).
(179) (a) M. C. Lin, R. G. Shortridge, and M. G. Umstead, *Chem. Phys. Lett.*, **37**, 279 (1976); (b) M. E. Umstead, R. G. Shortridge, and M. C. Lin, *Chem. Phys.*, **20**, 271 (1977); (c) M. E. Umstead and M. C. Lin [on $O(^3P)$ + butynes], *Chem. Phys.*, submitted for publication; (d) D. S. Y. Hsu, L. J. Calcord, and M. C. Lin, *J. Phys. Chem.*, **82**, 121 (1978).
(180) D. S. Y. Hsu and M. C. Lin, *Int. J. Chem. Kinet.*, **9**, 507 (1977).
(181) J. G. Moehlmann and J. D. McDonald, *J. Chem. Phys.*, **59**, 6683 (1973).
(182) (a) A. B. Callear and H. E. van den Bergh, *Chem. Phys. Lett.*, **8**, 17 (1971); (b) G. D. Downey, D. W. Robinson, and J. H. Smith, *J. Chem. Phys.*, **66**, 1685 (1977), on pure rotational, collisionally pumped OH laser.
(183) R. J. Jensen in ref 141, p 703.
(184) M. E. Whitson, Jr., L. A. Darnton, and R. J. McNeal, *Chem. Phys., Lett.*, 41, 552 (1976).
(185) (a) M. N. R. Ashfold and J. P. Simons, *J. Chem. Soc., Faraday Trans. 2*, **73**, 858 (1977); (b) M. J. Sabety-Dzvonik et al., *J. Chem. Phys.*, **66**, 125, 2145 (1977).
(186) M. Kawasaki, S. J. Lee, and R. Bersohn, *J. Chem. Phys.*, **66**, 2647 (1977).
(187) M. J. Berry, *J. Chem. Phys.*, **61**, 3114 (1974).
(188) D. S. King and J. C. Stephenson, prepublication report.
(189) H.-L. Chen et al., *J. Chem. Phys.*, **66**, 5513 (1977).
(190) V. M. Bierbaum et al., *J. Chem. Phys.*, **67**, 2375 (1977).
(191) M. J. Berry, *Annu. Rev. Phys. Chem.*, **26**, 259 (1975).
(192) J. H. Birely and J. L. Lyman, *J. Photochem.*, **4**, 269 (1975).
(193) J. P. Aldridge, J. H. Birely, C. D. Cantrell, and D. C. Cartwright, "Laser Photochemistry, Tunable Lasers and Other Topics" (Physics of Quantum Electronics), S. F. Jacobs et al., Ed., Addison-Wesley, New York, N.Y., 1977.
(194) S. Kimel and S. Speiser, *Chem. Rev.*, **77**, 437 (1977).
(195) I. W. M. Smith, (Specialist Periodical Reports), The Chemical Society, London, "Gas Kinetics and Energy Transfer" (Specialist Periodical Reports), Vol. 2, 1977, p. 1.
(196) J. Wolfrum, *Ber. Bunsenges. Phys. Chem.*, **81**, 114 (1977).
(197) I. P. Herman, R. P. Mariella, and A. Javan, *J. Chem. Phys.*, **65**, 3792 (1976).
(198) A. Burcat and A. Lifshitz, *J. Phys. Chem.*, **74**, 263 (1970).
(199) V. I. Balykin et al., *Chem. Phys.*, 17, 111 (1976).
(200) R. F. Heidner, III, and J. V. V. Kasper, *Chem. Phys. Lett.*, **15**, 179 (1972).
(201) (a) D. H. Stedman, D. Steffenson, and H. Niki, *Chem. Phys. Lett.*, **7**, 173 (1970); (b) L. B. Sims, L. R. Dosser, and R. S. Wilson, *ibid.*, **32**, 150 (1975); (c) L. Y. Nelson, A. L. Pindroth, and S. R. Byron, unpublished report.
(202) J. H. Birely et al., *Chem. Phys. Lett.*, **31**, 220 (1975).
(203) (a) S. H. Bauer, D. M. Lederman, and E. L. Resler, Jr., *Int. J. Chem. Kinet.*, **5**, 93 (1973); (b) A. Lifshitz and M. Frenklach, *J. Chem. Phys.*, **67**, 2803 (1977). (c) N. J. Brown and D. M. Silver, *ibid*, **65**, 311 (1976).
(204) J. E. Spencer and G. P. Glass, *Int. J. Chem. Kinet.*, 9, 111 (1977).
(205) J. E. Spencer, H. Endo, and G. P. Glass, 16th Symposium (International) on Combustion, 1976, p. 829.
(206) B. A. Blackwell, J. C. Polanyi, and J. J. Sloan, *Faraday Discuss., Chem. Soc.*, No. 62, 328 (1976); *Chem. Phys.*, **24**, 25 (1977).
(207) A. E. Potter, Jr., R. N. Coltharp, and S. D. Worley, *J. Chem. Phys.*, **54**, 992 (1971).
(208) G. E. Streit and H. S. Johnson, *J. Chem. Phys.*, **64**, 95 (1976).
(209) M. J. Berry, *J. Chem. Phys.*, **59**, 6229 (1973).
(210) G. J. Wolga and R. Chang, unpublished data, 1976.
(211) D. Arnoldi and J. Wolfrum, *Ber. Bunsenges. Phys. Chem.*, **80**, 892 (1976).
(212) P. F. Ambidge, J. N. Bradley, and D. A. Whylock, *J. Chem. Soc., Faraday Trans. 1*, 72, 1157 (1976).
(213) K. Kaufmann and J. Wolfrum, unpublished.
(214) (a) A. G. M. Ding et al., *Discuss. Faraday, Chem. Soc.*, No. 55, 252 (1973); (b) L. J. Kirsch and J. C. Polanyi, *J. Chem. Phys.*, **57**, 4498 (1972).
(215) (a) R. G. Macdonald et al., *J. Chem. Phys.*, **62**, 2934 (1975); (b) D. L. Thompson, *Acc. Chem. Res.*, 9, 338 (1976).
(216) (a) D. Arnoldi, K. Kaufmann, and J. Wolfrum, *Phys. Rev. Lett.*, **34**, 1597

(1975); (b) D. J. Douglas, J. C. Polanyi, and J. J. Sloan, *J. Chem. Phys.*, **59**, 6679 (1973); (c) S. R. Leone, R. G. Macdonald, and C. B. Moore, *Ibid.*, **63**, 4735 (1975).
(217) (a) Z. Karny, B. Katz, and A. Szoke, *Chem. Phys. Lett.*, **35**, 100 (1975); (b) R. Brown, G. P. Glass, and I. W. M. Smith, *Ibid.*, **32**, 517 (1975).
(218) (a) T. J. Odiorne, P. R. Brooks, and J. V. V. Kasper, *J. Chem. Phys.*, **55**, 1980 (1971); (b) J. G. Pruett, F. R. Grabiner, and P. R. Brooks, *Ibid.*, **63**, 1173 (1975).
(219) M. J. Berry, unpublished.
(220) J. M. White and D. L. Thompson, *J. Chem. Phys.*, **61**, 719 (1974).
(221) C. C. Badcock, W. C. Hwang and J. F. Kalsch, Aerospace Report No. ATR-77(8127)-1, 1976.
(222) H. Schacke, K. J. Schmatjko, and J. Wolfrum, *Ber. Bunsenges. Phys. Chem.*, **77**, 248 (1973).
(223) H. Schacke, H. Gg. Wagner, and J. Wolfrum, *Ber. Bunsenges. Phys. Chem.*, **81**, 670 (1977).
(224) G. Hancock, C. Moreley, and I. W. M. Smith, *Chem. Phys. Lett.*, **12**, 193 (1971).
(225) J. C. Stephenson and S. Freund, *J. Chem. Phys.*, **65**, 4303 (1976).
(226) R. J. Gordon and M. C. Lin, *Chem. Phys. Lett.*, **22**, 262 (1973).
(227) P. N. Clough and B. A. Thrush, *J. Chem. Soc., Faraday Trans. 1*, **63**, 915 (1967).
(228) M. J. Kuryio et al., *J. Photochem.*, **3**, 71 (1974).
(229) (a) D. I. Rosen and T. A. Cool, *J. Chem. Phys.*, **62**, 466 (1975); (b) S. M. Freund and J. C. Stephenson, *Chem. Phys. Lett.*, 41, 157 (1976); (c) K.-K. Hui and T. A. Cool, Ph.D. Dissertation, Cornell University, 1977.
(230) W. Baum et al., *J. Chem. Phys.*, **61**, 461 (1974).
(231) (a) M. J. Kuryio et al., *J. Chem. Phys.*, **62**, 2065 (1975); (b) A. Kaldor, W. Braun, and M. J. Kuryio, *Ibid.*, **61**, 2496 (1974).
(232) J. Moy, E. Bar-Ziv, and R. J. Gordon, *J. Chem. Phys.*, **66**, 5439 (1977).
(233) (a) D. J. Wren and M. Menzinger, *J. Chem. Phys.*, **63**, 4557 (1975); (b) T. P. Parr et al., *Ibid.*, **67**, 2181 (1977).
(234) A. Yokozeki, presented at the 31st Symposium on Spectroscopy, Columbus, Ohio, June 1976.
(235) R. G. Manning, W. Braun, and M. J. Kurylo, *J. Chem. Phys.*, **65**, 2609 (1976).
(236) (a) D. Arnoldi et al., "Lasers in Physical Chemistry and Biophysics", 27th International Meeting, Societe de Chemie Physique, June 1977; (b) I. Shamah and G. Flynn, *J. Am. Chem. Soc.*, **99**, 3191 (1977).
(237) B. L. Earl and A. M. Ronn, *Chem. Phys. Lett.*, **41**, 29 (1976).
(238) V. P. Strunin et al., *react. Kinet. Catal. Lett.*, submitted for publication.
(239) T. J. Manuccia, M. D. Clark, and E. R. Lory, *Chem. Phys. Lett.*, submitted for publication.
(240) J. L. Lyman and R. J. Jensen, *Chem. Phys. Lett.*, **13**, 421 (1972).
(241) (a) F. Bachman et al., *Ber. Bunsenges. Phys. Chem.*, **81**, 313 (1977); (b) D. F. Dever and E. Grunwald, *J. Am. Chem. Soc.*, **98**, 5055 (1976).
(242) E. R. Lory, T. J. Manuccia, and S. H. Bauer, *J. Phys. Chem.*, **79**, 545 (1975); and ref 49.
(243) S. H. Bauer and J. A. Haberman, *IEEE, J. Quantum Electron*, in press.
(244) M. Lamotte, H. J. Dewey, P. Keller, and J. J. Ritter, *Chem. Phys. Lett.*, **30**, 165 (1975).
(245) S. Datta, R. W. Anderson, and R. N. Zare, *J. Chem. Phys.*, **63**, 5503 (1975).
(246) J. L. Lyman, Ph.D. Dissertation, 1973; Report; LA-5365-T (UC-34).
(247) Michael J. Berry, preliminary disclosure.
(248) (a) N. Bloembergen, C. D. Cantrell, and D. M. Larsen in "Tunable Lasers and Applications", ref 28a; (b) S. Mukamel and J. Jortner, *J. Chem. Phys.*, **65**, 3735, 5204 (1976).
(249) M. F. Goodman, J. Stron, and D. A. Dows, *J. Chem. Phys.*, **65**, 5052, 5062 (1976).
(250) (a) R. B. Walker and R. K. Preston, *J. Chem. Phys.*, **67**, 2017 (1977); (b) L. M. Narducci *et et al.*, *Phys. Rev. A*, **16**, 247 (1977).
(251) (a) J. L. Lyman, *J. Chem. Phys.*, **67**, 1868 (1977); (b) E. R. Grant et al., *Phys. Rev. Lett.*, submitted for publication.
(252) (a) M. C. Gower and K. W. Billman, *Appl. Phys. Lett.*, **30**, 514 (1977); (b) P. Kolodner, C. Winterfeld, and E. Yablonovitch, *Opt. Commun.*, **20**, 119 (1977).
(253) (a) B. Perlmutter-Hayman, *Prog. Inorg. Chem.*, **20**, 229 (1976); (b) W. C. Gardiner, *Acc. Chem. Res.*, **10**, 273 (1977).
(254) S. H. Bauer, *J. Chem. Phys.*, **7**, 1097 (1939).
(255) R. L. Leroy, *J. Phys. Chem.*, **73**, 4338 (1969).
(256) M. Menzinger and R. Wolfgang, *Angew. Chem. Int. Ed. Engl.*, **8**, 438 (1969).
(257) J. C. Polanyi and J. L. Schreiber in ref 2c, Chapter 6.
(258) R. D. Kern in ref 73.
(259) H. O. Pritchard, *Acc. Chem. Res.*, **9**, 99 (1976).
(260) R. N. Porter, *Annu. Rev. Phys. Chem.*, **25**, 317 (1974).
(261) C. F. Bender, B. J. Garrison, and H. F. Schaefer, III, *J. Chem. Phys.*, **62**, 1188 (1975).
(262) C. Thompson, *Annu. Rep. Prog. Chem.*, **71**, 5 (1975).
(263) (a) *Faraday Discuss. Chem. Soc.*, No. 62 (1977); (b) Symposium, Physical Chemistry Division, 174th National Meeting of the American Chemical Society, 1977.
(264) (a) D. L. Miller and R. E. Wyatt, *J. Chem. Phys.*, **67**, 1302 (1977); (b) A. Komornicki, T. F. George, and K. Morokuma, **65**, 4312 (1976); **67**, 5012 (1977).
(265) (a) O. H. Crawford, *J. Chem. Phys.*, **55**, 2571 (1971); (b) W. H. Miller, *Adv. Chem. Phys.*, **30**, 77ff (1975); D. Micha, *Ibid.*, **30**, 7ff (1975).
(266) (a) S. A. Pace and J. M. White, *Int. J. Chem. Kinet.*, 7, 951 (1975); (b) R. B. Bernstein and R. D. Levine, *Chem. Phys. Lett.*, **29**, 314 (1974).
(267) R. K. Preston and R. T. Pack, *J. Chem. Phys.*, **66**, 2480 (1977).
(268) J. M. Farrar, J. M. Parson, and Y. T. Lee, Proceedings of the 4th International Conference on Molecular Beams, Cannes, France, 1973.
(269) (a) R. T. Pack, *J. Chem. Phys.*, **62**, 3143 (1975); (b) S. Chapman and S. Green, *ibid.*, **67**, 2313 (1977); (c) C. S. Lin and D. Secrest, *ibid.*, **67**, 1291 (1977).
(270) J. J. Suzukawa, Jr., Ph.D. Dissertation, University of California, Irvine, 1974.
(271) N. Sathyamurthy and L. M. Raff, *J. Chem. Phys.*, **66**, 2191 (1977).
(272) (a) U. Buck and P. McGuire, *Chem. Phys.*, **16**, 101 (1976); (b) J. C. Polanyi, N. Sathyamurthy, and J. L. Schreiber, *Ibid.*, **24**, 105 (1977).
(273) R. J. Gordon, *J. Chem. Phys.*, **65**, 4945 (1976).
(274) S. H. Bauer and S. C. Tsang, *Phys. Fluids*, **6**, 182 (1963).
(275) (a) D. L. Thompson, *J. Chem. Phys.*, **56**, 3670 (1972); (b) see also H. E. Bass and D. L. Thompson, *Ibid.*, **66**, 2545 (1977), for $Cl_2^{\dagger}$ + HCl (DCl).
(276) M. D. Pattengill, J. C. Polanyi, and J. L. Schreiber, *J. Chem. Soc. Faraday Trans. 2*, **72**, 897 (1976).
(277) (a) J. C. Brown, H. E. Bass, and D. L. Thompson, *Chem. Phys.* (LASL Report, 1976), submitted for publication; (b) H. E. Bass, L. S. Kenton, and D. L. Thompson, *Chem. Phys. Lett.*, **44**, 452 (1976).
(278) Selected examples: (a) H + DBr, H. Y. Su et al., *J. Chem. Phys.*, **62**, 1435 (1975); (b) H + I_2 (Br_2), R. N. Porter et al., *ibid.*, **62**, 2429 (1975); (c) Br + HCl† (DBr†), I. W. M. Smith, *Chem. Phys.*, **20**, 437 (1977); (d) O + $H_2^{\dagger}$, B. R. Johnson and N. W. Winter, *J. Chem. Phys.*, **66**, 4116 (1977).
(279) N. H. Hijazi and J. C. Polanyi, *J. Chem. Phys.*, **63**, 2249 (1975).
(280) L. W. M. Smith, *Chem. Phys. Lett.*, **47**, 219 (1977).
(281) D. L. Thompson, *J. Chem. Phys.*, **60**, 4557 (1974); **62**, 4241 (1975).
(282) N. C. Blais and D. G. Truhlar, *J. Chem. Phys.*, **66**, 772 (1977). See also D. T. Chang and G. Burns, *Can. J. Chem.*, **55**, 380 (1977). Re: Br_2 + Ar, and ref 57 for an analysis of the statistical problem.
(283) R. L. Johnson, K. C. Kim, and D. W. Setser, *J. Phys. Chem.*, 77, 2499 (1973).
(284) A. Gauss, Jr., *J. Chem. Phys.*, **65**, 4365 (1976).
(285) D. L. Thompson and D. R. McLaughlin, *J. Chem. Phys.*, **62**, 4284 (1975).
(286) L. M. Raff et al., *J. Chem. Phys.*, **56**, 5998 (1972); **60**, 2220 (1974).
(287) M. H. Mok and J. C. Polanyi, *J. Chem. Phys.*, **53**, 4588 (1970).
(288) E. R. Grant and D. L. Bunker, submitted for publication.
(289) S. Chapman and D. L. Bunker, *J. Chem. Phys.*, **62**, 2840 (1975).
(290) T. E. Orlowski, K. E. Jones, and A. H. Zewail, *Chem. Phys. Lett.*, **50**, 45 (1977).
(291) C. A. Parr, A. Kupperman, and R. N. Porter, *J. Chem. Phys.*, **66**, 2914 (1977).
(292) J. D. McDonald and R. A. Marcus, *J. Chem. Phys.*, **65**, 2180 (1976).
(293) L. Holmlid and K. Rynefors, *Chem. Phys.*, **19**, 261 (1977).
(294) A. B. Elkowitz and R. E. Wyatt, *J. Chem. Phys.*, **62**, 2504 (1975).
(295) J. N. L. Connor, W. Jakubetz, and J. Manz, *Chem. Phys. Lett.*, **39**, 75 (1976).
(296) V. Halavee and M. Shapiro, *J. Chem. Phys.*, **64**, 2826 (1976).
(297) (a) R. B. Bernstein and R. D. Levine, *J. Chem. Phys.*, **57**, 434 (1972); (b) A. Ben-Shaul, R. D. Levine, and R. B. Bernstein, *Ibid.*, **57**, 5427 (1972).
(298) R. D. Levine, "Jerusalem Symposia on Quantum Chemistry and Biochemistry VI", 1974, p 35.
(299) (a) R. D. Levine and J. Manz, *J. Chem. Phys.*, **63**, 4280 (1975); (b) E. Pollak and R. D. Levine, *Chem. Phys. Lett.*, **39**, 199 (1976).
(300) R. D. Levine and A. Ben-Shaul in "Chemical and Biological Applications of Lasers", C. B. Moore, Ed., Academic Press, New York, N.Y., 1977.
(301) (a) D. S. Perry and J. C. Polanyi, *Chem. Phys.*, **12**, 37 (1976); (b) R. B. Bernstein and R. D. Levine, *J. Chem. Phys.*, **61**, 4926 (1974).
(302) R. B. Bernstein and R. D. Levine, *Adv. At. Mol. Phys.*, 11, 215 (1975).
(303) R. D. Levine and R. B. Bernstein, "Modern Theoretical Chemistry", Vol. 2, W. H. Miller, Ed., Plenum, New York, N.Y., 1976, p 323.
(304) S. Lemont and G. W. Flynn, *Annu. Rev. Phys. Chem.* **28**, 261 (1077).
(305) K. Shibuya and E. K. C. Lee, in press.
(306) E. K. C. Lee, *Acc. Chem. Res.*, **10**, 319 (1977).
(307) R. G. Miller and E. K. C. Lee, *Chem. Phys. Lett.*, **33**, 104 (1975).
(308) J. J. Valentine, Y. T. Lee, and D. Auerbach, *J. Chem. Phys.*, **67**, 4866 (1977).
(309) L. Pasternack and P. J. Dagdigian, *J. Chem. Phys.*, **67**, 3854 (1977).
(310) B. Davies, A. McNeish, M. Poliakoff, M. Tranquille, and J. J. Turner, *Chem. Phys. Lett.*, 52, 477 (1977).
(311) G. P. Smith, J. C. Whitehead, and R. N. Zare, *J. Chem. Phys.*, **67**, 4912 (1977).
(312) I. Oref and B. S. Rabinovitch, *J. Phys. Chem.*, **81**, 2587 (1977); J. H. Richardson and D. W. Setser, *Ibid.*, **81**, 2301 (1977); D. Gutman, W. Braun, and W. Tsang, *J. Chem. Phys.*, **67**, 4291 (1977).
(313) J. Goodman and L. E. Brus, *J. Chem. Phys.*, **67**, 4398 (1977).